Gasification-Based Fuels and Electricity Production from Biomass, without and with Carbon Capture and Storage

Eric D. Larson,* Haiming Jin,** Fuat E. Celik*
* Princeton Environmental Institute, Princeton University, Princeton, NJ
**Thayer School of Engineering, Dartmouth College, Hanover, NH

1 Introduction

We report here on design, mass-and-energy-balance calculations, and production cost estimates for gasification-based thermochemical conversion of switchgrass into Fischer-Tropsch (F-T) fuels, dimethyl ether (DME), and hydrogen, in all cases with some level of co-production of electricity. Also, some process designs are developed and analyzed that include capture of by-product CO_2 for underground storage. Additionally, we present results for stand-alone electricity production using integrated gasification combined-cycle technology, both with and without carbon capture and storage (CCS).

The feedstock considered in all cases is switchgrass, and the reference production scale is an "as-received" input of 5,670 metric tons per day (tpd) of switchgrass having a moisture content of 20%.[1] This corresponds to a dry matter flow of 4,536 tpd (or 5000 dry short tons per day). The 20% moisture level is sufficiently low that active drying of the feed material is not necessary before gasification. This saves considerable capital cost by avoiding a dryer, while imposing little if any efficiency penalty relative to systems with active drying utilizing low-grade waste heat.

The physical and chemical characteristics of the assumed switchgrass are given in Table 1. The energy flow corresponding to 5,670 tpd of 20% moisture switchgrass is 983 MW higher heating value or 893 MW lower heating value.

Table 1. Characteristics of switchgrass assumed in this analysis.[a]

As-Received Proximate Analysis	
Fixed carbon (wt%)	17.1
Volatile matter (wt%)	58.4
Ash (wt%)	4.6
Moisture content (wt%)	20.0
Lower Heating Value (MJ/kg)	13.5
Higher Heating Value (MJ/kg)	15.0
Ultimate Analysis (dry basis)	
Carbon (wt%)	47.0
Hydrogen (wt%)	5.3
Oxygen (wt%)	41.4
Nitrogen (wt%)	0.5
Sulfur (wt%)	0.1
Ash (wt%)	5.7
Lower Heating Value (MJ/kg)	17.5
Higher Heating Value (MJ/kg)	18.7

(a) The proximate and ultimate analyses are for whole-plant Alamo Switchgrass as given in the US Department of Energy database available at http://www.ott.doe.gov/biofuels/properties_database.html (entry #74). We have normalized the original DOE ultimate analysis (carbon, 47.27%; oxygen, 41.59%; hydrogen, 5.31%; nitrogen, 0.51%; sulfur, 0.1%; and ash, 5.76%), so that the percentages sum to 100%. The higher heating value given in this DOE database is 7998 Btu/lb (dry basis), or 18.61 MJ/kg. We used the latter value as an input to our Aspen process simulation. Aspen uses the initial value in calculations involving values of other thermodynamic properties. The latter values vary slightly depending on which one of Aspen's internal thermodynamic property sets is selected for use in the simulation. As a result, back-calculating from the final Aspen simulation results yields a slightly different higher heating value (shown in the table), but one that is consistent with the overall Aspen calculations.

[1] The average as-received moisture content for large-scale production of field-dried switchgrass is expected to be 15% to 20% by weight (S. McGlaughlin, personal communication, October 2003).

For all process designs considered, we have developed energy and mass balances (using Aspen-Plus process simulation software) for "N^{th} plant" systems, i.e., systems for which it is assumed that all research, development, and demonstration hurdles to commercial implementation have been overcome. This requires projecting some performance characteristics and costs, since none of the systems under consideration have reached commercially mature performance, reliability, or cost levels today. There have been considerable technology developments in closely related areas, as discussed in Section 3, which provides a good basis for making N^{th} plant performance and cost projections.

As discussed by Larson (2003) and Larson, *et al.* (2004), the most important technical hurdles that have yet to be overcome, but which are assumed to have been overcome for the purposes of this analysis, relate to a) reliable feeding of low bulk-density biomass like switchgrass into a pressurized gasifier vessel without excessive feeding-energy requirements, b) high-reliability operation of commercial oxygen-blown fluidized-bed gasification, c) essentially complete cracking of tars in the raw gasifier product into non-condensible combustible gases, d) raw gas cleanup of particulates, alkali, sulfur, and other trace contaminants to the specifications needed for downstream processing, and d) tight process heat integration and control, resulting in maximum recovery and use of process waste heat.

Based on the required equipment capacities derived from our process simulations, we have developed capital cost estimates by major plant area drawing on literature sources, extensive discussions with industry experts, and our own prior work. The uncertainty in our capital cost estimates is ±30%, based on the level of detail (factored estimates for major plant areas), the nature of literature and industry sources (including some equipment-vendor quotes) from which we derived costs, and the inherent uncertainties in projecting "N^{th} plant" costs given the pre-commercial status of some of the major pieces of equipment included in the systems examined. Using widely-accepted equipment-level cost scaling exponents, we also estimate capital costs for plants of different capacities from the reference capacity to illustrate scale economies inherent in the technologies.

It may be noted that the reference biomass feed rate (5,670 tpd) is considerably larger than has been considered previously for biomass conversion facilities in most analyses, although a few commercial lignocellulosic-biomass processing facilities this size are in operation today.[2] The primary incentive for building plants this large is more favorable economics. While it is feasible and desirable to build large-scale biomass conversion facilities, most analysis and commercial implementation of bioenergy to date has focused on relatively small-scale conversion plants. This is due largely to the prevailing thinking that low-cost biomass feedstocks (residues and wastes) are necessary for the viability of projects in the near term. Residues and wastes are relatively dispersed resources, so large quantities cannot be cost-effectively brought to single sites, thereby limiting the size of conversion facilities.

With dedicated production of switchgrass for energy, it becomes plausible for large-scale conversion facilities to be supplied with feedstock from within reasonable distances (incurring

[2] For example, in Brazil there are an estimated 15 sugarcane processing facilities that consume sugarcane at a rate of 5,000 dry metric tons/day or greater (personal communication from J.H. Suleiman, Centro de Tecnologia Copersucar, Piracicaba, Sao Paulo, Brazil, 6 May 2004). Since typical Brazilian sugarcane has a moisture content of about 70% when it reaches a mill, 5000 dry tpd corresponds to about 17,000 as-received tpd.

only modest transport costs), particularly in areas where high switchgrass yields can be achieved. Figure 1 shows the approximate transport distances that would be involved in supply 5000 metric tonnes per day (dry matter) to a central conversion facility as a function of yield and planting density. Shown for reference are planting densities for corn across corn-growing regions of the United States, as well as the planting density for corn in the heavy corn-producing region of Southeastern Iowa.

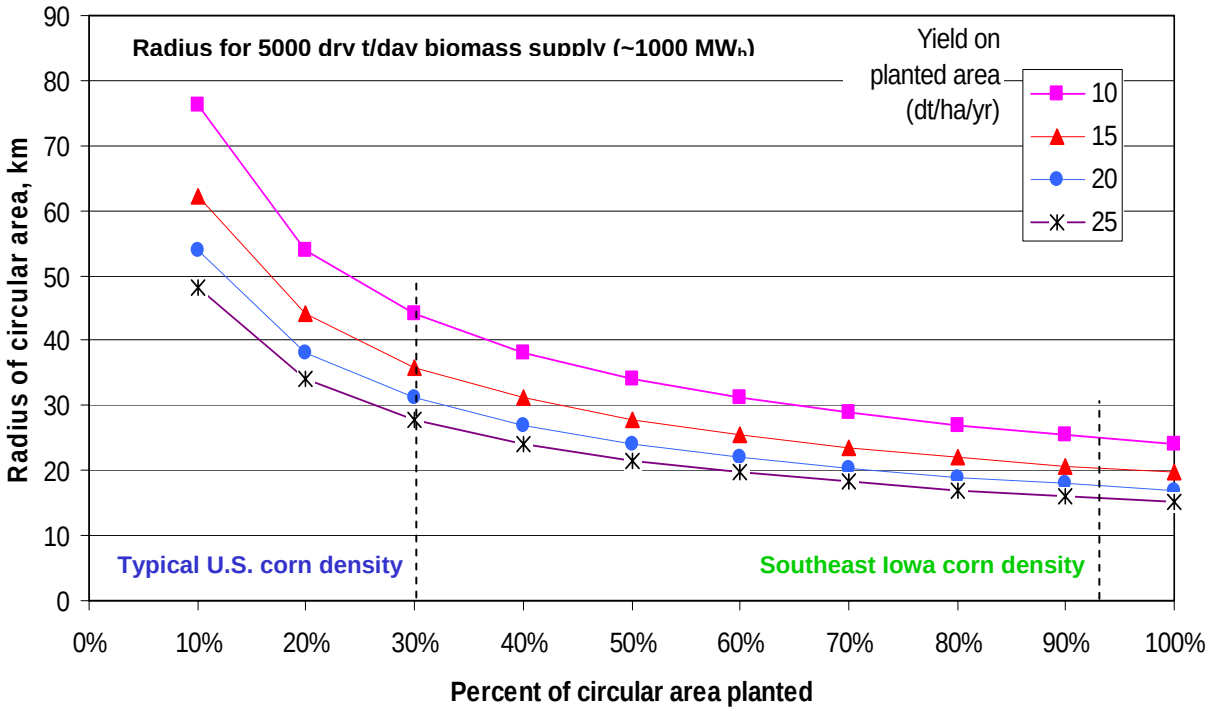

Figure 1. Calculated radius of circular area from which switchgrass would be harvested for delivery to a conversion site located at the center of the collection area. Radius is shown for different average yields (dry metric tonnes per hectare per year) and percent of area cultivated.

In this report, we begin with an overview of the process designs for converting switchgrass into fuels and/or electric power. We then summarize the commercial status of relevant technologies. Detailed process design and simulation results are then presented, followed by capital and production cost estimates. Some relevant comparisons between the estimated production costs of biomass-derived fuels and power and fossil-fuel based products are also given.

2 Overview of Conversion Processes

In a later section of this report we will present detailed results for a large number of different process configurations. To help the reader navigate through the different process designs, we begin here with simplified descriptions.

All processes examined here share a common upstream design for converting biomass into a clean synthesis gas. Switchgrass is brought from a short-term storage area into a feed preparation area where it is chopped and conveyed to the gasifier. Gasification is carried out in a pressurized, oxygen-blown, fluidized-bed gasifier, with oxygen provided from an air separation

unit (ASU). Oxygen gasification is preferred to air-blown gasification because it minimizes downstream equipment sizes (by eliminating nitrogen dilution in process streams) and improves reaction rates in fuels synthesis steps.[3] The gasifier produces a mixture of light combustible species (primarily CO and H_2, with some CH_4), heavy hydrocarbons ("tars and oils") and unwanted minor contaminants (H_2S, NH_3, HCN, and others). In our simulations, all carbon in the biomass is assumed to be completely converted to gas. The raw gas (at about 1000°C) is subjected to several cleaning and cooling steps before further processing. These include thermal/catalytic cracking of tars/oils, partial gas cooling (to about 350°C), and particle removal by filtration (which also removes alkali compounds condensed on the particles).

After a clean synthesis gas is produced, the downstream processing of the gas varies depending on what products are being made and on whether or not CO_2 is captured for storage. Table 2 summarizes all cases considered in this work. The case names shown there are used throughout this report. All case names ending in "VENT" involve no capture of CO_2. All cases with names ending in "CAP" or "CCS" involve some extent of carbon capture and storage (CCS). In all cases, electricity is generated in excess of the amount needed to meet onsite process needs. For three of the cases (indicated in Table 2), the amount of excess electricity is relatively modest, for reasons explained below.

Table 2. Process designs examined in this work.

Abbreviation for Process Configuration	Products				Carbon Captured?	
	Electricity	**F-T Fuels**	**DME**	**H_2**	**NO**	**YES**
Electricity only						
BIGCC-VENT	✓				✓	
BIGCC-CCS	✓					✓
Dimethyl Ether						
D-OT-VENT	✓		✓		✓	
D-RC-VENT	low ✓		✓		✓	
D-OT-UCAP	✓		✓			✓
D-RC-UCAP	low ✓		✓			✓
D-OT-DCAP	✓		✓			✓
Fischer-Tropsch Fuels						
FT-OT-VENT	✓	✓			✓	
FT-OT-UCAP	✓	✓				✓
Hydrogen						
HMAX-VENT	low ✓			✓	✓	
H50/50-VENT	✓			✓	✓	
HMAX-CCS	✓			✓		✓
H50/50-CCS	✓			✓		✓

Two designs for stand-alone electricity production are developed. Both involve the combustion of the clean synthesis gas in a gas turbine combined cycle. In the case with venting of CO_2

[3] Synthesis involves reactions that are driven by the partial pressures of the CO, H_2, and other reacting species in the gas. Inert nitrogen would reduce the partial pressures of the reacting species and lead to lower synthesis rates. An alternative to oxygen-blown gasification for producing a synthesis gas undiluted with nitrogen is gasification driven by heat delivered indirectly to the biomass. Two indirectly-heated gasifier technologies have received considerable development and demonstration support from the US Dept. of Energy during the past 15 years. These include the technology originally developed at the Battelle Columbus Laboratory, in which hot sand delivers heat to a fluidized-bed reactor, and the technology of the company, MTCI, in which heat exchanger tubes are immersed in a fluidized bed. Both of these technologies operate at near-atmospheric pressure, which makes it difficult and/or costly to scale up to the large plant sizes being considered here.

(BIGCC-VENT), the clean syngas is sent directly to the gas turbine combined cycle (Figure 2, upper). In the case with CO_2 capture (BIGCC-CCS), the clean syngas undergoes water gas shift reaction followed by CO_2 removal, resulting in a hydrogen-rich fuel gas stream going to the GTCC (Figure 2, lower).

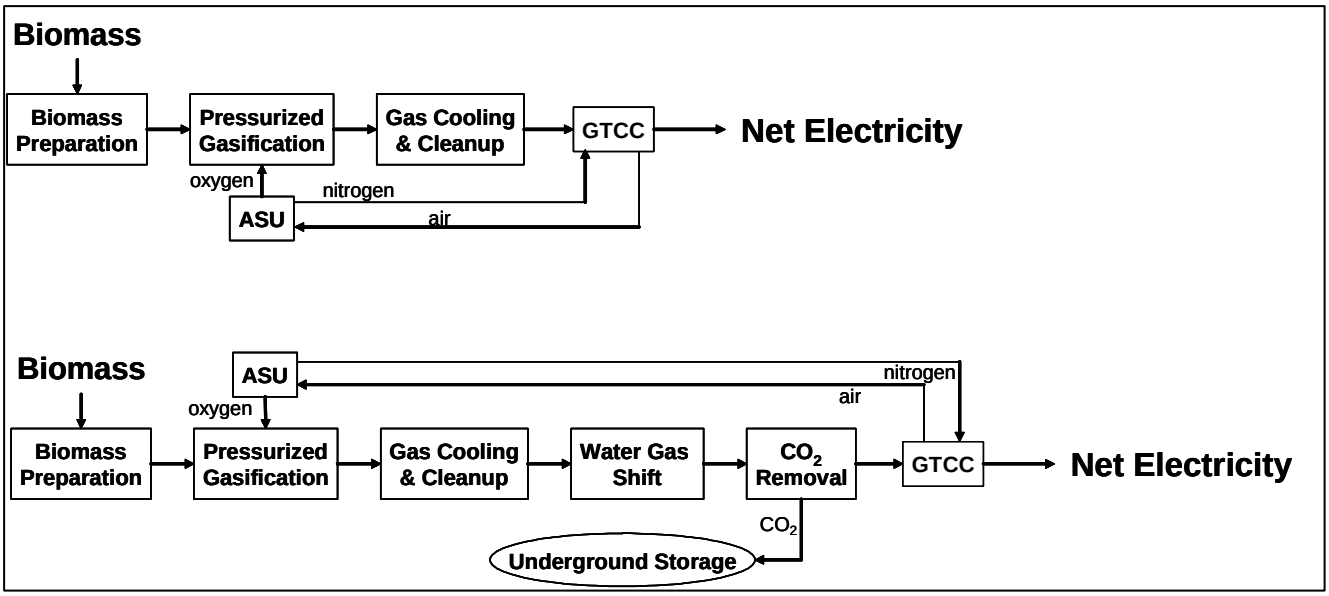

Figure 2. Simplified process diagram for electricity production from biomass without carbon capture (upper figure) and with carbon capture (lower figure).

For production of dimethyl ether, two basic process designs are examined for the case without carbon capture (Figure 3). In both designs, the small amount of H_2S (~ 500 ppmv) remaining in the clean syngas is removed prior to synthesis to avoid poisoning of the downstream catalyst, and most of the CO_2 in the gas is also removed in order to improve conversion rates in the synthesis reactor. CO and H_2 catalytically combine in the synthesis reactor, which produces a mix of DME and unconverted synthesis gas. In one design (D-OT-VENT, Figure 3, upper), the syngas is passed once through ("OT") the synthesis reactor. The DME is then separated from the unconverted gas, and the latter is burned in a gas turbine combined cycle to generate electricity, a small portion of which is consumed on site and the balance of which is sold. In the second design (D-RC-VENT, Figure 3, lower), most of the unconverted syngas after synthesis is recycled ("RC") to the synthesis reactor to produce additional DME. A small purge gas stream is burned in the power island to generate a modest amount of electricity, most of which is consumed on site to meet process needs.

For DME production with CCS, three process designs have been developed (Figure 4). With once-through synthesis, CO_2 is captured upstream of the synthesis reactor (D-OT-UCAP, Figure 4, upper) or both upstream and downstream of the reactor (D-OT-DCAP, Figure 4, middle). For the latter case, the unconverted synthesis gas leaving the DME separation area is subjected first to a water gas shift reaction to increase the amount of CO_2 that can be subsequently removed. The third DME process design with CCS is with recycle synthesis (D-RC-UCAP, Figure 4, lower). In this design CO_2 is captured only upstream of the synthesis reactor, since there is relatively little CO_2 available for capture downstream.

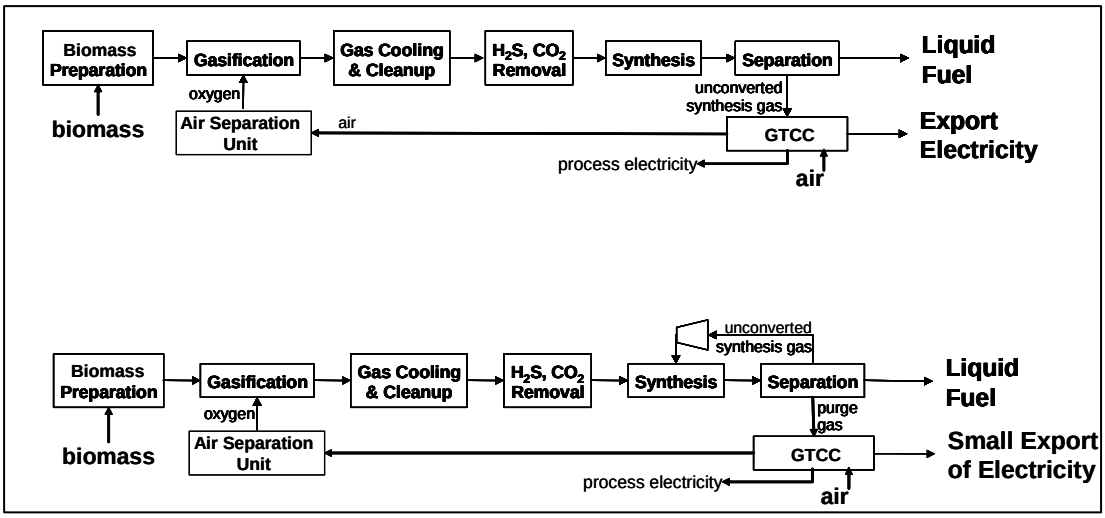

Figure 3. Simplified process diagrams for co-production of liquid fuels (DME or FT) and electricity without CCS. The upper configuration shows once-through synthesis, with co-production of a significant amount of electricity from unconverted syngas. The lower configuration (D-RC-VENT) shows recycle of unconverted syngas to synthesis, resulting in less electricity co-production.

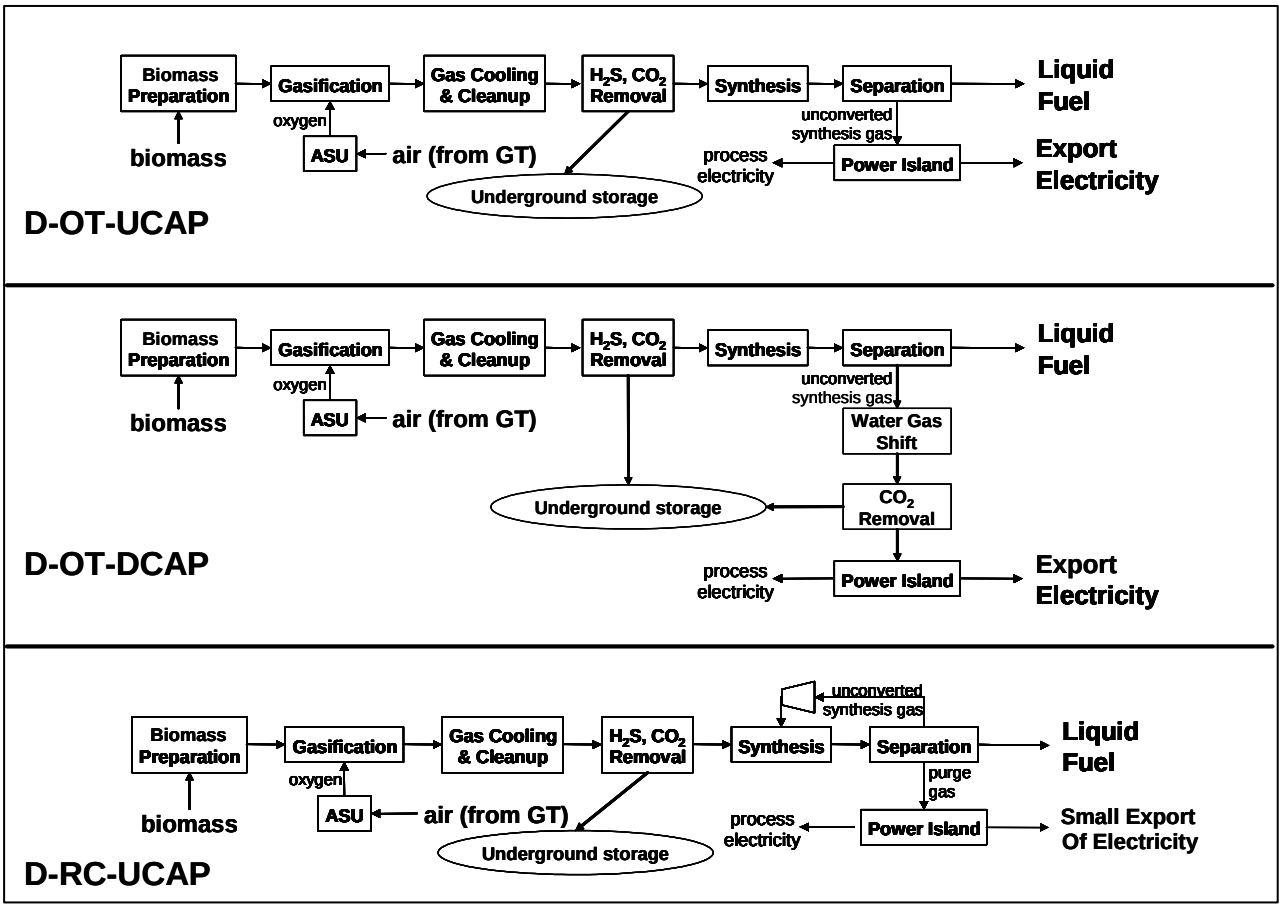

Figure 4. Simplified process diagrams for co-production of DME and electricity with carbon capture and storage. The upper and middle configurations involve once-through synthesis, with co-production of a significant amount of electricity from unconverted syngas. The lower configuration involves recycle of most of the unconverted syngas to the synthesis reactor, resulting in a smaller amount of electricity co-production.

For the production of F-T fuels, we have developed two process designs, both involving once-through synthesis. The case without CCS is depicted in the upper diagram in Figure 3 (FT-OT-VENT). The design of the case with CCS, FT-OT-UCAP, is analogous to the DME case, D-OT-UCAP, shown in the upper diagram of Figure 4. We have considered only once-through synthesis for F-T fuels, because the high single-pass conversion of syngas that can be achieved with F-T synthesis (compared with DME synthesis) leaves relatively little unconverted gas for recycle.

For hydrogen production, the clean syngas leaving the gasifier/gas cleanup area is subjected to water gas shift, after which CO_2 is removed (for venting or for capture) and hydrogen in the remaining gas is purified. The purge gas from the purification process is burned to generate electricity. Two process designs are considered with CO_2 vented. One case maximizes the production of hydrogen (H-MAX-VENT, Figure 5) by the design of the separation area. The amount of exportable electricity generated in this case is relatively small. In the second case, the separation area is designed so that roughly equal amounts of hydrogen and exportable electricity are produced (H-50/50-VENT, Figure 5). For hydrogen production with CCS, essentially the same designs as with CO_2 venting would be utilized, but rather than venting the CO_2 before the hydrogen purification step, the CO_2 would be captured and compressed for transporting to storage (Figure 5, lower two diagrams).

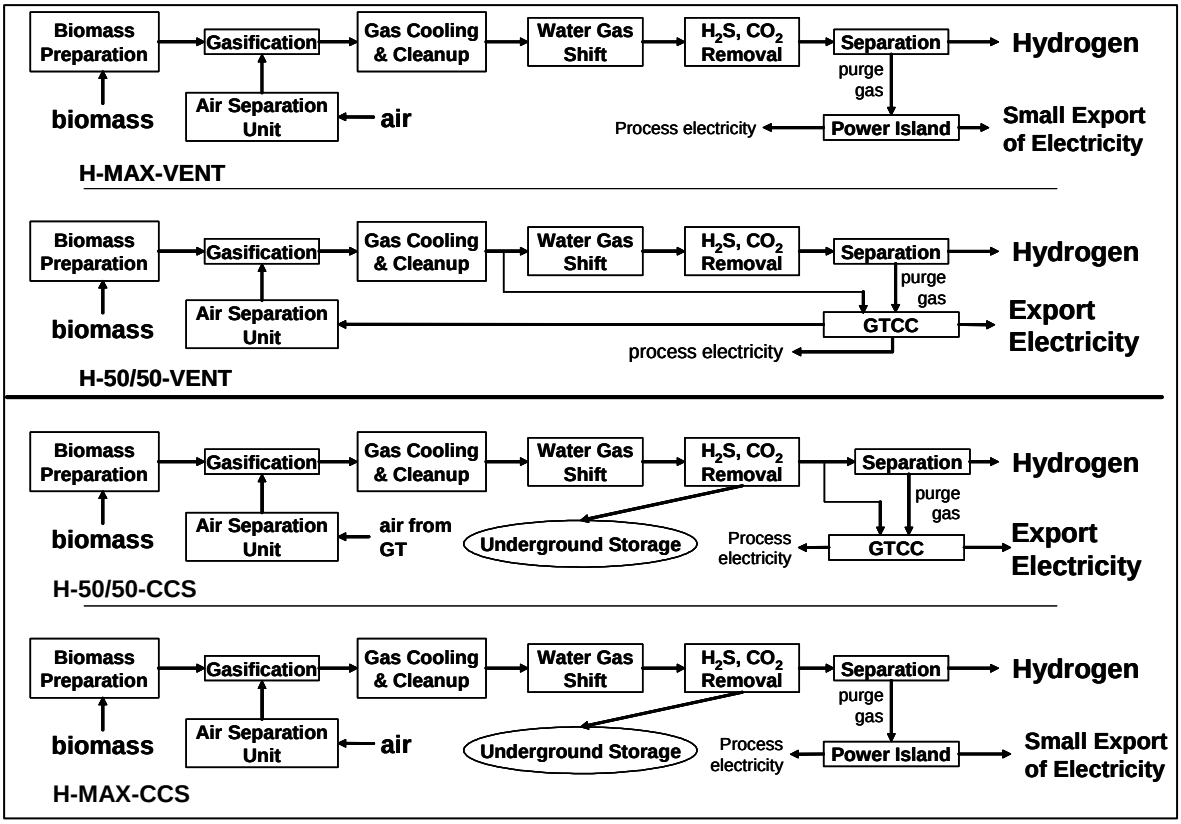

Figure 5. Simplified process diagrams for co-production of hydrogen and electricity with carbon capture and storage. The upper two configurations are with venting of CO_2. The lower two configurations are with carbon capture and storage.

3 Status of Technologies

Many of the key component technologies in the process designs sketched above are already commercial, while a few key ones are yet to see any commercial use. In this section we discuss the development status of key biomass-specific technologies and also the status of synthesis gas processing technologies that are not specific to any particular starting feedstock.

3.1 Production of Clean Synthesis Gas

3.1.1 Biomass Gasification

Biomass gasifiers are not commercial for the scale and type of application considered in this analysis, but there is a worldwide transition underway in the fossil fuel sectors toward gasification—a transition that is so far confined mainly to petroleum refining/chemical process industries for the co-production of chemicals and electricity [60 GW syngas capacity installed worldwide, growing at about 3 GW per year (Simbeck, 2004)]. The cost-cutting experience being accumulated for large-scale fossil-fuel gasification technologies is likely to spill over to gasification-based conversion of any low-grade carbonaceous feedstock, including biomass, so that once biomass gasification technologies are introduced commercially at large-scale, costs and reliability may approach N^{th} plant levels relatively quickly.

While there are no large-scale pressurized biomass gasifiers in commercial operation, development and pilot-plant demonstration efforts with oxygen-blown fluidized bed gasification (the gasification design utilized in our analysis) date to the early-1980s in Sweden (Engstrom *et al*., 1981; Strom *et al*., 1984) and the mid-1980s in the USA (Kosowski *et al*., 1984; Evans *et al*., 1987). Most such efforts were curtailed when world oil prices fell in the late 1980s. With growing interest in hydrogen as an energy carrier, there has been some recent re-assessment of pressurized oxygen-blown gasification (Lau *et al*., 2003). Thus, a not-insignificant knowledge base already exists relating to pressurized oxygen-blown gasification technology.

The ability to efficiently feed a low-density biomass like switchgrass into a pressurized gasifier is important for achieving good overall process conversion efficiencies and lower costs, especially at larger scales. Pressurized biomass feeding is a technology area where additional development is needed. The conventional approach for feeding low-density biomass such as chopped switchgrass against pressure is through use of lock-hoppers. Conventional lock-hopper technology suffers from high consumption of inert pressurizing gas and the associated gas compression work required. A number of efforts have been made to develop alternative feeder systems to address the drawback of lock-hoppers (Wilen and Rautalin, 1993), including rotary types and plug types (screw, piston, and hybrid screw/piston). None of these have been yet proven viable for large-scale commercial operation. Lau, *et al.* (2003) provide the most comprehensive recent review and evaluation of alternative feeder systems for pressurized gasifiers.[4] They conclude that for elevated reactor pressures (> 30 bar) lock-hoppers are the only well-proven option. For these pressures, they are pessimistic about the future feasibility of the plug-type feeder designs, especially for fibrous feedstocks such as bagasse and switchgrass. Nevertheless, they recommend further investigation of one of the piston-type feeder designs they evaluated. They propose double lock-hopper and hybrid lock-hopper/plug concepts that might considerably reduce the consumption of inert gas without significant added cost.

[4] See Appendix B in Lau *et al.* (2003).

3.1.2 Gas Cleanup

Maniatis (2001) and others have identified gas cleanup (especially tar removal or destruction) as the most important area where technological advances are needed in order to facilitate widespread commercialization of gasification-based biomass conversion systems. Different authors report different required contaminant removal levels, but by any measure the tolerance to contaminants of downstream fuels synthesis and advanced power generation processes is low.

3.1.2.1 Tars

Much work has been done on various aspects of tar production and destruction as related to biomass gasification since the 1970s. Several of the more recent and comprehensive review articles on the subject are discussed here.

Milne *et al.* (1998) provide an authoritative review of issues and literature relating to biomass-gasifier tars, their production, their measurement and analysis, their tolerance by end-use devices, and their removal or destruction. The article includes a bibliography of some 400 publications that were reviewed in the course of that work.

Stevens (2001) defines tars as any organic molecule with molecular weight greater than benzene. Raw gas from a circulating fluidized bed gasifier (CFB) without any primary or secondary treatment of tar, typically has a tar concentration in the range of 1 to 15 g/Nm^3. Tar removal (as distinguished from tar cracking) is most commonly done by cooling it to condense the tar into droplets and then removing the droplets much the way particles can be removed (using scrubbers, electrostatic precipitators, etc.). Collected tars can be re-injected into the gasifier, which will cause a portion of them to crack to lighter molecules (a generally desirable result since the energy content of the tars is then largely maintained in the gas). However, it will also cause a portion of the tars to undergo further dehydration and condensation reactions to form highly-aromatic and more-refractory tars (a generally undesirable result).

Devi *et al.* (2003) provide a comprehensive review of tar removal by "primary" treatments, which he defines as those applied inside the gasifier, as contrasted to treatments of tar-laden gas in external reactors. A positive feature of successful primary treatment is the elimination of the cost and added operating complexity with "secondary" (post-gasifier) treatments. The main negative feature of primary treatment is the potential detrimental impact on gas quality (e.g., injection of secondary oxidant may lead to a reduced heating value for the fuel gas). Primary treatments include staging of the gasification process, using catalysts, and using injection of secondary oxidant. The authors conclude that for some applications of the product gas, primary treatment approaches that are already known can provide sufficient tar removal.[5] They indicate that the tar removal requirements for *any* application can be met by a combination of known primary and/or secondary treatments. They indicate that further research is needed before primary treatment alone will be able to meet tar removal requirements for the most stringent applications.

Tars can be cracked using heat alone (thermal cracking) at temperatures > 1200^{o}C, although this is too high a temperature for most biomass applications (wherein ash melting would likely be a

[5] For example, Pan *et al.* (1999) showed in laboratory-scale experiments that injection of secondary air to a fluidized-bed gasifier operating on forestry residues at temperatures above about 840^{o}C decreased tar content in the raw product gas by 90%, which will be sufficient for a number of applications.

problem). With assistance of catalysts, cracking can occur at 750-900^{o}C. Tar cracking can be carried out in the gasifier bed itself. Difficulties with using catalysts in a gasifier can include physical attrition and catalyst deactivation. Based on tests at a Swedish biomass-IGCC demonstration plant in the 1990s (Sydkraft et al., 2001) in situ dolomite catalysts were successful in reducing, though not entirely eliminating tar leaving a pressurized air-blown fluidized-bed gasifier.

Using a separate tar cracker, 95-99% of tars in gas streams at 750-900^{o}C have been cracked using dolomite under laboratory conditions. A proprietary, disposable, non-metallic catalyst, identified as DN34, developed at Battelle Columbus Laboratory (BCL), has been tested in a fluid-bed tar cracking unit operating at 800^{o}C with a feed gas from the pilot-scale (10 tonne per day biomass feed) pyrolytic BCL gasifier in Columbus, Ohio. Tar levels in the gas were reduced from 23 g/m^3 to 1.4 g/m^3. Tar conversion was lower at lower temperatures. The syngas was subsequently run through a wet scrubber, and the resulting tar concentration was reported to be "essentially zero". Metallic tar cracking catalysts, particularly those based on Ni/Co/Mo blends, also have been shown to be effective at tar cracking. They also destroy ammonia (see below). Tar cracking (with metallic or non-metallic catalysts) in continuously operating, full commercial-scale biomass systems has not yet been demonstrated.

Finally, Boerrigter and van der Drift (2004) conclude from a careful evaluation and analysis of tar issues around biomass gasification that the optimum technology for large-scale biomass conversion to fuels and chemicals is entrained flow gasification – essentially the same gasifier design used commercially for modern coal gasification. The high gasification temperatures with the technology ensure complete tar cracking in the gasifier. The authors acknowledge other technology challenges that entrained gasification would bring (feed preparation and feeding, slag handling, etc.), but are more optimistic about the prospects for finding solutions to these issues than solving the problems associated with tar cracking with lower-temperature biomass gasifiers. Interestingly, the Shell Company, which offers one of the leading commercial entrained-flow coal gasifiers, recently announced a partnership with Choren, a German company developing a biomass gasification system for liquid fuels production based on entrained-flow gasification (Shell, 2005).

3.1.2.2 Other Gas Contaminants

Stevens (2001) provides the most recent comprehensive review of the status and future prospects for conditioning of gasified biomass for a range of applications, from those that are relatively tolerant of contaminants in the gas to those that have very stringent gas quality requirements. In addition to tar, his review addresses particulates, alkali compounds, ammonia, and sulfur. Many of the gas conditioning technologies that he mentions are well established commercially in applications other than with biomass gasification. Other of the technologies have been shown to work in small-scale or short-duration tests with gasified biomass, but require scaled-up longer-term testing before they can be considered proven.

Removal of alkali vapors is required upstream of devices on which the vapors would otherwise condense due to low temperatures, and thereby cause deposition and corrosion problems. Condensation of alkali vapors typically begins around 650^{o}C. At temperatures below this, the vapors will condense on particles in the gas stream or simply condense to form fine (<5 micron) solids. Removal of the particles/solids from the gas has been shown to be effective at reducing alkali content to required limits set by downstream equipment. Some work also has been done

on removal of alkali compounds at higher temperatures (650-725^{o}C) using alkali "getters", but additional R&D is needed on this approach.

Stevens also addresses ammonia control. Ammonia forms in most biomass gasifiers from fuel-bound nitrogen. Ammonia production is higher in pressurized gasifiers due to equilibrium considerations and in pyrolytic (indirectly-heated) gasifiers due to the stronger reducing environment. Ammonia removal is required for regulatory, but not generally for technical reasons. Removal will be required where there are strict NO_x emissions regulations. For biomass conversion systems not located in ozone non-attainment areas, ammonia control is unlikely to be needed for regulatory reasons. Complete thermal decomposition of ammonia occurs only at >1000^{o}C, which is above temperatures typical for biomass gasification. At lower temperatures, ammonia has been shown to be destroyed (>90-99%) by dolomite, nickel-based steam reforming catalysts, alumino-silicate catalysts (Qadar *et al.*, 1996), and other tar cracking catalysts at approximately the same temperatures required for tar cracking. Iron-based catalysts also work at somewhat higher temperature (900^{o}C). Such concepts have not been proven for large-scale, continuous operation. Wet scrubbing (with sulfuric acid) is well proven for ammonia removal at low temperatures.

Removal of particles to some extent or other, which Stevens discusses at length, is essential for any biomass conversion system. There are a variety of commercially-established particle removal technologies available. Cyclones are a well-established technology for removing particles at any operating temperature relevant to biomass. Cyclones can remove >90% of particles larger than 5 microns with only a modest pressure drop. Partial removal of 1-5 micron particles is possible. Cyclones are not effective for removal of sub-micron particles. So-called barrier filters can remove particles down to 0.5 micron at elevated temperatures. For removal of smaller particles than this, the pressure drop through such filters is prohibitively high. Ceramic and metallic barrier filters have been tested. In limited-duration tests (170 hours) with hot gas derived from sugarcane bagasse by air-blown pressurized fluidized-bed gasification, ceramic candle filters showed good mechanical integrity. On the other hand ceramic filters have shown some susceptibility to reaction with alkali vapors. Metallic candle filters have successfully undergone longer-duration demonstration (at 350^{o}C) at the Varnamo biomass IGCC plant. Dry electrostatic precipitators (ESP) can operate at 500^{o}C or higher. Wet ESP operate only up to 65^{o}C. ESPs are best suited for large-scale facilities due to physical size and cost scale economies. Venturi wet scrubbers can remove >99.9% of particles larger than 2 microns and 95-99% of particles over 1 micron with pressure drop between 2.5 and 25 kPa.

Sulfur removal is less of a concern with most biomass systems than with coal due to intrinsically low sulfur levels in raw biomass. For gas turbine power generation applications, removal of H_2S from biomass-derived gas generally will not be required because the H_2S will be oxidized to SO_2 in the gas turbine combustor, and the SO_2 concentrations in the exhaust gas will be well below regulated levels (due to intrinsically low sulfur content of biomass). For fuel cell use of biomass gas or for synthesis of many liquid fuels, H_2S can be present only at sub-ppm levels, since the catalysts involved are poisoned by sulfur. Active removal of H_2S from biomass gas will typically be required in these cases. Because most biomass conversion systems considered to date would not require H_2S removal from the gas, sulfur removal is not addressed in any detail in the biomass conversion literature. Others, particularly in the coal field, have addressed H_2S removal. Cicero *et al.* (2003) review both commercially-available sulfur removal technologies (typically operating at low temperatures -- < 100^{o}C), as well as promising advanced systems that

are still under development. These latter systems are generally aiming to remove sulfur at elevated temperatures (250-450°C).

For process designs requiring H_2S removal developed in this work, we utilize commercially established Rectisol™ technology, a low-temperature physical absorption processing that uses methanol as an absorbent. This is discussed further in the next section.

3.1.2.3 CO_2 Removal

Bulk CO_2 removal from syngas streams is required in some of our process designs. We simulate CO_2 removal based on the performance of the commercial Rectisol™ process. A Rectisol process (operating in the range of 20 to 70 bar) can be designed for either separate removal of CO_2 and sulfur species from a gas stream or for co-removal of these species. Separate removal is required when the sulfur is to be converted to elemental sulfur for storage or sale. If co-removed with CO_2, H_2S must either be oxidized (by processing with the CO_2 through a combustor, e.g., in the gas turbine power island) or be co-stored (with the CO_2) underground. (The low sulfur concentrations in raw syngas make feasible the oxidation route when H_2S is co-removed with CO_2.)

Rectisol plants with co-removal of CO_2 and sulfur species use a single absorber column. For separate removal of CO_2 and H_2S, a two-column design is needed, with each species removed in a separate column and recovered separately.

In either design, typically any CO_2 removal rate (up to 100%) can be achieved, and nearly all of the sulfur species can also be removed. Due to the small but finite solubilities of other syngas components (H_2, CO, and CH_4) in methanol, some quantities of these syngas components will be incidentally removed. In a one column design, one may expect a loss rate of 0.3% of the H_2, 1.5% of the CO, and 3% of the CH_4. (In a two column design, the loss rates would be about 50% higher, or 0.45%, 2.25%, and 4.5% respectively.) It is feasible, however, to recover these incidentally removed species at the Rectisol stripping column and recycle them, such that net loss rates are essentially zero.

Some of our plant designs include CO_2 capture at two different places in the process. For such designs, some cost savings can be achieved by utilizing two absorbers with a common solvent regeneration column. (In the regenerator, the acid gases are stripped from the solvent by steam heating, and the solvent is recycled to the absorbers.) Solubilities of acid gases in methanol increase with decreasing temperature, so operating temperatures for good Rectisol performance are relatively low, necessitating a refrigeration plant. Aside from refrigeration, the only electricity consumption for a Rectisol plant comes from pumping solvent. (If incidental syngas components are recovered and recompressed for recycling, then there is additionally compressor power consumption.)

3.1.2.4 Example Gas Conditioning Strategies

Stevens (2001) describes the overall gas conditioning approaches used at several existing biomass-gasification demonstration facilities. For producing clean, cool (35-100°C) fuel gases he describes plants in the Netherlands, the UK, and the USA.

The Amergas power station in Geertruidenberg, Holland, uses a Lurgi circulating fluidized-bed gasifier operating at 850-900°C on waste biomass materials and making gas that is co-fired with

coal in a boiler. This is currently the largest biomass gasification facility in the world (85 MW_{th} gas output, or the equivalent of approximately 700 tonnes per day dry biomass input). The gas conditioning system consists of cyclones for particulate removal, followed by gas cooling (by steam raising) to 200-240^{o}C, followed by bag (fabric) filters for additional particulate removal, followed by wet scrubbers for tar removal and gas cooling. The tars are collected and injected into the gasifier. There is an additional final wet scrubbing for ammonia removal, with the ammonia being re-injected into the gasifier for thermal destruction and reaction with NO_x.

The UK project, called ARBRE, is a biomass-gasifier IGCC (8 MW_e) that is intended to operate on short-rotation woody biomass fuel grown by farmers in the area (Pitcher *et al.*, 1998; Maniatis, 2001). Plant construction was completed and commissioning started in 2002, but the plant is not yet operating due to ownership uncertainties. The gasifier is an air-blown, atmospheric-pressure circulating fluidized-bed designed by the Swedish company, TPS. After bed solids are captured (via cyclone) for recycle, the raw product gas passes to a high-temperature fluidized-bed tar cracker that uses dolomite as a catalyst. The cracker is followed by a syngas cooler generating steam. The warm gas (350^{o}C) then passes through fabric filters for capture of particles and condensed alkali. Finally, wet scrubbing with dilute H_2SO_4 (sulfuric acid) is used as the final conditioning to remove particles, residual tars, and ammonia.

The USA project is located in Burlington, Vermont. It consists of a FERCO/Battelle indirectly-heated (pyrolytic) gasifier with a capacity to gasify 200 dry tonnes per day of forest residues. The pyrolytic gases leave the gasifier at about 800^{o}C and are passed through a cyclone for bulk particle removal and then sent at elevated temperature to be burned in an existing boiler. The plan (which has not yet been put into effect) is to install a catalytic tar cracker following the cyclone, pass the cracked gas through a syngas cooler to raise some steam, and then use a fabric filter and wet scrubbing to remove remaining particles, tars, and ammonia. The proposed catalyst for tar cracking is DN34, mentioned earlier.

Stevens also describes the overall gas conditioning strategy for producing warm (200-500^{o}C) or hot (> 500^{o}C) clean fuel gases. He cites the Varnamo project in Sweden where this strategy was pursued with success. The Varnamo facility included a pressurized air-blown gasifier with limestone or dolomite bed material to provide partial tar cracking. The resulting tar level in the gas was about 5 g/Nm^3. By insulating downstream pipes/filters to keep the gas temperature above ~350^{o}C, tar condensation was prevented. Bulk particulate removal was effected with a primary cyclone, which was followed by a syngas cooler generating steam and dropping the gas temperature to about 350^{o}C. A barrier filter operating at this temperature provided the final contaminant removal step. Ceramic candle filters were initially tested, but subsequently metallic candle filters were found to have more satisfactory performance.

3.1.2.5 Gas Conditioning for Ultra Clean Applications

For fuel cell and liquid fuels synthesis applications (e.g., production of dimethyl ether or Fischer-Tropsch liquids), gas contaminant levels, including sulfur, generally must be considerably lower than for gas turbine applications. There is considerably less analysis or empirical results published on biomass-related gas conditioning issues for such ultra clean applications. Dayton (2001) reviews gas quality requirements relating to particulates, sulfur, ammonia, halogens (e.g., hydrochloric acid), and alkali metals for different fuel cell designs (proton exchange membrane, phosphoric acid, molten carbonate, and solid oxide). For synthesis of liquid fuels, Graham and Bain (1993), as cited by Stevens (2001), define gas quality requirements for syngas to be used

for fuels synthesis. Nitrogen-dilution of the gas is unacceptable due primarily to the increased costs associated with the higher volumetric flow of gas that would need to be processed. Pressurized gasification is preferred since synthesis processes are favored by higher pressures. Particle loading in the clean synthesis gas must be <0.02 mg/Nm^3. Tar loading in the clean gas must be < 0.1 mg/Nm^3. Sulfur loading in the syngas must be < 0.1 mg/Nm^3.

3.2 Conversion of Synthesis Gas to Final Products

There is considerable commercial activity relating to conversion of synthesis gas to liquid fuels and to hydrogen. With a few important exceptions (discussed below), in most such commercial facilities, the synthesis gas is produced from natural gas.

The conversion of clean synthesis gas to liquid fuels, including F-T fuels and DME, involves passing the gas over catalysts that promote the desired synthesis reactions. These reactions are exothermic, and the reactor temperature will increase as the reactions proceed if no heat is removed. Higher temperatures promote faster reactions, but maximum conversion is favored by lower temperatures. Also, catalysts are deactivated when overheated. Thus, the temperature rise in a synthesis reactor must be controlled. In practice, a reactor operating temperature of 250-280^{o}C balances kinetic, equilibrium, and catalyst activity considerations.

Two available synthesis reactor designs, gas-phase (or fixed-bed) and liquid-phase (or slurry-reactor), handle temperature control using different approaches. The basic gas-phase design involves the flow of syngas over a fixed-bed of catalyst pellets. The basic liquid-phase design involves bubbling syngas through an inert mineral oil containing powdered catalyst in suspension.

In a gas-phase reactor it is difficult to maintain isothermal conditions by direct heat exchange (due to low gas-phase heat transfer coefficients). To limit temperature rise, the synthesis reactions are staged, with cooling between reactor stages. Also, by limiting the initial concentration of CO entering the reactor (to 10-15 vol%) the extent of the exothermic reactions can be controlled. Control of the CO fraction is achieved in practice by maintaining a sufficiently high recycle of unconverted H_2-rich syngas back to the reactor.

In a liquid phase reactor, the feed gas is bubbled through an inert oil in which catalyst particles are suspended (Figure 6). Much higher heat release rates (i.e., extents of reaction) can be accommodated without excessive temperature rise as compared to a gas-phase reactor because of more effective reactor cooling by boiler tubes immersed in the fluid. The vigorous mixing, intimate gas-catalyst contact, and uniform temperature distribution enable a high conversion of feed gas to liquids in a relatively small reactor volume. Conversion by liquid-phase F-T synthesis is especially high – achieving a single-pass fractional conversion of CO to F-T liquids of about 80% (Bechtel Group, 1990). This compares to less than 40% conversion with traditional fixed-bed F-T reactors.

High single-pass conversion rates make liquid-phase reactors especially attractive from an overall cost perspective for co-production process designs (Larson and Ren, 2003), whereby the synthesis gas is passed once through the synthesis reactor, and any unconverted gas is used to generate co-product electricity for sale (e.g., Figure 3, upper). Liquid-phase reactors are commercially available for F-T synthesis. They have been demonstrated at pilot scale for DME

synthesis (and at commercial scale for methanol synthesis, a catalytic process closely related to DME synthesis). In our work, we have examined both "once-through" and recycle synthesis configurations for producing DME, but given the very high single-pass conversion achievable with F-T synthesis, we have chosen to consider only once-through configurations for F-T synthesis.

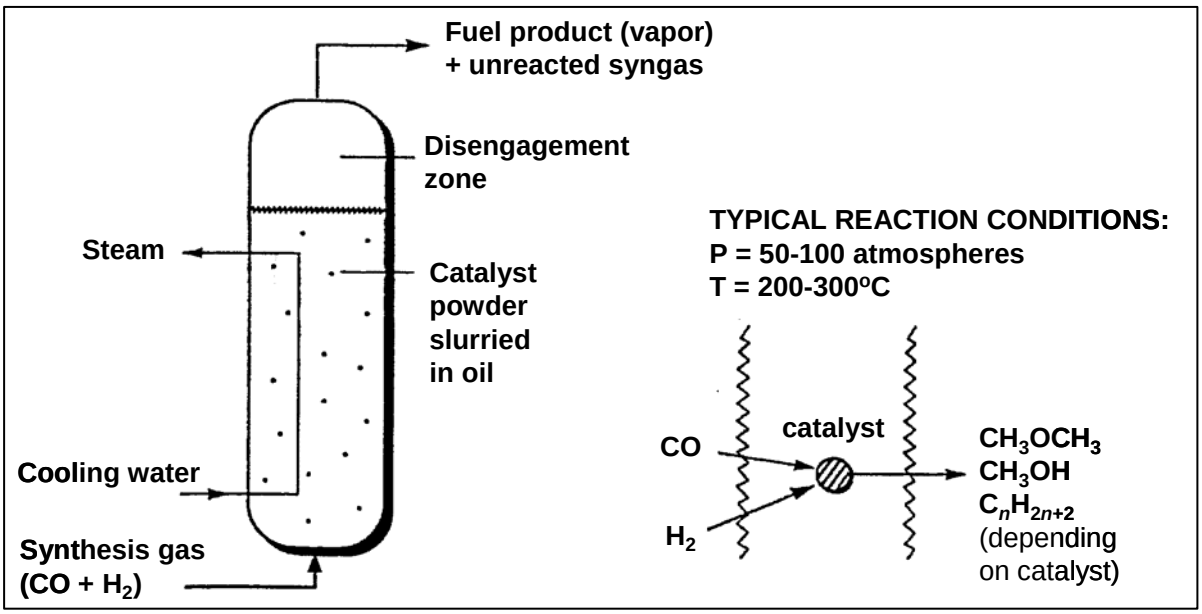

Figure 6. Simplified depiction of a liquid-phase synthesis reactors, which yield higher one-pass conversion of ($CO+H_2$) to liquids than traditional gas-phase reactors.

3.2.1 Synthesis of Fischer-Tropsch Fuels

Fischer-Tropsch conversion was first done commercially, based on gas-phase technology, in the 1930s when Germany started producing F-T liquids from coal syngas as vehicle fuel (Dry, 2002). A coal-to-fuels program has been operating in South Africa since the early 1950s. Starting in the 1990s, there has been renewed interest globally in F-T synthesis to produce liquids from large reserves of remote "stranded" natural gas that has little or no value because of its distance from markets (Oukaci, 2002; Rahmim, 2003). Of particular interest is the production of middle distillate fuels (diesel-like fuels) with unusually high cetane numbers and containing little or no sulfur or aromatics. Such fuels (derived by natural gas F-T conversion) are now beginning to be blended with conventional diesel fuels, e.g., in California, to meet increasingly strict vehicle fuel specifications designed to reduce tailpipe emissions.

In addition to Shell's well-known gas-to-liquids (GTL, used synonymously with gas-to-FT liquids) plant (using gas-phase synthesis technology) in Malaysia that has been operating for nearly a decade, there are additional large commercial GTL facilities under construction or at advanced planning stages, including:

- 34,000 barrels/day plant, Qatar Petroleum project that will use Sasol liquid-phase synthesis technology; slated to come on line in 2005.
- 34,000 b/d, Chevron project in Nigeria, also using Sasol FT technology; to come on line by 2006

- 140,000 b/d, Shell project in Qatar, using Shell's gas-phase FT technology; to come on line in 2009
- 154,000 b/d ExxonMobil project in Qatar, using ExxonMobil liquid-phase technology; to come on line in 2011

There is also a growing resurgence of interest in production of F-T fuels from gasified coal. Coal-based FT fuel production was commercialized beginning with the Sasol I, II, and III plants (175,000 b/d total capacity) built between 1956 and 1982 in South Africa. (Sasol I is now retired). In the U.S., a major assessment was recently completed for the U.S. Department of Energy on co-production of F-T liquids and electricity from coal via gasification at large scales (Bechtel *et al*. 2003a; 2003b), and the U.S. Department of Energy is cost-sharing a $0.6 billion demonstration project in Gilberton, Pennsylvania, that will make from coal wastes 5,000 b/d of F-T liquids using liquid-phase synthesis and 41 MW_e of electricity. Also, there are proposals for 33,000 b/d and 57,000 b/d facilities for FT fuels production from coal in the state of Wyoming. China's first commercial coal-FT project is under construction by the Shenhua Group in Inner Mongolia. The plant is slated to produce 1 million tonnes of oil products/year (20,000 barrels/day or 0.3 billion gallons per year) when it comes on line in 2007. China has also signed a letter of intent with Sasol for two coal-FT plants that will produce together 6 million tonnes of liquid fuels per year (120,000 b/d). Prefeasibility analysis is ongoing for these plants. The projected capital investment required for these plants is a total of $6 billion. Meanwhile, Chinese researchers have been developing pilot-scale slurry phase FT synthesis technology for coal-derived syngas (e.g., Li *et al.*, 2001; Yang *et al.*, 2003).

The process for converting biomass into F-T liquids is similar in many respects to that for converting coal. Preliminary technical/economic analyses on biomass conversion was published by Larson and Jin (1999a and 1999b). More recently, there have been several detailed technical and economic assessments published (Bechtel, 1998; Tijmensen, 2000; Tijmensen *et al.*, 2002; Hamelinck *et al.*, 2003; Boerrigter and van der Drift, 2003; Hamelinck *et al.*, 2004). There is considerable current interest in Europe in production of FT fuels from biomass, motivated by large financial incentives. For example, in the UK a 20 pence per liter ($1.40/gal) incentive for biomass-derived diesel fuel has been in place since July 2002. Incentives are also in place in Germany, Spain, and Sweden. Such incentives have been introduced in part as a result of European Union Directive 2003/30/EC, which requires all member states to have 2% of all petrol and diesel consumption (on an energy basis) be from biofuels or other renewable fuels by the end of 2005, reaching 5.75% by the end of 2010.

3.2.2 Synthesis of Dimethyl Ether

The leading commercial developer of fixed-bed DME synthesis reactor designs is Halder-Topsoe.[6] Mobil and Snamprogetti S.p.A. hold patents for DME synthesis processes (Zahner, 1977; Pagani, 1978), but at present are not pursuing commercial development of the technology. Leading private developers of slurry-bed DME synthesis reactors are Air Products and Chemicals, Inc. (APCI) (Lewnard *et al.*, 1990; Brown *et al.*, 1991; Lewnard *et al.*, 1993; Air Products and Chemicals, 1993; Peng *et al.*, 1999a; Peng *et al.*, 1999b) and the NKK Corporation

[6] The fixed-bed design of Halder-Topsoe includes three stages of synthesis reactors with cooling between each stage and recycle of unconverted syngas (Hansen et al., 1995). The patent for this process specifies a feed gas CO concentration of less than 10% and a recycle volume of unconverted syngas ranging from 93% to 98% of the total unconverted syngas (Voss et al., 1999). The fraction of CO converted on a single pass through each reactor stage (assuming a three-stage intercooled set of reactors) ranges from 16% to 34%, depending on the H_2/CO ratio.

(Adachi *et al.*, 2000; Fujimoto *et al.*, 1995). The Institute of Coal Chemistry of the Chinese Academy of Sciences (CAS) (Niu, 2000) has also been developing slurry-phase DME synthesis technology since 1995. The CAS Institute of Chemical Physics (Dalian) has done some work on fixed-bed DME synthesis technology (Xu *et al.*, 2001).

The DME reactor design of APCI is derived from its liquid-phase methanol (LPMEOH) synthesis process that was developed in the 1980s. A commercial-scale LPMEOH demonstration plant (250 tonnes per day methanol capacity) has been operating since 1997 with gas produced by the Eastman Chemical Company's coal gasification facility in Kingsport, Tennessee (Eastman Chemical and Air Products and Chemicals, 2003). The construction of this facility was preceded by extensive testing in a 10 tpd capacity process development unit (PDU) in LaPorte, Texas. The PDU was operated in 1999 to generate test data on direct DME synthesis (Air Products and Chemicals, 2001 and 2002).

DME Development, Inc., a Japanese consortium of nine companies led by NKK and Nippon Sanso, is currently in the design/build stage for a 100 tpd DME slurry-phase reactor planned for testing during 2004-2006 in Kushiro, Hokkaido. This effort builds on initial testing of a five ton per day capacity reactor that was completed in 1999 by NKK (2003), who prior to that (with support from the Japanese Ministry of International Trade and Industry) worked with the Taiheiyo Coal Mining Co., Sumitomo Metal Industries, and Japan's Center for Coal Utilization to develop the DME slurry reactor technology, with coal applications in mind. There is interest in commercial DME from coal in China (Lucas, 2002).

In addition to the emerging industry making FT fuels from fossil fuels, there is also an emerging industry making DME from fossil fuels for energy applications. (There is already a small amount of DME produced by dehydration of methanol – about 150,000 tonnes per year globally – for use as aerosol propellants and in other chemicals applications.) The initial energy market for DME is primarily as an LPG substitute. Construction of a plant for natural gas conversion to DME (110,000 t/yr production capacity) will be completed in 2005 in Sichuan Province, China. Toyo Engineering (Japan) is managing the construction effort. An 800,000 tons per year DME-from-gas facility will come on line in Iran in 2006 using Halder Topsoe DME synthesis technology. At least one large coal-to-DME facility is also in the works: China's State Development Planning Commission approved plans in 2002 for a plant to be built in Ningxia, one of China's coal-rich provinces. The first phase of the project would build 210,000 tons per year of capacity. A second phase would add 630,000 tons per year. Construction has not yet started.

3.2.3 Hydrogen Production

Technology for production of hydrogen from syngas is well established commercially (Chiesa et al., 2005; Kreutz *et al.*, 2005), with applications found most commonly in petroleum refining and ammonia production. Globally, natural gas is the most commonly used feedstock to make syngas for hydrogen production, but in China the predominant feedstock is coal.

4 Detailed Process Descriptions and Mass/Energy Balances

In this section we present detailed descriptions of 13 process designs developed in this work (Table 2). Table 3 summarizes the mass and energy balances, discussed in detail below, for each of these designs as developed from Aspen-Plus simulations. The Technical Appendix (available

on request) provides detailed information regarding our Aspen-Plus simulations and input parameter values.

Table 3. Summary of mass and energy balances for all process designs examined in this work.

	DME + Electricity					FT+Elec		Electricity Only		Hydrogen			
	OT-VENT	OT-UCAP	OT-DCAP	RC-VENT	RC-UCAP	OT VENT	OT UCAP	B-IGCC VENT	B-IGCC CCS	H-5050 VENT	H-MAX VENT	H-5050 CCS	H-MAX CCS
Biomass input (20% moisture), MW_{th} (HHV)	983	983	983	983	983	983	983	983	983	983	983	983	983
Biomass input (20% moisture), MW_{th} (LHV)	893	893	893	893	893	893	893	893	893	893	893	893	893
Biomass input, tC/hr	88.9	88.9	88.9	88.9	88.9	88.9	88.9	88.9	88.9	88.9	88.9	88.9	88.9
ENERGY BALANCE													
Internal power use, MW_e													
Air separation unit	-8.48	-6.68	-6.68	-7.54	-6.82	-8.48	-6.81	-5.76	-5.64	-8.48	20.68	-8.48	20.68
Oxygen Compressor	5.44	5.44	5.44	5.44	5.44	5.44	5.44	5.31	5.36	5.44	7.26	5.44	7.26
Nitrogen Compressor (Expander)	-2.57	11.2	11.2	5.40	13.4	-2.57	13.23	11.14	10.93	-2.57	0	-2.57	
Biomass handling and preparation	0.66	0.66	0.66	0.66	0.66	0.66	0.66	0.66	0.66	0.66	0.66	0.66	0.66
Lock-hopper	0.52	0.52	0.52	0.52	0.52	0.52	0.52	0.52	0.52	0.52	0.52	0.52	0.52
CO_2 removal	2.19	2.19	2.19	2.19	2.19	2.18	2.19		3.84	1.83	3.82	3.82	3.82
CO_2 compression	11.7	16.9	26.3	12.5	18.2	12.5	18.2		31.79	6.51	1.38	31.66	31.71
Syngas compressor	11.6	11.7	11.7	11.4	11.4	0.0	0.0						
Refrigeration	3.01	3.54	5.02	2.76	2.76	2.41	2.42		3.05	1.49	3.04	3.05	3.04
Syngas expansion	-1.68	-1.69	-1.69	-12.11	-12.07								
Recycle Compressor				41.79	41.66								
FT upgrading area						6.03	6.03						
PSA purge gas compressor										3.39	7.27	2.96	7.24
Hydrogen compressor										4.43	9.74	4.59	9.77
Other auxiliary power uses[a]	3.00	2.87	4.23	1.95	2.21	2.29	2.15	3.48	3.48	3.18	2.95	2.83	3.37
Total internal power use, MW_e	25.4	46.7	58.8	65.0	79.5	21.0	44.0	15.3	54.0	16.4	57.3	44.5	88.1
Gas turbine gross output, MW_e	150.7	164.0	156.6	53.3	56.4	86.69	99.40	267.5	241.6	166.6	0	138.9	0
Steam turbine gross output, MW_e	144.2	139.3	131.4	90.5	90.5	140.90	135.44	190.3	164.0	131.1	98.56	123.3	97.73
Net power output, MW_e	269.6	256.6	229.2	78.8	67.3	206.6	190.8	442.4	351.6	281.4	41.2	217.7	9.7
H2 output, MW (HHV)										283.5	621.9	294.0	623.9
H2 output, MW (LHV)										239.9	526.2	248.8	527.8
F-T Gasoline output, MW (HHV)						128.5	128.8						
F-T Gasoline output, MW (LHV)						116.9	117.2						
F-T Diesel output, MW (HHV)						200.8	201.3						
F-T Diesel output, MW (LHV)						188.1	188.6						
DME output, MWth (HHV)	238.8	239.5	239.6	514.0	515.9								
DME output, MW_{th} (LHV)	217.2	217.9	217.9	467.5	469.3								
Liquid output, barrels diesel-equivalent per day	3357	3368	3368	7226	7253	4630	4641						
Electric efficiency, % of biomass LHV	30.2%	28.7%	25.7%	8.8%	7.5%	23.1%	21.4%	49.5%	39.4%	31.5%	4.6%	24.4%	1.1%
Fuels efficiency, % of biomass LHV	24.3%	24.4%	24.4%	52.3%	52.5%	34.1%	34.2%			26.9%	58.9%	27.8%	59.1%
Total efficiency, % of biomass LHV	54.5%	53.1%	50.0%	61.1%	60.1%	57.3%	55.6%	49.5%	39.4%	58.3%	63.5%	52.2%	60.2%
Fuels effective efficiency (LHV basis)	62.2%	58.1%	70.1%	63.7%	62.0%	64.1%	60.2%			73.8%	64.9%	54.8%	60.4%
CARBON BALANCE													
Total captured CO2, t/h	0	150	240	0	162	0	162	0	294	0	0	293	293
Total captured C02, tC/h	0	41	66	0	44	0	44	0	80	0	0	80	80
Captured at upstream AGR, % of biomass C	0%	46%	46%	0%	50%	0%	50%			0%	0%	0%	0%
Captured downstream of synthesis, % of biomass C	0%	0%	28%	0%	0%	0%	0%		90%	0%	0%	90%	90%
Vented to atmosphere, % of biomass C	84%	38%	10%	66%	16%	75%	26%	100%	10%	100%	100%	10%	10%
Carried in Fuel product, % of biomass C	16%	16%	16%	34%	34%	25%	25%			0%	0%	0%	0%
Total	100%	100%	100%	100%	100%	100%	100%	100%	100%	100%	100%	100%	100%
Total carbon captured, % of biomass C	0%	46%	74%	0%	50%	0%	50%	0%	90%	0%	0%	90%	90%

4.1 Producing Clean Synthesis Gas

The upstream design for producing synthesis gas is largely the same for all of our process designs. Switchgrass is transported from a short-term storage area to the feed preparation area, where it is chopped for feeding to the gasifier. The feeder model adopted in our simulation assumes successful development of double lock-hopper or hybrid lock-hopper/plug-feed concepts that would considerably reduce the consumption of inert gas without significant added cost (Lau et al., 2003). Nitrogen (98.5% purity) is available at low pressure from the air separation unit (ASU), and in some of the process designs is used to pressurize the biomass feeding system. (CO_2 is used for this purpose in other designs.)

The gasifier in all cases is a pressurized (29.9 bar) oxygen-blown fluidized bed reactor. We have modeled the gasifier based on empirical data for pilot-plant operation of the gasifier design of the Gas Technology Institute[7,8] (Katofsky, 1993; OPPA, 1990). Switchgrass is injected near the bottom of the reactor together with 0.61 m^3/s of oxygen (95% purity) and 0.90 m^3/s of steam.[9]

[7] The license for the Gas Technology Institute (GTI) technology is currently owned by Carbona.

The gasifier produces a mix of light combustible gases, unconverted carbon (char), ash, heavy hydrocarbons (condensable tars and oils), and small amounts of hydrogen sulfide, ammonia, alkali compounds, and other gaseous polar impurities. A cyclone separates the gas from entrained ash and unconverted char, and the latter is recirculated to the gasifier, where the char is assumed to be ultimately completely consumed. Ash is removed from the bottom of the gasifier. (Heat is not recovered from the ash, but if a viable means for doing so were available, overall plant efficiency could be increased modestly.)

We simulate the cracking of tars and oils to light gases as either a one or two-step process, depending on the downstream requirements for syngas cleanliness. In the first step, a small amount of oxygen is injected into the freeboard of the gasifier (above the bubbling fluidized bed) to promote cracking of the tars and oils to lighter molecules. The literature suggests that 90% conversion of tars and oils to CO and H_2 can be achieved by this oxygen injection (Pan et al., 1999). The heat released in these reactions raises the temperature of the raw syngas to about 1000^{o}C as it leaves the gasifier. A fusion temperature for switchgrass ash (under oxidizing conditions) of 1016^{o}C has been reported in the literature (McLaughlin et al., 1999). If this temperature is also representative for reducing conditions (gasification), then it may be necessary to introduce an additive in the gasifier bed material to suppress ash fusion. Additives have been demonstrated to be able to raise ash fusion temperatures in biomass combustors (Steenari and Lindqvist, 1998; Ohman and Nordin, 2000).

After the gasifier (in some of our designs) we include an external catalytic tar cracker to ensure that all tars are converted to light gases. This reactor is assumed to operate adiabatically. The heat needed to drive the endothermic cracking reactions is drawn from the gas itself, resulting in an exit gas temperature of about 800^{o}C. The Technical Appendix (available on request) describes the details of our tar cracking model.

The gas is subsequently cooled to 350^{o}C in a syngas cooler, a vertical fire-tube design (hot gas inside the tubes) that minimizes deposition of small particles still in the gas, as well as of alkali species that condense during cooling. Subsequent particle removal by a barrier filter (ceramic or sintered metal) is carried out at 350^{o}C. [An alternative approach to particle filtration might be to use a baghouse filter. However, baghouse filters generally operate at lower temperatures (<200^{o}C) and pressures (< 4.5 bar), so are not suitable for the systems considered here.] At 350^{o}C, any residual tar or other impurities remain as vapor. Whether and how these components

---

[8] Since biomass gasification is a kinetically controlled process, and kinetic parameters values are not well known, we have developed an approach to modeling biomass gasifier heat and mass balances that relies on empirical data. We use a combination of Aspen reactor modules. Since Aspen Plus is not able to model solid biomass explicitly, we first convert the biomass into fictional components using Aspen's RYIELD reactor. There, the biomass is converted into gaseous H_2, O_2, N_2, H_2O, S, and solid C, as well as ash. These components, together with some 98.5% pure nitrogen (used for feeder pressurization), some 95% pure oxygen, and some steam are fed to an RGIBBS reactor. The steam input rate is set to simulate the overall dry biomass-to-moisture input ratio indicated in empirical data and the oxygen rate is set to achieve a target reactor temperature (1003^{o}C). We allow the RGIBBS module to calculate a product composition at chemical equilibrium, subject to the following constraints: we specify the output of tar (modeled as abietic acid, $C_{20}H_{30}O_2$) to be 1% by weight of the dry biomass, and we specify the following volume fractions in the product gas based on empirical data: CH_4 (8.2%), C_2H_4 (0.15%) and C_2H_6 (0.15%). We assume 1% of the biomass higher heating value is heat loss. Following the RGIBBS reactor, an RSTOIC reactor is used to adjust the product H_2/CO ratio to be 0.72 to match empirical data.

[9] Unless otherwise noted, all volumetric gas flows are expressed in this paper in terms of actual volume (not at standard or normal conditions).

are removed depends on what downstream processing of the gas is to be undertaken. Our calculated "cold gas efficiency" (chemical energy in the cleaned syngas divided by energy in the input switchgrass), is 79.8% on a lower heating value basis (or 79.1% on HHV basis).

All 13 process designs that we have developed share all of the features described above. The processing of the syngas from this point on varies depending on the products being made.

4.2 Stand-Alone Electricity Production

4.2.1 Electricity Production with No Carbon Capture and Storage

The detailed process configuration and mass and energy balance for the stand-alone electricity production design without carbon capture and storage, BIGCC-VENT, is shown in Figure 7. The raw synthesis gas leaves the gasifier at about 1000°C. Because the syngas is maintained at elevated temperatures until it is burned in the gas turbine, the external tar cracking step (described above) is not needed for this design. The raw syngas is cooled to 350°C and passes through the particle filter before being delivered to the gas turbine generator.[10]

An air separation unit (ASU) produces oxygen [95% (volume) purity] for the gasifier. In the BIGCC-VENT design, the ASU is integrated with the gas turbine, as contrasted with a stand-alone ASU. A stand-alone design takes ambient air and compresses it in a dedicated air compressor. Product oxygen and nitrogen are further compressed after the ASU to required pressures. An integrated ASU takes pressurized air from the gas turbine compressor and delivers oxygen and nitrogen at slightly higher pressure than a stand-alone ASU. Because of the integration, operating pressures within an integrated ASU are higher than for a stand-alone unit (the air compressor for a stand-alone ASU will typically deliver 6 bar air, whereas the gas turbine compressor delivers 19 bar air). This reduces the size of the "cold box" equipment and reduces the need for post-ASU compression of the oxygen and nitrogen. Moreover, the integrated ASU itself actually produces some electricity (5.8 MW_e in this design, Table 3) by partial expansion of some pressurized flows within the ASU.[11]

Removing air at the exit of the gas turbine compressor for delivery to the ASU disturbs the mass balance between the gas turbine compressor and expander. This is corrected by returning to the turbine through several streams most of the air sent to the ASU. The nitrogen leaving the ASU (98.5% purity) is pressurized in a two-stage intercooled compressor and returned to the gas turbine combustor. Also, the nitrogen used to pressurize the gasifier feeder returns as a

[10] Any ammonia in the gas will be carried to the gas turbine combustor, where it will form NO_x. NO_x emissions may exceed the levels allowed in geographic regions where NO_x is regulated, e.g., many urban areas. Most biomass power plants are likely to be located in rural areas, however, where NO_x regulations are less stringent. If control of NO_x emissions is needed, ammonia can be removed at high temperature by placing a catalytic ammonia decomposition reactor between the gasifier and the syngas cooler (Stevens, 2001). The unit decomposes NH_3 into N_2 and H_2. The pressure drop through the reactor would reduce only slightly the overall system efficiency.

[11] Within the ASU area, the pressurized air is first cleaned to remove CO_2 and moisture in a molecular sieve unit, and then passes to the "cold box", where distillation takes place at low temperature. Input air is cooled against cold product streams by heat exchange. A cryogenic expander further cools the air by Joule-Thompson cooling. Liquefied air is separated into purified oxygen and nitrogen streams (and argon if desired) in cryogenic distillation towers. The high pressure tower reduces the nitrogen content of the oxygen, allowing pure oxygen to be drawn from the bottom of the low pressure tower. Waste nitrogen is removed from the top of the low pressure column to purge the molecular sieve and for other uses as needed. Liquid products may also be drawn directly from the columns. The Technical Appendix (available on request) provides additional details.

component of the syngas, as does the oxygen supplied to the gasifier. Only a small amount of nitrogen (accounting for roughly 25% by mass of the input air to the ASU) is used internally in the ASU and purged to the atmosphere.

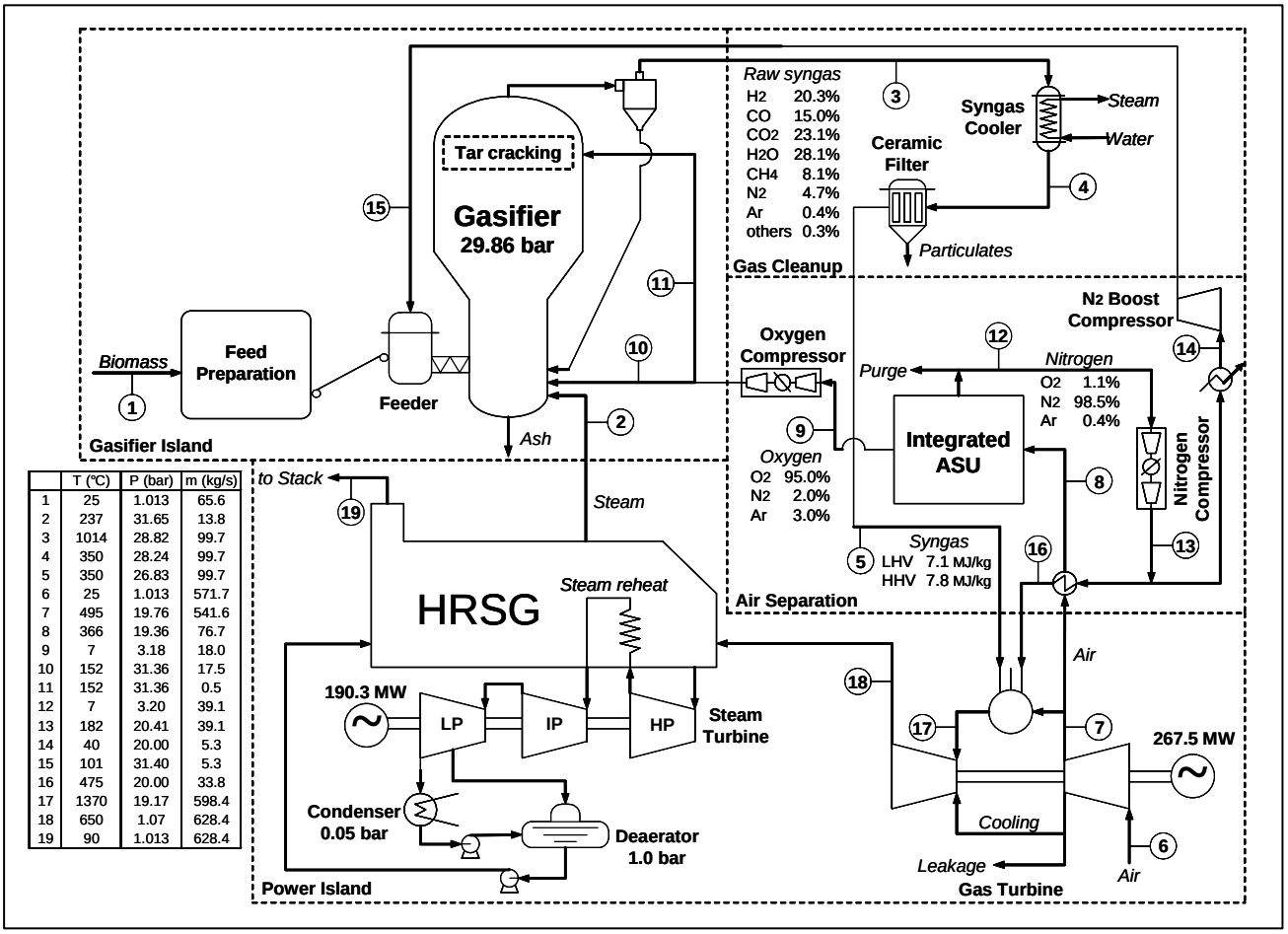

Figure 7. Detailed energy and mass balance for power generation from biomass without carbon capture and storage (BIGCC-VENT case).

An important additional reason for returning nitrogen to the gas turbine combustor is for control of thermal NO_x emissions. The latter are controlled by diluting the gas turbine fuel gas with N_2 (or with H_2O or CO_2 in some cases). For simulation purposes, the dilution rate is controlled such that the adiabatic flame temperature in the gas turbine combustor does not exceed 2300 K.[12]

The net power generating efficiency of a BIGCC system with an integrated ASU will not be significantly different from one with a stand-alone ASU. The power output of the gas turbine itself is lower with the integrated ASU arrangement (due to reduced mass flows through the gas turbine expander), compensating for the reduced auxiliary power consumption compared with a stand-alone ASU (including required compression of air, N_2, and O_2 streams). However, an integrated ASU should decrease the net cost of power generation (due to decreased capital cost) compared to a case with a stand-alone ASU (Smith *et al.*, 1997).

[12] S. Consonni, Department of Energetics, Politecnico di Milano, Italy, personal communication, 2004.

The power island consists of a gas turbine/steam turbine combined cycle and associated generator, piping, ducting, and auxiliary equipment. The gas turbine performance is based on that for a General Electric MS7001FB turbine firing natural gas (Table 4). The "7FB" is in the class of most-advanced gas turbines currently in commercial use with natural gas firing. (Historically, natural gas-fired gas turbine performance has improved steadily over time, so some future improvements can be expected before systems described in this report are commercially implemented. On the other hand, 7FB-class technology is not commercially mature for syngas firing, so assuming that future syngas-fired turbines achieve performance comparable to that of today natural gas-fired turbines may be a reasonable estimate for N^{th} plant systems.) To simulate the performance of the 7FB, we first matched the performance of the 7FB on natural gas quoted by the manufacturer by tuning the expander and compressor efficiencies to match power output and overall thermal efficiency for a fixed natural gas fuel rate and turbine inlet pressure. (We also fixed values of some other parameters, as shown in Table 4.)

To simulate the performance of the gas turbine firing syngas, which has a considerably lower volumetric heating content than natural gas, we assume that the turbine inlet temperature (TIT) with syngas will be the same as with natural gas (Larson et al., 2003).[13] We also assumed that the turbine expander operates with a "choked" flow condition at its inlet. Under this condition, the mass flow into the expander cannot be increased (as would be required since a higher mass flow of fuel is required in the turbine combustor to achieve the same energy input as with natural gas firing) without increasing the pressure upstream of the inlet, i.e. raising the compressor pressure ratio and/or lowering the flow rate of combustion air. We increased the compression ratio over the quoted value for a natural gas machine by about 5%, a percentage increase that is within the range typically tolerated by compressors of heavy-duty gas turbines. Table 4 shows the resulting performance prediction for the gas turbine.

Finally, in our BIGCC and all other simulations involving a gas turbine, we assume the turbine is a "rubber" gas turbine, i.e., the unit performance characteristics based on our 7FB simulation are achieved regardless of the scale of the turbine.[14]

The hot exhaust from the gas turbine enters the HRSG, where it cools to 90°C and is vented to the atmosphere. (Lower exhaust temperatures would enable greater steam production for power generation, but may cause corrosion problems from formation of sulfuric or other acids.) The steam generated at the syngas cooler is integrated into the HRSG output. The HRSG produces steam at 160 bar to drive a steam turbine and a small amount of steam at 31.65 bar for injection

[13] Due to the different flow rate and thermo-physical properties of syngas with respect to natural gas, maintaining the same TIT as with the natural-gas version implies higher temperatures throughout the expansion and thus - everything else equal - higher blade metal temperatures and shorter lifetime for the hot parts of the engine. Running a syngas-fired gas turbine at the same TIT as rated for natural gas implies an increase in blade metal temperatures of 20-25°C (when the ambient temperature is 20°C) and an increase in turbine outlet temperature (TOT) of 10-20°C (Larson et al, 2003). This is why syngas-fired gas turbines today are typically de-rated (TIT lower by 20-30°C) to match the lifetime and reliability of natural gas-fired versions. However, by the time the Nth BIGCC plant is realized in practice, TIT and TOT of state-of-the-art gas turbines will be significantly higher than those adopted today, so our assumption of TIT equal to today's TIT with natural gas firing is reasonable.

[14] In practice, gas turbines are available commercially only in discrete capacities. By assuming a "rubber" turbine in our simulations we avoid complications involved in modeling any specific commercial gas turbines. Adding such complications would give somewhat more precise results, but the conclusions we draw in this report regarding overall system performance would not be materially different.

into the gasifier. Steam for expansion is produced at only one pressure level because there is insufficient low-grade waste heat available to produce intermediate or low pressure steam.

After expanding through the first stage of the steam turbine, the steam is reheated before passing to the second expansion stage. Steam leaving the turbine is condensed and the resulting water is pumped to modest pressure (1.5 bar) before traveling to the deaerator, after which it is further pressurized and returned to the HRSG. A bleed of steam from a low-pressure stage of the turbine is used for deaerator heating.

An important design consideration for maximizing the energy efficiency of the overall process is effective heat integration, whereby heat from various process streams that require cooling is transferred to others that require heating. To provide a consistent basis for optimal heat integration within practical constraints, we have carried out a pinch analysis (Linnhoff, 1993) for each of our process designs. The temperature and mass flows of all process streams requiring heating and all process streams requiring cooling are used as inputs to this analysis.[15] The pinch methodology matches streams that need heating with those that need cooling, taking into account the practical issues of having enough temperature difference between streams for effective heat transfer. After meeting all process heating needs, any remaining process waste heat is used to boost steam production in the HRSG. (Some process waste heat is at too low a temperature to generate useful steam. Such heat is rejected to cooling water.)

As summarized in Table 3, the simulated net power output for the BIGCC-VENT design is 442 MW_e, and the electricity-from-switchgrass efficiency is 45.0% on a higher heating value (HHV) basis or 49.5% on a lower heating value (LHV) basis. This efficiency is higher than found in many other studies for BIGCC systems – a result that is consistent with assumptions here of a large facility based on advanced N^{th} plant technology.

4.2.2 Electricity Production with Carbon Capture and Storage

Our system design for stand-alone production of electricity with carbon capture and storage (BIGCC-CCS) resembles the BIGCC-VENT design, with some important variations. The key changes include the introduction of an external tar cracker (to ensure complete tar destruction prior to syngas processing), a water gas shift area (to maximize CO_2 content in the gas), CO_2 removal, and CO_2 compression to supercritical pressure for pipeline transmission and underground injection. The external tar cracker is needed since the gas temperature must be reduced below the tar dew point (for CO_2 capture) before the gas reaches the gas turbine combustor. Following gasification and tar cracking, a two-stage WGS unit converts most of the CO in the gas to CO_2, which in turn is removed using a Rectisol system. The resulting hydrogen-rich gas is burned in a gas turbine combined cycle to generate power. The removed CO_2 is compressed for pipeline transport to an underground storage site. As in the BIGCC-VENT design, we use an air separation system integrated with the gas turbine and return the separated nitrogen to the gas turbine combustor. The steam cycle utilizes a three pressure-level HRSG with one steam reheat. (The Technical Appendix, which is available on request, gives more details regarding the steam cycle.)

[15] Note that in Figure 7 (and other detailed process diagrams shown later), some heat exchangers are shown incompletely, i.e., the properties (temperature, mass flow, composition) of the material flowing on one side of the heat exchanger are detailed, but no information is provided on the characteristics of the stream to or from which heat is being transferred. The indicated heat exchange is included in the pinch analysis.

Table 4. Comparison of quoted and simulated performance of the General Electric 7 FB gas turbine. Quoted and simulated results are compared for natural gas. Simulation results are shown for syngas.

	GE Quoted[a]	*Aspen Simulated*	
	Natural gas[a]	*Natural gas*[a]	*Syngas*
Natural Gas Flow (kg/s)	9.985	9.985	0
Syngas flow rate (kg/s)	0	0	99.71
Air Mass Flow (kg/s)	438.07	438.07	571.64
Compressor Pressure Ratio	18.5	18.5	19.5
Net Electric Output (MW_e)	184.4	184.43	267.5
Exhaust Temperature, C	623	623	650.1
Thermal Efficiency (%)	36.92	36.92	37.9
Exhaust Flow (kg/s)	448.06	448.06	628.4
Turbine Inlet Temperature (^oC)	1370	1370	1370
GT Air Filter Pressure drop, bar	N/A	0	0
GT Compressor Polytropic Efficiency, % [b]	N/A	87	87
GT Compressor Mech Efficiency, %	N/A	98.65	98.65
Air Leakage, %	N/A	0.1	0.1
Cooling flow bypass%	N/A	5.161	5.161
Combustion Heat Loss, % fuel LHV	N/A	0.5	0.5
GT Turbine Isentropic Efficiency, % [b]	N/A	89.769	89.769
GT Turbine Mech Efficiency, %	N/A	98.65	98.65
Generator Efficiency	N/A	98.6	98.6
GT Exhaust Pressure, bar	N/A	1.01	1.065

(a) Quoted performance is from: Brooks (2000), Scholz (2002), and Cerovski (2003). For the parameters shown below turbine inlet temperature, representative values have been assumed based on discussion with Consonni (Politecnico di Milano, Italy, personal communication).

(b) These parameter values were tuned to match as closely as possible the quoted net power output and exhaust temperature.

As summarized in Table 3, the simulated net power output for the BIGCC-CCS design is 354 MW_e, corresponding to an 88 MW (or 10 percentage point efficiency) penalty relative to our BIGCC-VENT design. The reduced output is due to higher process electricity consumption (primarily for capturing and compressing CO_2) and lower gross power output from both the gas turbine and steam turbine. The gas turbine output is lower because there is less energy input to it (due to energy impacts of adding the WGS reactor). The steam turbine output is lower because there is less gas turbine exhaust heat available for steam raising and some steam is diverted to the WGS reactor.

4.3 DME Production

For production of DME, the post-gasifier external tar cracker (discussed in Section 3.1.2.1) is included before syngas cooling and particle filtration. The tar cracker is needed to ensure complete tar destruction since, as in the BIGCC-CCS case, the synthesis gas must be cooled (for downstream processing) to temperatures below which any remaining tar would condense. Leaving the particle filter at 350^{o}C, the gas is subsequently cooled to 40^{o}C before it goes to the acid-gas removal area.

Acid gas removal consists of processing the syngas through a Rectisol™ unit, which removes all H_2S and most of the CO_2. H_2S must be removed to avoid poisoning of downstream catalysts.[16] CO_2 is removed to increase reaction rates in the DME synthesis reactor. Complete CO_2 removal is possible and theoretically would considerably accelerate the conversion of syngas to DME, since the presence of CO_2 acts to reduce the partial pressures of the main reacting gases, CO and H_2. However, a small amount of CO_2 is necessary to ensure sufficient catalyst activity in a liquid-phase DME synthesis reactor (Larson and Ren, 2003), the reactor design we have assumed here.

Following acid-gas removal, the syngas is compressed and heated in preparation for delivery to the DME synthesis reactor. The synthesis of DME (CH_3OCH_3) has similarities to synthesis of methanol (CH_3OH), the production technology for which is well-established commercially.[17] Methanol synthesis is carried out over a catalyst, typically $CuO/ZnO/Al_2O_3$, and can be (simplistically) represented by the following principal reaction:

$$CO + 2H_2 \Leftrightarrow CH_3OH \qquad \text{(-90.7 kJ/mol)} \qquad (1)$$

DME is produced today exclusively in small-scale facilities by dehydration of methanol over a γ-alumina catalyst:

$$2CH_3OH \Leftrightarrow CH_3OCH_3 + H_2O \qquad \text{(-23.4 kJ/mol DME)} \qquad (2)$$

By combining some methanol catalyst and dehydration catalyst in the same reactor, reactions (1) and (2) proceed simultaneously, resulting in direct synthesis of DME. The idea of direct synthesis of DME from syngas was first reported in the literature long ago (Brown and Galloway, 1929), but efforts to commercialize direct synthesis technology did not begin in earnest until around 1990. As noted earlier, single-step DME synthesis technologies are now approaching commercial readiness.

Syngas conversion to methanol (equation 1) can be accomplished today to nearly the extent predicted by chemical equilibrium, i.e., to the theoretical maximum extent. Substituting methanol dehydration catalyst for some of the methanol synthesis catalyst results in methanol being reacted away (by Equation 2) as it forms. This effectively by-passes the equilibrium limits of Equation 1. The presence of methanol catalyst can also promote the water gas shift reaction:

$$H_2O + CO \Leftrightarrow H_2 + CO_2 \qquad \text{(-40.9 kJ/mol)} \qquad (3)$$

The overall single-step DME synthesis chemistry can be represented as a combination of Equations 1, 2, and 3:

---

[16] The sulfur content of the switchgrass considered in this analysis is 0.1% by dry weight, which is high for biomass (but very low compared to most coal). The H_2S content of the raw gasifier product is about 100 ppm(v). The acceptable H_2S content in synthesis gas depends on the downstream catalyst to be used, but is generally in the 100 to 500 ppb range (Spath and Dayton, 2003).

[17] Most commercial methanol is produced today from syngas derived from natural gas (except in China, where most domestic production of methanol – 3.3 million metric tons used in 2001) is via coal gasification (Larson and Ren, 2003).

$$3CO + 3H_2 \Leftrightarrow CH_3OCH_3 + CO_2 \qquad \text{(-246 kJ/mol DME)} \quad (4)$$

This reaction suggests that the optimum H_2:CO ratio in the feed gas for DME synthesis is 1:1. In practice, modest departures from this ratio (1.35 for the process configurations considered in this work), do not significantly change the synthesis yields.[18]

Our simulation of the reaction kinetics in a liquid phase DME synthesis reactor is based on a model developed by Larson and Ren (2003). That model is based on rate equations for methanol synthesis developed by Graaf [Graaf, et al. (1988a and 1988b) and Graaf and Beenackers (1996)] from laboratory measurements with a batch liquid-phase reactor and a $CuO/ZnO/Al_3O_3$ catalyst. Among the rate equations in the literature for which complete information is provided by authors, Graaf's equations appear to be relatively conservative in their prediction of the fractional conversion of CO to methanol. For the DME synthesis model, Larson and Ren added to these reactions a kinetic expression for methanol dehydration (over a γ–alumina catalyst) developed by Ng, *et al.* (1999). By appropriate selection of gas space velocity [6000 lit/hr-kg_{cat} was used (standard liters input syngas per hour per kilogram of methanol synthesis catalyst)] and ratio of dehydration catalyst to methanol catalyst (0.3 was used), Larson and Ren obtained synthesis reactor performance predictions that compared well with the predictions of synthesis models developed internally at Air Products and Chemicals, Inc. The Air Products' models were based on typical lifecycle reactor performance, including an assumed catalyst activity level of 50% of the level for fresh catalyst.

The raw synthesis product leaving the liquid-phase reactor is sent to the downstream separation area, where a series of flash tanks and cryogenic distillation steps are used to produce separate streams of DME, by-product methanol, a CO_2-rich gas stream, and unconverted synthesis gas. After the initial flash separation steps, one stream containing mostly DME and methanol plus a small amount of other species undergoes distillation. A CO_2-rich stream comes off the top of this distillation tower, and a concentrated DME/methanol liquid mixture leaves at the bottom. The liquid mixture is distilled in a second tower, producing a 99.9% pure DME product stream at the top. The bottom methanol-rich stream passes to a third distillation tower where remaining water is separated out, leaving a pure stream of methanol exiting the top of the tower. A small amount of this methanol is used as make-up for the Rectisol plant. The remaining methanol is passed to a catalytic reactor, where 80% of it is converted to additional DME by dehydration.

The downstream DME separation area is based on equipment configurations proposed by Air Products and Chemicals, Inc. (Air Products and Chemicals, Inc., 1993), as implemented by Celik *et al.* (2004) in Aspen-Plus models of DME production from coal. Celik *et al.* updated Larson and Ren's model of the downstream area to improve DME separation effectiveness, and hence DME recovery. Among other modifications made by Celik *et al.* was the addition of the methanol dehydration reactor to convert methanol by-product to DME, rather than recycling the methanol to the synthesis reactor. Separately dehydrating the methanol provides for somewhat improved overall DME yield.

[18] Our sensitivity analyses indicate about a 10% higher DME production with H_2/CO of 1 instead of 1.35.

4.3.1 DME Production with No Carbon Capture and Storage

4.3.1.1 D-OT-VENT

Figure 8 shows the detailed mass and energy balance for co-producing DME and electricity based on once-through synthesis, with no carbon capture and storage. In this design, the operating parameters of the system are set such that the volume fraction of CO_2 in the syngas leaving the Rectisol area is 3%. After stripping the captured acid gases from the Rectisol solvent, most of the mixture of H_2S and CO_2 is compressed and delivered to the gas turbine combustor. This serves three purposes. It helps maintain the requisite mass balance between the gas turbine compressor and expander, it's diluting effect ensures that NO_x emissions are kept below regulated levels, and by converting the small amount of H_2S in the gas into SO_2, (giving acceptably low concentrations in the exhaust stack) it obviates the need for any dedicated H_2S capture system. The portion of the acid gas mixture that is not compressed for gas turbine use is used to pressurize the biomass gasifier feeder.

The unconverted syngas, which is rich in methane, passes through a saturator where it picks up moisture before reaching the gas turbine combustor. The saturator serves three purposes. It provides a use for low-grade waste heat generated elsewhere in the process, it adds mass flow to help maintain the mass balance between gas turbine compressor and expander, and it's diluting effect contributes to keeping NO_x emissions below regulated levels.

We have modeled the gas turbine on the most advanced generation of operating machines now available on the market ("F" technology), as discussed in Section 4.2.1.

The hot gas turbine exhaust passes to a heat recovery steam generator (HRSG), wherein steam is raised to run a steam turbine. As noted earlier, where feasible the recovery of waste heat generated elsewhere in the process is integrated with the HRSG to augment steam generation for the steam turbine. Steam is generated at three different pressure levels (160, 21, and 3.5 bar), and the condenser operates at 0.05 bar.

Some air is taken from the gas turbine compressor exit to provide feed air to the air separation unit generating the oxygen needed for gasification. The pressurized nitrogen available at the ASU is expanded through a free turbine to contribute to overall electricity generation from the plant.

Overall, the D-OT-VENT design converts 30% of the input biomass energy (LHV basis) into DME and 24% into electricity, for a total efficiency of 54% (Table 3). To facilitate comparisons with other fuels production designs, we calculate an "effective efficiency" of fuels production as the ratio of the liquid fuel energy produced divided by the following quantity: the total amount of biomass consumed less an amount of biomass that would be consumed in producing the same amount of power in a stand-alone biomass power plant.[19] This gives an effective efficiency for the D-OT-VENT case of 62% (LHV basis).

[19] For all cases shown in Table 3 except one, we use the efficiency of the BIGCC-VENT estimated in this report for the stand-alone electricity generating efficiency in the calculation of effective efficiency. For the D-OT-DCAP case (discussed later) we use the efficiency of the BIGCC-CCS case for the effective efficiency, since the D-OT-DCAP case is designed specifically to maximize carbon capture unlike the other cases.

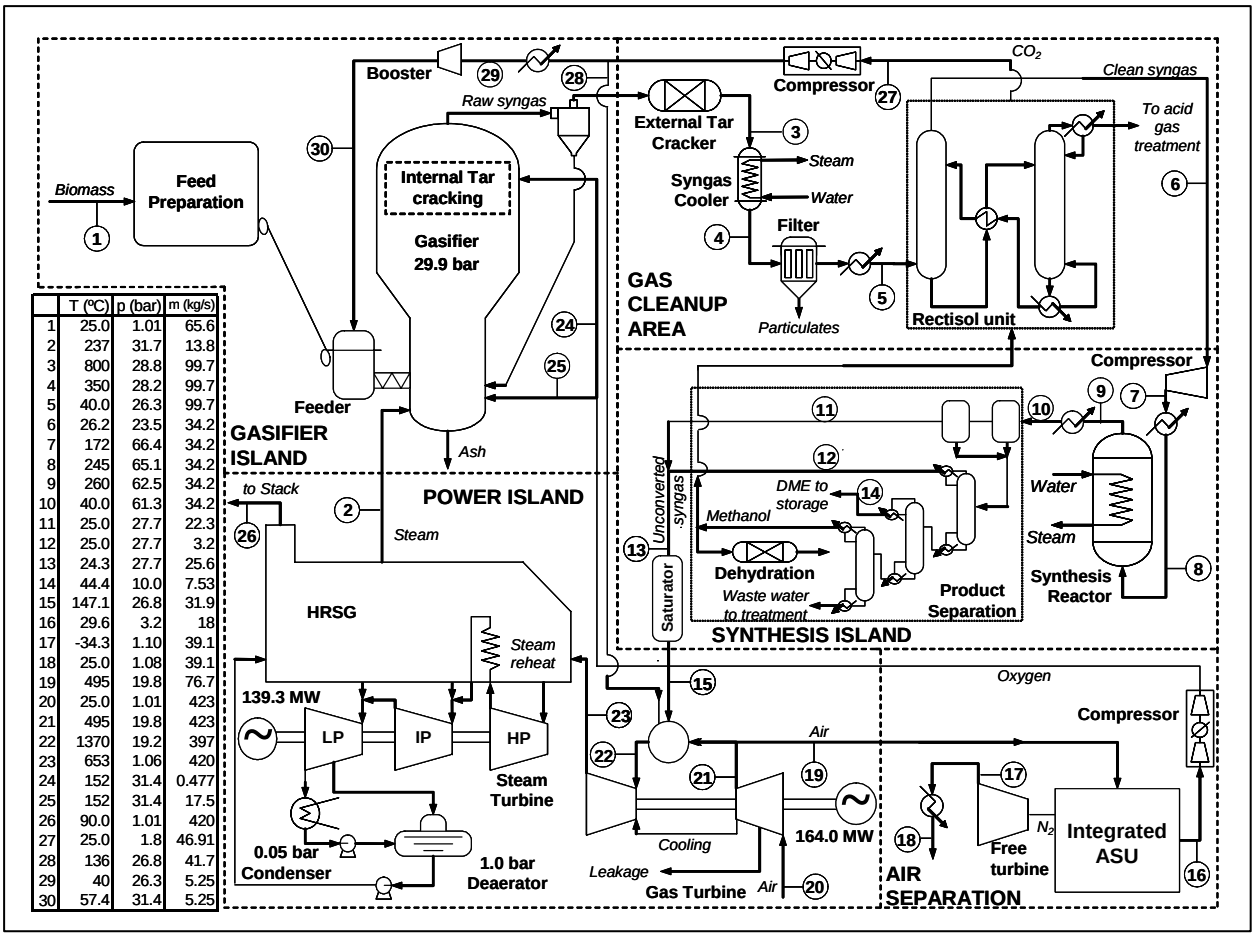

	T (ºC)	p (bar)	m (kg/s)
1	25.0	1.01	65.6
2	237	31.7	13.8
3	800	28.8	99.7
4	350	28.2	99.7
5	40.0	26.3	99.7
6	26.2	23.5	34.2
7	172	66.4	34.2
8	245	65.1	34.2
9	260	62.5	34.2
10	40.0	61.3	34.2
11	25.0	27.7	22.3
12	25.0	27.7	3.2
13	24.3	27.7	25.6
14	44.4	10.0	7.53
15	147.1	26.8	31.9
16	29.6	3.2	18
17	-34.3	1.10	39.1
18	25.0	1.08	39.1
19	495	19.8	76.7
20	25.0	1.01	423
21	495	19.8	423
22	1370	19.2	397
23	653	1.06	420
24	152	31.4	0.477
25	152	31.4	17.5
26	90.0	1.01	420
27	25.0	1.8	46.91
28	136	26.8	41.7
29	40	26.3	5.25
30	57.4	31.4	5.25

Figure 8. Detailed energy and mass balance for DME production from switchgrass with once-through processing of syngas in a liquid-phase synthesis reactor and production of electricity from unconverted syngas (D-OT-VENT case). No carbon capture and storage included in this design.

4.3.1.2 D-RC-VENT

The second plant design for DME production with venting of CO_2 (Figure 9) involves recycle of 97% of the unconverted synthesis gas from the product separation area to the synthesis reactor. This more than doubles the net output of DME relative to the D-OT-VENT case (514 MW vs. 249 MW, HHV basis) at the expense of electricity generation (79 MW vs. 270 MW), and results in an effective efficiency of 64% (LHV basis) (Table 3). Even higher recycle percentages are possible in theory, but the not-insignificant level of methane in the syngas would lead to prohibitively large recycle volumes in that case.

Key design differences between the D-RC-VENT and D-OT-VENT cases are

- In the D-RC-VENT case all CO_2 in the syngas is removed at the Rectisol plant (rather than leaving 3% CO_2 in the gas). Because the post-Rectisol feed gas to the synthesis reactor is a mixture of fresh and recycled syngas, the needed CO_2 (for maintaining synthesis catalyst activity) is provided by the recycled syngas.
- In the D-RC-VENT case most of the unconverted syngas leaving the product separation area is compressed and recycled to the synthesis reactor. The lower flow of un-recycled gas results in a smaller power island, but one that produces sufficient electricity to provide for on-site needs and a modest level of net exports (Table 3).

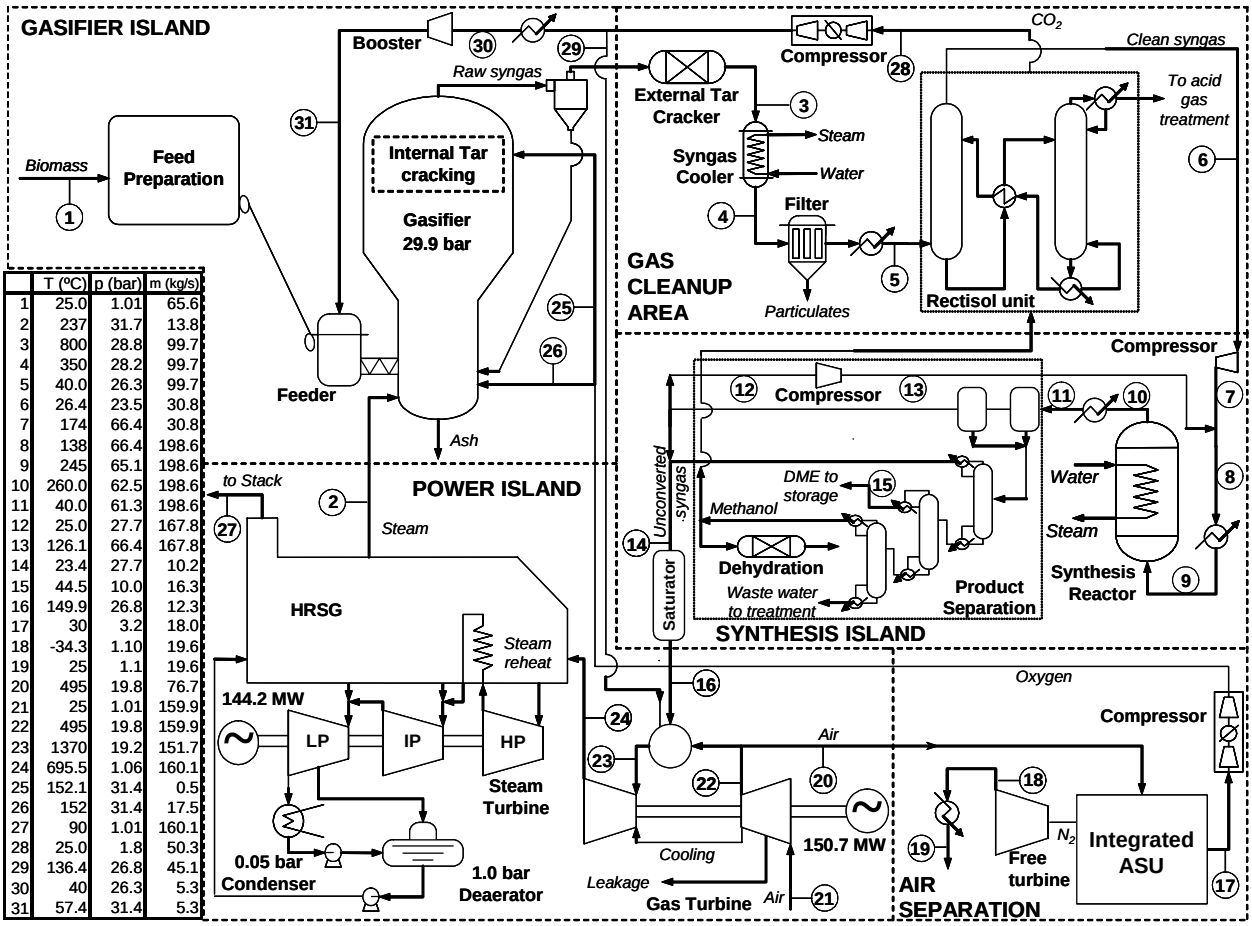

	T (ºC)	p (bar)	m (kg/s)
1	25.0	1.01	65.6
2	237	31.7	13.8
3	800	28.8	99.7
4	350	28.2	99.7
5	40.0	26.3	99.7
6	26.4	23.5	30.8
7	174	66.4	30.8
8	138	66.4	198.6
9	245	65.1	198.6
10	260.0	62.5	198.6
11	40.0	61.3	198.6
12	25.0	27.7	167.8
13	126.1	66.4	167.8
14	23.4	27.7	10.2
15	44.5	10.0	16.3
16	149.9	26.8	12.3
17	30	3.2	18.0
18	-34.3	1.10	19.6
19	25	1.1	19.6
20	495	19.8	76.7
21	25	1.01	159.9
22	495	19.8	159.9
23	1370	19.2	151.7
24	695.5	1.06	160.1
25	152.1	31.4	0.5
26	152	31.4	17.5
27	90	1.01	160.1
28	25.0	1.8	50.3
29	136.4	26.8	45.1
30	40	26.3	5.3
31	57.4	31.4	5.3

Figure 9. Detailed energy and mass balance for DME production from switchgrass with recycle processing of syngas through a liquid-phase synthesis reactor and production of some electricity from recycle purge gas (D-RC-VENT case). No carbon capture and storage included in this design.

4.3.2 DME Production with Carbon Capture and Storage

In each of the two DME production plant designs described above, CO_2 is removed following gasification/gas cleanup to ensure adequate conversion rates in the synthesis reactor. With a relatively minor addition of equipment to the plant, the stream of removed CO_2 can be captured for underground storage rather than vented to the atmosphere (Figure 4, D-OT-UCAP and D-RC-UCAP). Moreover, for the process configuration involving once-through synthesis, the syngas burned in the power island could be decarbonized before combustion to further increase the overall amount of CO_2 captured for storage (Figure 4, D-OT-DCAP). We have designed and simulated in detail the three plant configurations sketched in Figure 4 for production of DME with CCS. In all cases, the captured CO_2 (with all H_2S co-captured) is compressed to supercritical pressure (150 bar) for pipeline transport to a long-term underground storage site.

The idea of co-capture and co-storage of H_2S and CO_2 has been proposed by Chiesa, *et al.* (2005) for coal-based systems. With coal gasification for DME production, it would have cost advantages for sulfur management compared to separate removal of H_2S (Larson and Ren,

2003). The extent to which underground co-storage of CO_2 and H_2S is a viable option is not yet known, although there has been good operating experience with about 40 small projects in western Canada (starting in 1989) involving co-storage of various mixtures of H_2S and CO_2 in depleted oil and gas fields and in deep aquifers as an acid-gas management strategy in conjunction with sour natural gas production (Bachu and Gunter, 2005).

4.3.2.1 D-OT-UCAP

The D-OT-UCAP design (Figure 10) is similar to the D-OT-VENT design (Figure 8), with the following key differences:

- CO_2 removed with H_2S from the syngas by the Rectisol unit is compressed to 150 bar for pipeline transport to an underground storage site.
- To compensate for eliminating the flow of CO_2 from the Recitsol area to the gas turbine combustor, nitrogen from the ASU is compressed and delivered instead. (The N_2 expander present in the D-OT-VENT case is eliminated.)

The net overall effect of these changes is that, compared to the D-OT-VENT case, DME output increases very slightly, while net electricity output falls by about 5% (from 270 MW to 257 MW). The carbon capture rate in the D-OT-UCAP design is 41 metric tonnes C per hour (150 tCO_2 per hour), representing nearly half of the carbon in the original switchgrass (Table 3).

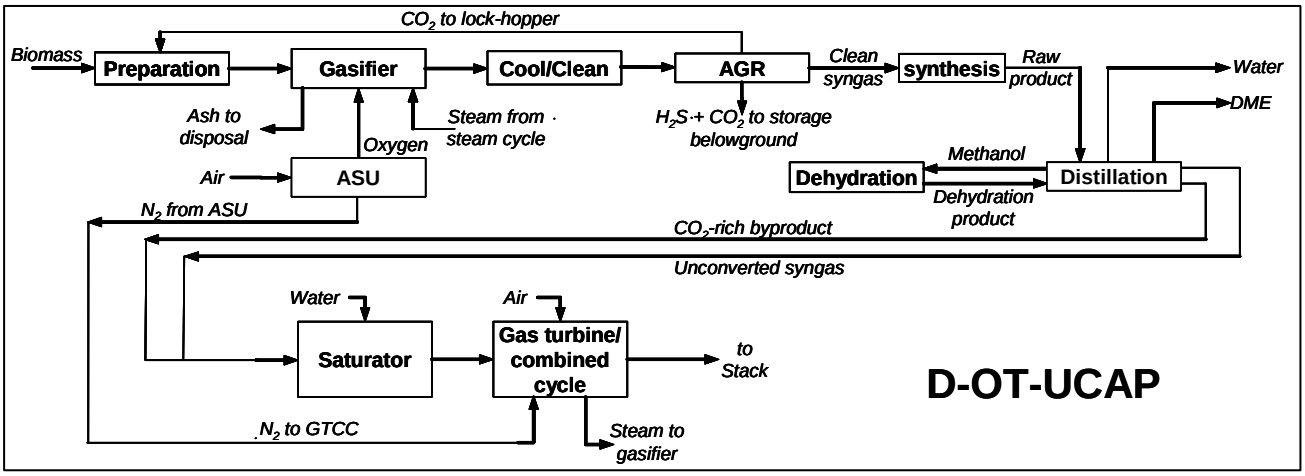

Figure 10. Simplified process diagram for DME production with once-through synthesis, electricity production from unconverted syngas, and capture of carbon upstream for storage.

4.3.2.2 D-RC-UCAP

The D-RC-UCAP design (Figure 11) is similar to the D-RC-VENT design (Figure 9), with the following key differences:

- CO_2 removed with H_2S from the syngas by the Rectisol unit is compressed to 150 bar for pipeline transport to an underground storage site.
- To compensate for eliminating the flow of CO_2 from the Recitsol area to the gas turbine combustor, nitrogen from the ASU is compressed and delivered instead. (The N_2 expander present in the D-RC-VENT case is eliminated.)

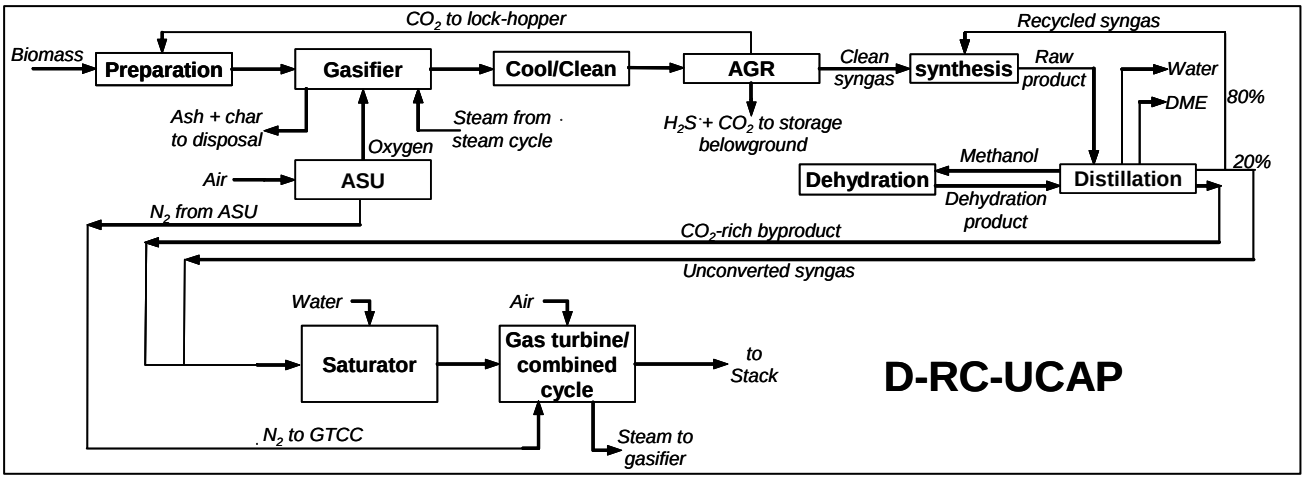

Figure 11. Simplified process diagram for DME production with recycle synthesis processing of sygnas, with electricity production from recycle purge gas and capture of carbon upstream for storage.

The net overall effect of these changes is that, compared to the D-RC-VENT case, DME output increases very slightly, while net electricity output falls by about 15% (from 79 MW to 67 MW). The percentage reduction in electricity output is greater than in the D-OT-UCAP case mainly because approximately the same CO_2 compression work is added compared to the D-RC-VENT case, but the starting (VENT case) level of power output is considerable lower.

The carbon capture rate in the D-RC-UCAP design is slightly higher than in the D-OT-UCAP case (44 tC/hr, 162 tCO_2 per hour) due to the greater amount of CO_2 removal allowable with the recycle design (see Section 4.3.1.2). The captured carbon represents exactly half of the carbon in the original switchgrass (Table 3).

4.3.2.3 D-OT-DCAP

The D-OT-DCAP design (Figure 12) is similar to the D-OT-UCAP design described above, but with additional carbon capture downstream of the synthesis area. The unconverted syngas leaving the separation area is passed through a saturator to add humidity, following which it is subjected to a two-stage water gas shift process designed to shift as much remaining CO to CO_2 as possible. Following the WGS, the CO_2-rich stream from the DME separation area is merged with the WGS output before the mixture passes to a Rectisol column where CO_2 is removed. (Separate upstream and downstream Rectisol absorbers share a common absorbent stripping column in our process design.) The hydrogen-rich gas leaving the Rectisol area is passed through a second saturator and then diluted with nitrogen from the ASU before going to the gas turbine combustor. Without the added moisture and nitrogen in the fuel gas, unacceptably high NO_x emissions would result during gas turbine combustion.

The net effect of including both upstream and downstream decarbonization, compared to the D-OT-VENT case, is an unchanged output of DME, but a 15% drop in electricity output (from 270 MW to 229 MW), due primarily to the power required to compress captured CO_2 to pipeline pressure. The carbon capture rate in the D-OT-DCAP case, 66 tC/hour (74% of the carbon in the input switchgrass, or 88% of the input carbon that is not contained in the DME product). The carbon capture rate is the highest of any of the DME cases examined here (Table 3).

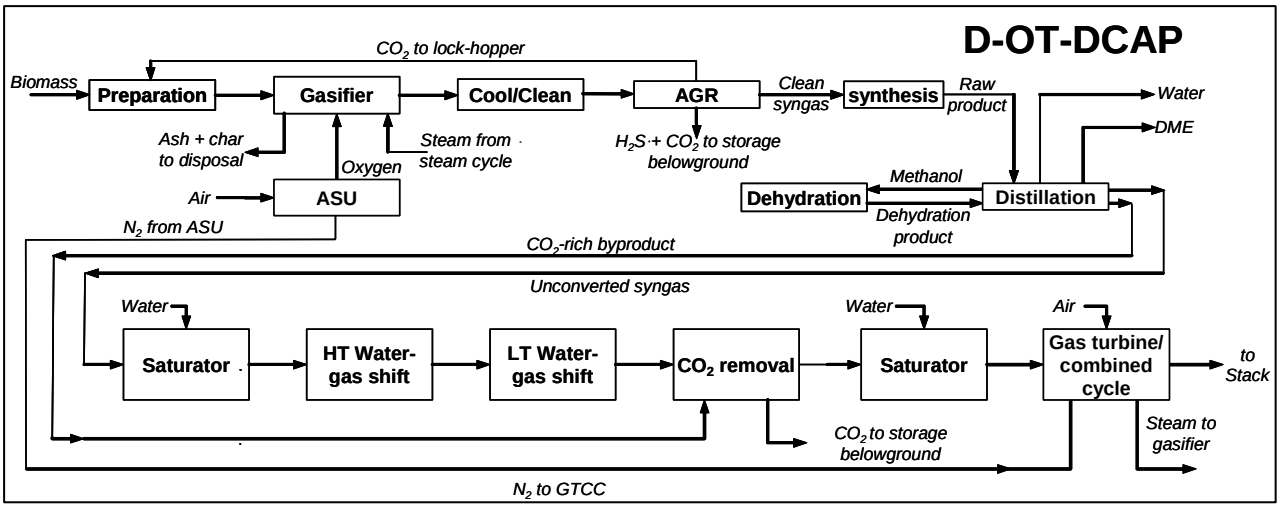

Figure 12. Simplified process diagram for DME production with once-through synthesis, electricity production from unconverted syngas, and capture of carbon for storage both upstream and downstream of the synthesis reactor.

4.4 Fischer-Tropsch Fuels Production

The upstream portion of process designs for producing Fischer-Tropsch fuels from switchgrass are similar to the upstream process designs for DME production: tars in product gas from the gasifier must be cracked to light molecules (or removed), particulates and trace contaminants must be removed, sulfur must be removed to protect downstream F-T synthesis catalysts, and CO_2 should be removed to achieve higher conversion rates in the synthesis reactor. Unlike the catalyst used for DME synthesis, F-T catalysts do not require any residual CO_2 in the feed gas, so all CO_2 present in the clean syngas can be removed upstream of the synthesis reactor.

The cool, clean syngas is fed to a slurry-phase Fischer-Tropsch reactor, where the CO and H_2 combine exothermically in the presence of a catalyst under moderate pressure and temperature conditions (ranging from 20-35 bar and 180-350^{o}C, depending on the specific design) to produce a mixture of straight-chain hydrocarbons, namely paraffins (C_nH_{2n+2}) and olefins (C_nH_{2n}), ranging from methane to high molecular weight waxes. The reactor must be actively cooled to maintain the desired reaction temperature. The output from the synthesis reactor includes a mix of different-length hydrocarbons, CO_2, H_2O, inert species in the feed gas, and other minor compounds.

The relative proportion of different hydrocarbons produced by the F-T reactions is determined primarily by feed gas composition, catalyst type and loading, reaction temperature, pressure, and residence time, the net result of which can be characterized in terms of the "alpha" number for a given reactor design and operation. This characterization derives from a single-parameter (α) model that can relatively accurately predict empirically-observed carbon number distributions (Anderson, 1984). The model accounts for the fact that longer hydrocarbons are formed by the linear addition of -CH_2- segments to shorter hydrocarbons in the synthesis process. The carbon number distribution predicted by this model is called the Schulz-Flory or Anderson-Flory-Schulz distribution[20] (Eilers *et al*., 1990). Commercial F-T synthesis reactors are characterized by 0.65

[20] The distribution of carbon number species (C_n) is given by $\log(C_n) = \log[(1-\alpha)/\alpha] + n\log(\alpha)$.

$< \alpha < 0.95$. Lower α will give a lower average molecular weight synthesis product compared to higher-α synthesis.

In GTL plants operating today, the F-T synthesis reactor is typically operated at high-end α values. The resulting heavy waxy product is easily and with high selectivity formed into desired lighter products by subsequent hydrocracking, which involves the breaking up of the large hydrocarbon molecules into desired final products in a hydrogen-rich environment. Hydrocracking of large straight-chain hydrocarbons can be done under much less severe temperature conditions (350-400^{o}C for cracking to C_5-C_{18} range) than is required for hydrocracking of aromatic molecules in conventional petrochemical refining. Lighter hydrocarbons leaving the hydrocracker can be recycled for further conversion or burned to produce co-product electricity, e.g., using a gas turbine.

As noted previously (Section 3.2), an important recent technological development in commercial F-T conversion is "liquid-phase" synthesis. The vigorous mixing, intimate gas-catalyst contact, and uniform temperature distribution enable conversion of feed gas to F-T liquids of about 80% in a single pass, as measured by fraction of CO converted (Bechtel Group, 1990). This compares to less than 40% conversion with traditional fixed-bed F-T reactors, such as those used commercially in the Shell Malaysia plant and in South Africa. Considerable recycling is required with fixed-bed reactors to achieve high overall yield. The higher gas throughput capacity per unit volume with liquid-phase synthesis reduces capital costs compared to a fixed-bed reactor, and catalyst consumption per unit of product is reduced dramatically (Jager, 1997). Liquid-phase reactors are now commercially available for F-T synthesis (Rahmim, 2003). Both of the process designs we have developed for F-T fuels production from biomass involve once-through liquid-phase synthesis, with electricity co-production using unconverted syngas.

We have modeled the F-T synthesis reactor based on the triple-α model of Fox and Tam (1995), as discussed in the Technical Appendix (available on request). The simplicity of a single-α model[20] is appealing, but multiple-α models can provide better matching to empirical data. Building on Fox and Tam's model, we developed our own multi-α model, drawing on more recent empirical results (than used by Fox and Tam) for the kinetics of F-T reactions over iron-based catalysts in slurry-bed reactors (Bukur *et al.*, 2004; Raje *et al.*, 1997). We use an iron-based catalyst because the H_2/CO ratio of the syngas produced by the gasifier is less than the optimal value of slightly above 2 for F-T synthesis, and iron-based catalysts promote the water gas shift reaction (converting some CO to H_2), in addition to the F-T reactions. Moreover, iron catalysts are less costly than cobalt and other metal catalysts.[21]

The Technical Appendix (available on request) provides a detailed description of our kinetic FT reaction model. The assumed synthesis reactor conditions are 260^{o}C and 22 bar pressure, with an average gas hourly space velocity of 5800 liters/$kg_{catalyst}$/hr (standard liters input syngas per hour per kilogram of catalyst). These assumptions, together with the syngas volume flowrate and density, enable calculation of the required catalyst mass, which in turn provides the basis for calculating the overall reaction results.

[21] On a relative basis, if scrap iron costs 1.0, the approximate cost of other metals is 250 for nickel, 1000 for cobalt, and 15000 for ruthenium (Dry, 2002).

The synthesis step produces a raw mix of products that must be separated and upgraded. The design of our separation/upgrading area (Figure 13) is based on a Bechtel design (Bechtel, 1998). The liquid product streams leaving the F-T synthesis reactor are separated into light-gas, naphtha, distillate and heavy-wax fractions. A small amount of syngas is bypassed around the synthesis reactor and processed through a water gas shift reactor. Then, together with a hydrogen-rich stream from the naptha reformer located in the upgrading area, the gas passes to a pressure-swing adsorption (PSA) unit to generate the hydrogen needed for product upgrading. The product upgrading area includes five major sub-units: (1) a wax hydrocracking plant cracks the raw waxes into naphtha, distillate and light gas; (2) a distillate-fraction hydrotreater and (3) a naphtha hydrotreater that stabilize these F-T fractions by hydrogen addition (saturating the olefins). The distillate product is then ready for use, e.g., for blending with petroleum diesel; (4) a catalytic reforming area that treats the naphtha fractions (from the wax hydrocracker and the naphtha hydrotreater) and produces a high-octane gasoline blending component and a hydrogen-rich stream (sent to the PSA unit); and (5) an isomerization unit that increases the octane number of the pentane/hexane stream produced by the naptha hydrotreater, producing additional high-grade gasoline blending component. Some light gases are unavoidably produced in each of the five sub-units, and these are collected and fed with unconverted syngas to a gas turbine combined cycle in the power island.

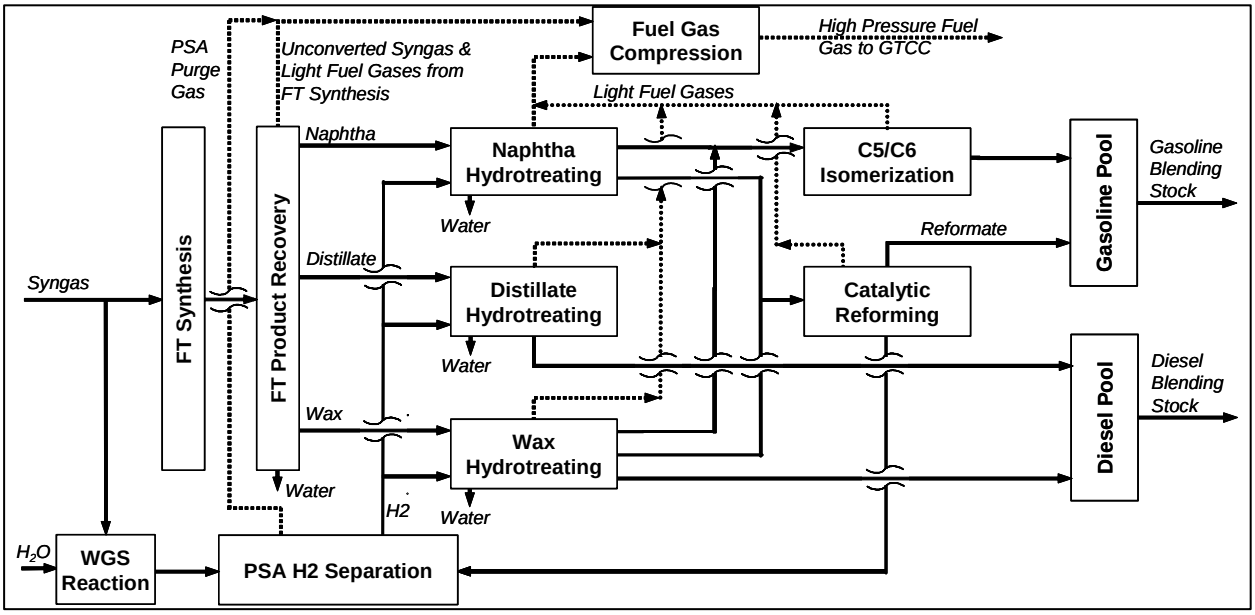

Figure 13. Schematic of the separation and refining area of the F-T production facilities simulated in this work.

4.4.1 F-T Fuels Production with No Carbon Capture and Storage

Figure 14 shows the detailed mass and energy balance for co-producing F-T fuels and electricity via once-through synthesis, with no CO_2 capture for storage. It is instructive to compare the results for this case (FT-OT-VENT) with the parallel case for DME production (D-OT-VENT). As noted earlier, the details of the upstream portion of the design are similar in both cases, including gasification, gas cleanup, CO_2 capture, and CO_2 delivery from the Rectisol plant to the gas turbine. However, there are some significant differences downstream. These are reflected in part in the ratio of fuels-to-electricity produced, which is considerably higher for the FT case

(1.5) than for DME (0.8) as a result of the much higher one-pass conversion achievable with FT synthesis. Also, because of the greater exothermicity of the FT reactions as compared to DME reactions, waste heat recovery plays a more significant role in the FT design. Cooling the FT reactor (by steam raising) extracts 105 MW of thermal energy from the synthesis reactor, compared to 40 MW in the case of DME synthesis. The greater availability of waste heat from synthesis reactor cooling in the FT case contributes to more steam being generated to drive the steam turbine in the power island. The result is that the steam turbine accounts for 62% of the gross power generated in the FT case, while it accounts for only 49% in the DME case.

Overall, the FT-OT-VENT design converts 34% of the input biomass energy (LHV basis) into liquid fuels (60% diesel, 40% gasoline) and 23% into exportable electricity, giving an effective efficiency of 64% (Table 3), the highest among all the liquid fuel process designs we have examined without CCS.

4.4.2 F-T Fuels Production with Carbon Capture and Storage

With CO_2 capture and storage incorporated into the design of a once-through F-T synthesis plant, the fuels output remains unchanged from the case without CCS, but electricity output falls by about 2 percentage points, resulting in an effective efficiency of 60% (Table 3). The amount of carbon captured, 44 tC/hr, is 50% of the carbon in the input biomass. The capture rate is slightly greater than in the D-OT-UCAP case (and identical to the D-RC-UCAP case), because all CO_2 in the syngas ahead of the synthesis reactor is captured in the FT-OT-UCAP case. The drop in electricity is due to compression work on the captured acid gases to prepare them for pipeline transport to an injection site and to nitrogen compression for delivery to the gas turbine (substituting for CO_2 in the FT-OT-VENT design). (In the FT-OT-VENT case, nitrogen leaving the ASU was expanded through a free turbine to generate some electricity.) Because carbon in the unconverted syngas used for power generation in this FT plant design is largely in the form of methane, effectively capturing carbon downstream of the synthesis reactor would require a methane reforming step. We chose not to examine this option.

4.5 Hydrogen

Hydrogen production from biomass has been the subject of several detailed studies by others (e.g., Katofsky, 1993; Hamelinck and Faaij, 2002; and Lau *et al.*, 2003). Here we have carried out process design and simulation of hydrogen production using a consistent framework and set of assumptions as for the other fuel and power products examined in this study. We have developed two basic process designs, one of which produces about as much hydrogen as electricity co-product and the second of which produces mostly hydrogen, but with enough electricity co-production to meet onsite needs and export a small amount. We have developed each of these designs with no CCS in one case and with CCS in another case.

4.5.1 Hydrogen Production with No Carbon Capture and Storage

In the design producing mostly hydrogen with no CCS (H-MAX-VENT), the clean synthesis gas leaving the particle filter is passed directly to a two-stage water gas shift reactor with sulfur-tolerant catalyst (Figure 15). The first stage of the WGS is operated adiabatically and the second is operated isothermally to convert as much of the CO as possible to CO_2: $CO + H_2O \rightarrow CO_2 + H_2$. Steam is injected in the first stage. Following the WGS, CO_2 and sulfur species are removed together at the Rectisol™ plant and passed to a downstream boiler for combustion (to fully oxidize the sulfur species – without exceeding sulfur emissions limits). The CO_2-free gas

leaving the Rectisol area is passed to a pressure-swing adsorption (PSA) system that separates hydrogen (99.999% purity) from residual gas components. The hydrogen is compressed to 60 bar for storage or pipeline transport. Typically, a single PSA unit will remove 70-90% of the hydrogen from a gas stream, with the highest removal possible when the initial H_2 concentration is high (Weist, 2005), as in our designs (90.4% H_2 in feed gas to PSA). We have modeled the PSA assuming an 87% one-pass H_2 recovery, but with recycle of some of the tail gas (containing residual H_2 plus other minor components) to achieve an overall H_2 capture of 95% of the available H_2. The heating value of the remaining tail gas is insufficient for gas turbine combustion, so it is passed to a boiler where it is burned to raise steam to drive a steam turbine generator. Since no gas turbine is present in this design, the air separation unit is a stand-alone design, with nitrogen vented to the atmosphere.

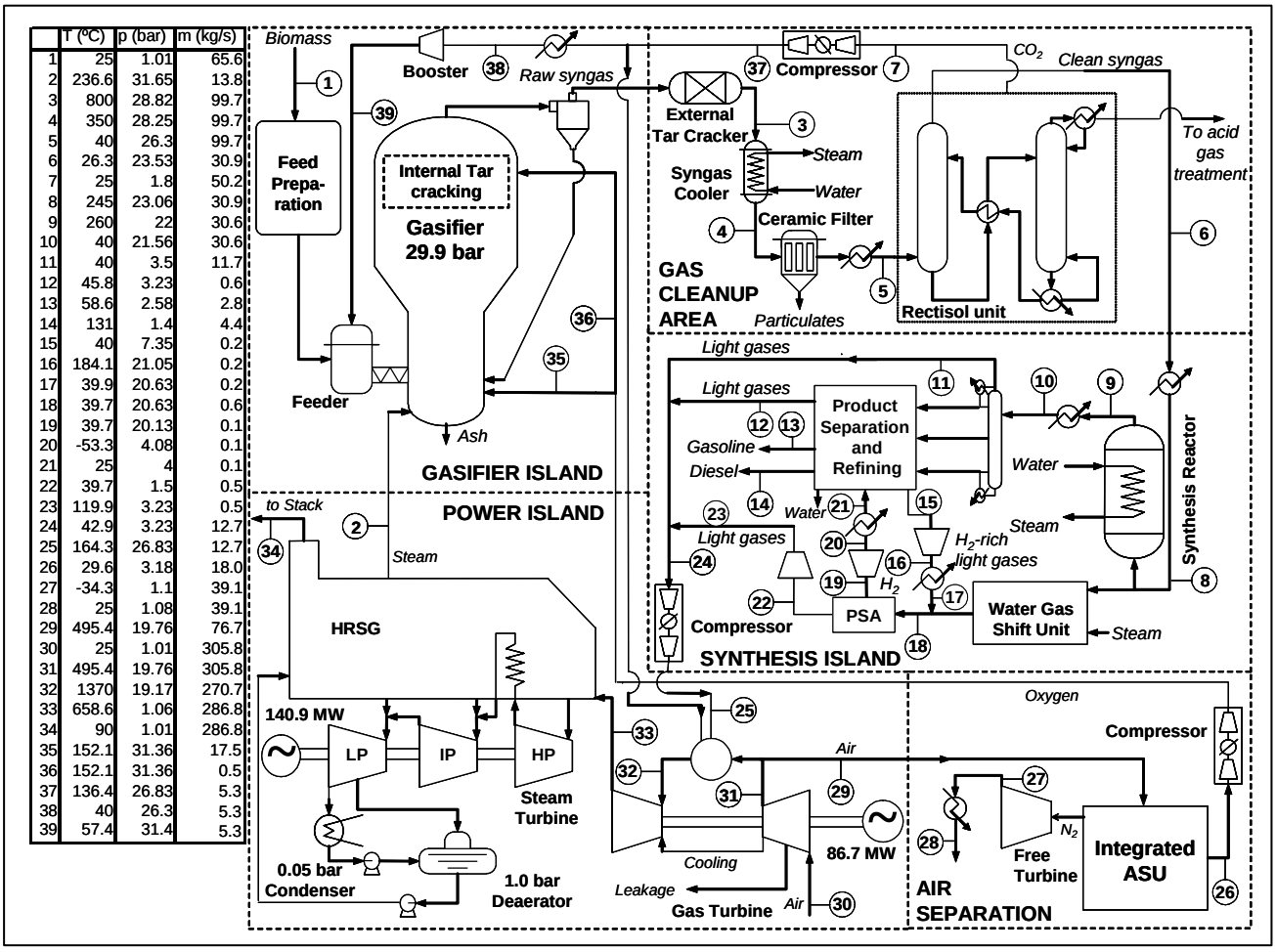

	T (°C)	p (bar)	m (kg/s)
1	25	1.01	65.6
2	236.6	31.65	13.8
3	800	28.82	99.7
4	350	28.25	99.7
5	40	26.3	99.7
6	26.3	23.53	30.9
7	25	1.8	50.2
8	245	23.06	30.9
9	260	22	30.6
10	40	21.56	30.6
11	40	3.5	11.7
12	45.8	3.23	0.6
13	58.6	2.58	2.8
14	131	1.4	4.4
15	40	7.35	0.2
16	184.1	21.05	0.2
17	39.9	20.63	0.2
18	39.7	20.63	0.6
19	39.7	20.13	0.1
20	-53.3	4.08	0.1
21	25	4	0.1
22	39.7	1.5	0.5
23	119.9	3.23	0.5
24	42.9	3.23	12.7
25	164.3	26.83	12.7
26	29.6	3.18	18.0
27	-34.3	1.1	39.1
28	25	1.08	39.1
29	495.4	19.76	76.7
30	25	1.01	305.8
31	495.4	19.76	305.8
32	1370	19.17	270.7
33	658.6	1.06	286.8
34	90	1.01	286.8
35	152.1	31.36	17.5
36	152.1	31.36	0.5
37	136.4	26.83	5.3
38	40	26.3	5.3
39	57.4	31.4	5.3

Figure 14. Detailed energy and mass balance for production of FT fuels (diesel and gasoline blendstocks) from switchgrass with once-through processing of syngas in the liquid-phase synthesis reactor and production of electricity from unconverted syngas (FT-OT-VENT case). No carbon capture and storage included in this design.

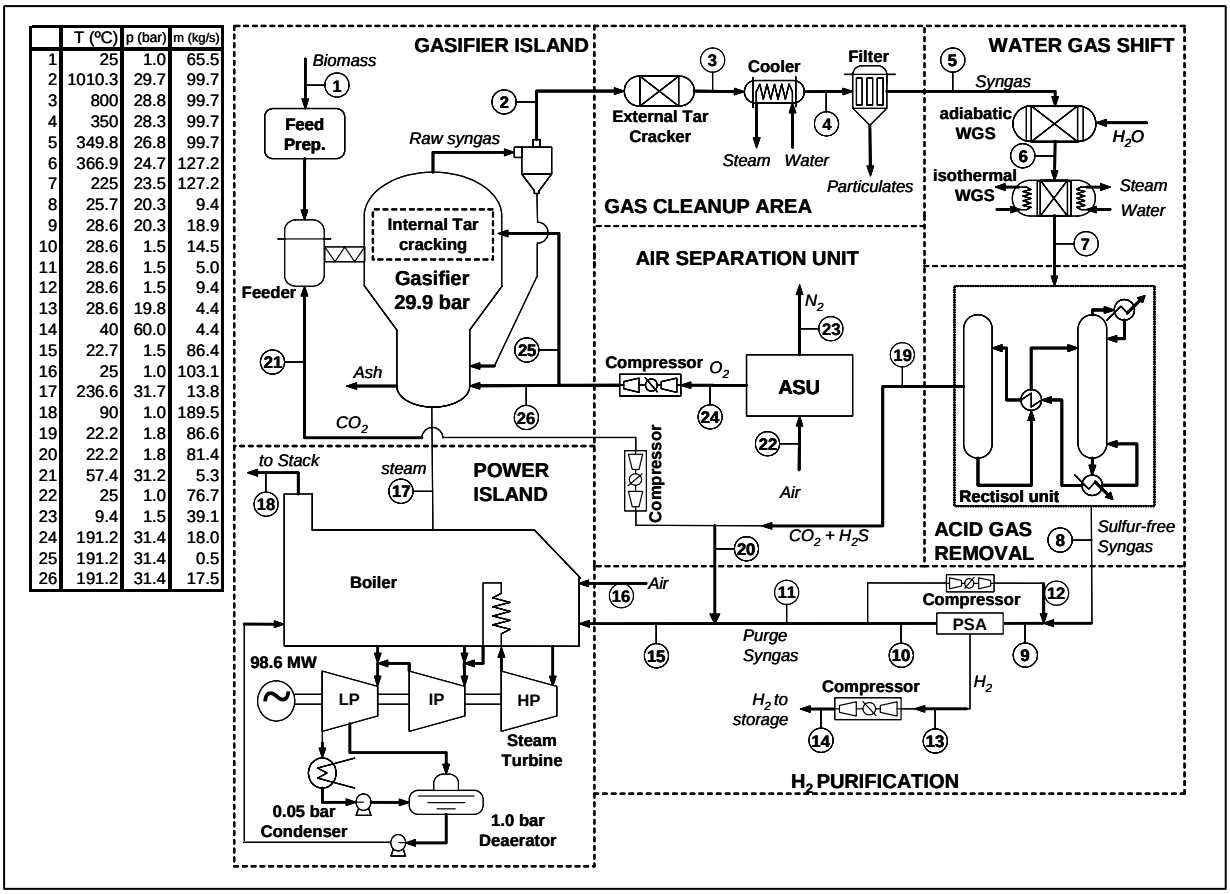

	T (ºC)	p (bar)	m (kg/s)
1	25	1.0	65.5
2	1010.3	29.7	99.7
3	800	28.8	99.7
4	350	28.3	99.7
5	349.8	26.8	99.7
6	366.9	24.7	127.2
7	225	23.5	127.2
8	25.7	20.3	9.4
9	28.6	20.3	18.9
10	28.6	1.5	14.5
11	28.6	1.5	5.0
12	28.6	1.5	9.4
13	28.6	19.8	4.4
14	40	60.0	4.4
15	22.7	1.5	86.4
16	25	1.0	103.1
17	236.6	31.7	13.8
18	90	1.0	189.5
19	22.2	1.8	86.6
20	22.2	1.8	81.4
21	57.4	31.2	5.3
22	25	1.0	76.7
23	9.4	1.5	39.1
24	191.2	31.4	18.0
25	191.2	31.4	0.5
26	191.2	31.4	17.5

Figure 15. Detailed energy and mass balance for production of hydrogen from switchgrass. This design (H-MAX-VENT) seeks to maximize hydrogen production without carbon capture and storage.

The second hydrogen production configuration (Figure 16, H-50/50-VENT) is designed such that approximately equal quantities (MW HHV) of electricity and hydrogen are produced. In this design, exactly half of the clean syngas from the particle filter bypasses the WGS area, going directly to a gas turbine in the power island. The WGS consists of a single, adiabatically-operated reactor. CO_2 is removed following the WGS, a PSA system (with no purge gas recycle) purifies the remaining H_2-rich stream, and the H_2 is compressed for storage or pipelining. The PSA purge gas is mixed with the WGS bypass syngas and passes through a saturator before being burned in a gas turbine to generate electricity. The ASU is integrated with the gas turbine. Steam raised using gas turbine exhaust and waste heat streams from elsewhere in the process powers a three-stage steam turbine to produce additional electricity.

The H-MAX-VENT configuration converts nearly 60% of the input biomass energy into hydrogen (LHV basis), with exportable electricity accounting for another 5% of the biomass energy input (Table 3). Because of the modest amount of electricity generated, the effective efficiency (65%) is only modestly higher than the fraction of biomass energy converted to hydrogen. The H-50/50-VENT case produces much less hydrogen (32% of input biomass on LHV basis), but much more electricity (27%), and as a consequence yields the highest effective efficiency (74%) of any of the fuel production configurations we have examined (Table 3).

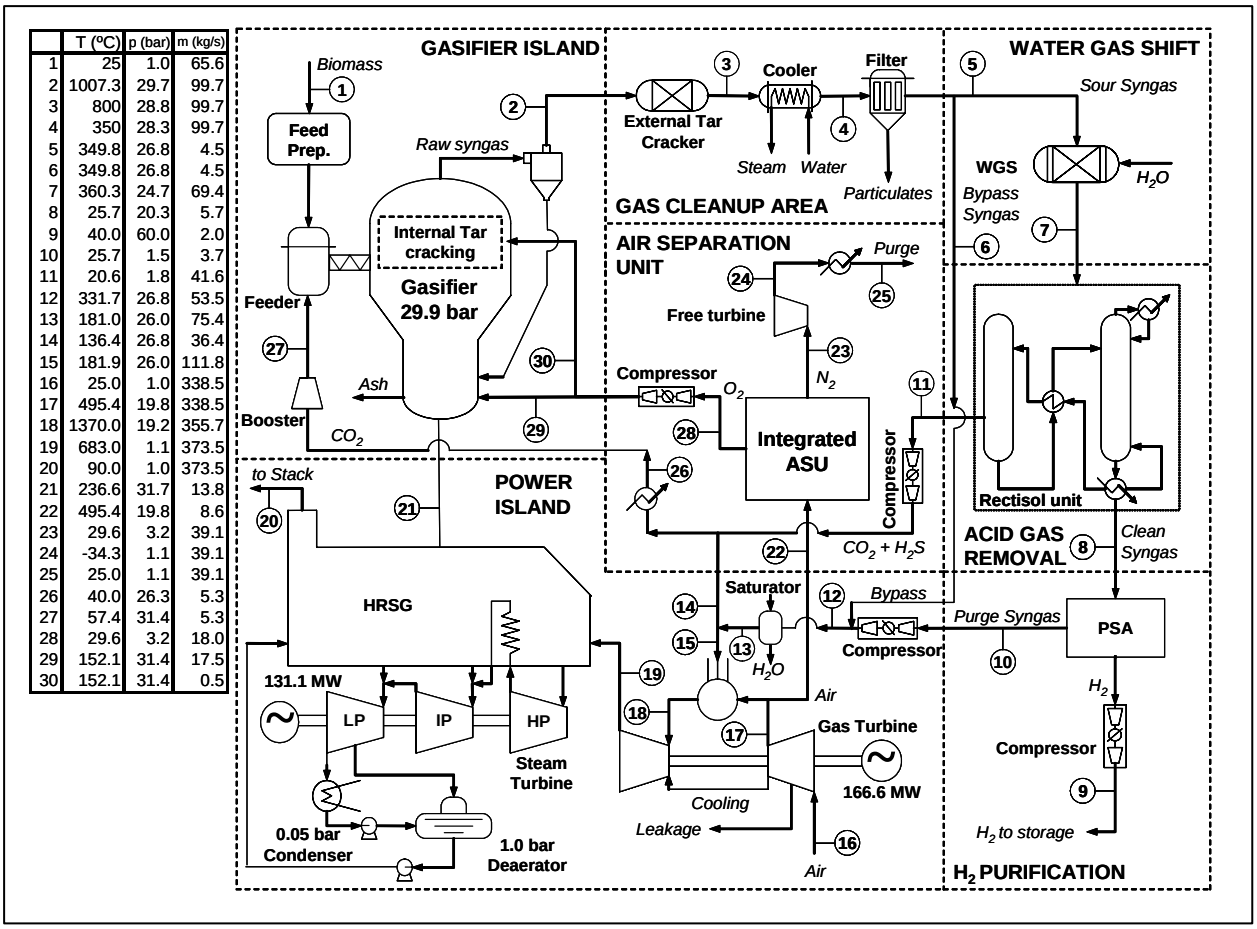

	T (ºC)	p (bar)	m (kg/s)
1	25	1.0	65.6
2	1007.3	29.7	99.7
3	800	28.8	99.7
4	350	28.3	99.7
5	349.8	26.8	4.5
6	349.8	26.8	4.5
7	360.3	24.7	69.4
8	25.7	20.3	5.7
9	40.0	60.0	2.0
10	25.7	1.5	3.7
11	20.6	1.8	41.6
12	331.7	26.8	53.5
13	181.0	26.0	75.4
14	136.4	26.8	36.4
15	181.9	26.0	111.8
16	25.0	1.0	338.5
17	495.4	19.8	338.5
18	1370.0	19.2	355.7
19	683.0	1.1	373.5
20	90.0	1.0	373.5
21	236.6	31.7	13.8
22	495.4	19.8	8.6
23	29.6	3.2	39.1
24	-34.3	1.1	39.1
25	25.0	1.1	39.1
26	40.0	26.3	5.3
27	57.4	31.4	5.3
28	29.6	3.2	18.0
29	152.1	31.4	17.5
30	152.1	31.4	0.5

Figure 16. Detailed energy and mass balance for production of approximately equal MW of hydrogen and electricity from switchgrass without carbon capture and storage (H-50/50-VENT). In this design, exactly half of the clean syngas from the particle filter bypasses the water gas shift, going directly to a gas turbine in the power island.

4.5.2 Hydrogen Production with Carbon Capture and Storage

We have designed and simulated two additional H_2 production cases. These parallel the two scenarios described in the previous section, but have the added feature that CO_2 is captured and compressed for underground storage.

For the case with maximum H_2 production, the design of the plant with carbon capture and storage (H-MAX-CCS, Figure 5) is nearly identical to that with venting of CO_2. The main difference is that CO_2 removed ahead of the PSA H_2 recovery area is compressed to supercritical pressure (150 bar) for pipeline transport in the H-MAX-CCS case, whereas it is delivered to the purge-gas boiler in the H-MAX-VENT case. The power consumed in compressing the CO_2 in the H-MAX-CCS case leads to a significant increase in the internal power consumption of the process relative to the H-MAX-VENT case, resulting in less exportable power, with approximately the same H_2 output (Table 3). The effective efficiency falls from 65% for the H-MAX-VENT case to 60% for the H-MAX-CCS case.

For the case in which roughly equal amounts of hydrogen and electricity are produced with CCS (H-50/50-CCS, Figure 5), the process design departs from the parallel case with CO_2 vented in

order to maximize carbon capture. In the H-50/50-CCS design, the full flow of syngas following gas cleanup is processed through a two-stage water gas shift area before the flow is split to deliver some gas to a gas turbine and some to a PSA for hydrogen purification. The removed CO_2 is compressed for pipeline delivery to an underground injection site. In the H-50/50-VENT case, most of the CO_2 had been delivered to the gas turbine for NO_x emission control and mass balance purposes, as well as to fully oxidize trace amounts of H_2S co-removed with the CO_2. In the H-50/50-CCS case, a small fraction of the captured CO_2 is used to pressurize the gasifier feeding system. The majority of the CO_2 is compressed for underground storage.

Overall, compared to the H-50/50-VENT design, hydrogen production is modestly higher in the H-50/50-CCS case due the 2-stages of WGS used. However, the production of exportable electricity falls considerably compared to the H-50/50-VENT case due in part to the greater onsite need for power (for CO_2 compression) and in part to the reduced output from the gas turbine and the steam turbine. The net result is that the effective efficiency of H_2 production falls from 74% in the H-50/50-VENT case to 55% in the H-5050-CCS case.

5 Cost Analysis

For each of the detailed plant designs discussed in Section 4 (and summarized in Table 3), we have developed capital costs and total production costs using a consistent set of data sources and values for financial parameters and other input assumptions (as will be discussed). We develop the detailed cost estimates for a reference plant size of 4,536 dry metric tons/day switchgrass input (5,000 dry short tonnes per day). Using component-level scaling exponents, we examine the impact of plant size on economics.

We have estimated capital costs at the sub-unit level for each major plant area in each process configuration, drawing on a variety of open and gray literature and industry experts. We have scrutinized the numbers given by these sources and made adjustments to original figures as appropriate (as discussed below) to develop a self-consistent set of capital cost estimates. For all process designs, we assume annual operating and maintenance costs are 4% of the overnight capital cost. For illustrative purposes, we assess production costs for three plant-gate prices of switchgrass: $\$2/GJ_{HHV}$, $\$3/GJ_{HHV}$, and $\$4/GJ_{HHV}$. For comparison, McGlaughlin *et al.* (2002), using the detailed agricultural sector model, POLYSIS, have estimated the switchgrass prices at which U.S. farmers could profitably convert farmland from current crops to switchgrass. McGlaughlin *et al*. found that delivered prices for switchgrass of $2.1/GJ, $3.0/GJ, and $3.4/GJ (HHV basis), corresponding to $30.3/dry metric ton (dmt), $44.0/dmt, and $52.4/dmt, would lead to conversion of 3.1 million ha, 16.8 million ha, and 21.3 million ha, respectively.

With capital, O&M, and biomass cost inputs, we calculate overall economic performance in terms of a levelized cost of stand-alone electricity generation or of fuels production. For fuels production plants we consider revenue from by-product electricity as a credit against total production costs, and we examine the influence of the electricity sale price on overall economics. We express all cost inputs and results in terms of constant 2003 U.S. dollars. We have used the GDP implicit price deflator to adjust cost inputs from other-year dollars when necessary (Council of Economic Advisors, 2004).[22]

[22] Some literature sources did not specify the cost basis year. In these cases we assumed a cost basis year one calendar year prior to the publication date. (For example, costs given in a report published in 1996 were assumed to be 1995 dollars.)

5.1 Definitions and Methodology

We first describe in generic terms the approach used to estimate costs. Notes in tables that appear later provide additional detailed information and assumptions.

Total Overnight Installed Capital Cost. We subdivided each plant into major process areas and sub-units within these areas. We estimate the capital cost for each sub-unit and sum all of these to obtain the total "overnight" installed capital cost (TOC). (We separately calculate interest during construction.) Calculating the TOC involved identifying from the literature or in consultation with experts appropriate reference costs for identical or similar equipment.[23] We refer to this as the base cost (C_o) for that type of equipment. The base cost includes installation, but generally excludes balance of plant (BOP) and indirect costs (IC) such as engineering and contingencies. Our approach for estimating BOP and IC are discussed further below.

The base cost refers to a particular equipment size (capacity), S_o, which in most cases is different from the required size (S_r) determined from our process simulations. We therefore scale the base cost (C_o) to estimate the cost of the equipment (C) at the scale of our simulation.[24]

In some cases, there are maximum allowed equipment sizes. These might be determined by structural limits for the operation or construction of a unit, or by the size of equipment that can be practically transported, e.g., by truck or by rail, to the construction site. Maximum scales assumed here are for truck delivery. If the required capacity or size (S_r) exceeds the practical maximum capacity (S_{max}) then multiple units must be installed. The number of units required (n) is calculated by rounding the right side of Equation 5 up to the nearest integer.

$$n = S_r / S_{max} \tag{5}$$

For our process designs where multiple gasifiers are required, we have assumed each gasifier would have associated with it a separate feed preparation area and separate gas cleaning train. We refer to each set of identical units in sequence surrounding the gasifier as a gasifier train. The capacity of each unit in a train, S, is given by Equation 6.

$$S = S_r / n \tag{6}$$

The cost of a unit of size S is determined from the base cost and size for that unit:

$$C = C_o \cdot \left(\frac{S}{S_o} \right)^f \tag{7}$$

[23] If the operating pressure of the reference equipment differed from the pressure used in this study, the reference cost was multiplied by a standard pressure factor to arrive at a new reference cost. Pressure multipliers for the cost of vessels and heat exchangers are from Guthrie (1969).

[24] For vessels handling gases or liquids, the volumetric flow rate of fluid defines the required size (assuming that residence time is constant or nearly so for similar units of different sizes). For solids handling, the solid mass feed rate defines the size. The size parameter of a compressor or pump is the amount of electricity consumed, and that of a heat exchanger is the amount of heat removed. The cost of power island equipment is assumed to scale with the electricity generating capacity.

where *f* is a scaling exponent that ranges between zero and one in value, and is close to 0.67 for many types of equipment.[25]

For multiple unit trains of equal size, the installed cost of each additional train will be somewhat less than the cost of the first train. This is because the two units may share some auxiliary equipment, the labor required to install two units is generally less than double that required for one, and the special machining and shop costs to construct the first unit are not all duplicated to construct the second. We capture this idea using the trained cost, C_m, of a unit, given by Equation 8:

$$C_m = C \cdot n^m \tag{8}$$

where *m* is the scaling exponent for multiple trains. We assume a value for *m* of 0.9.

For most of the equipment costs, the values of C_m were developed excluding balance of plant (BOP) costs (instrumentation and controls, building, civil works, electrical connections, piping, insulation, and site preparation). We then estimated the BOP cost for each unit as a percentage of C_m (except in the case of some units, as discussed below).[26] Hamelinck and Faaij (2001) have noted that the absolute cost of a power plant will grow more quickly with capacity than the BOP portion of the cost, so BOP as a % of total cost will be smaller the larger the plant size. We confirmed this by a careful review of literature cost studies for similar plants at varying scales. We have estimated an overall BOP percentage as a function of the higher heating value biomass energy input from a best fit of several literature estimates (Katofsky 1993; DeLong 1995; Stone and Webster *et al*. 1995; Weyerhaeuser 2000; Hamelinck and Faaij 2001; and Kreutz *et al*. 2005):

$$\text{BOP (\%)} = 0.8867 \,/\, \{(\text{biomass MW}_{\text{th}})^{0.2096}\} \tag{9}$$

For the reference plant size in this project (4,536 tonne/day), the thermal input is 983 MW_{HHV}, so BOP is 20.9 % of the installed cost. (At one-tenth this scale, the figure would be 33.9%.).

For the power island area, BOP is calculated differently, following the methodology of Kreutz *et al*. (2005). Power island BOP includes the components indicated above and also the cost of an electrical substation connection and equipment costs not included elsewhere.

The sum of C_m and BOP gives the total direct costs (TDC).

---

[25] While the value of 0.67 turns out to apply, approximately, for many types of equipment, it's origin is most apparent when considering a spherical reaction vessel. For such a vessel, the cost scales roughly with the amount of material needed to make the vessel, which in turn is closely related to its surface area: cost ~ $4\pi r^2$. Thus, for two vessels with different capacities, the ratio of costs is $\text{cost}_1/\text{cost}_2 \sim (r_1/r_2)^2$. Since the capacity of a spherical vessel is proportional to its volume $(4/3)\pi r^3$, we can write $\text{capacity}_1/\text{capacity}_2 \sim (r_1/r_2)^3$ or rearranging, this gives $(r_1/r_2) \sim (\text{capacity}_1/\text{capacity}_2)^{1/3}$. Putting this latter expression into the cost ratio gives $\text{cost}_1/\text{cost}_2 \sim (\text{capacity}_1/\text{capacity}_2)^{2/3}$.

[26] When an original equipment cost included BOP, these costs were stripped out (where the original data sources were sufficiently disaggregated to do this) for the purpose of developing consistent values of *C*. In some cases, the BOP fraction of an original cost estimate could not be disaggregated. These cases have been noted in tables presented in the next section.

Indirect costs (IC) are also incorporated into the analysis as percentages of TDC: 15% for engineering and head office, 5% for startup costs (including initial catalyst loadings), 1% for spares, and 1% for royalties. These values were obtained by comparing literature estimates for similar plants (Katofsky 1993; DeLong 1995; Stone and Webster *et al*. 1995; Mann and Spath 1997; Washington Group and Southern Company 2000; Weyerhaeuser 2000; Hamelinck *et al*. 2003; and Kreutz *et al*. 2005). Contingency costs are also included. Contingencies will vary with the level of experience with a technology and its manufacture and installation. For new and unproven technologies, contingencies could be 50% or more of TDC. Since we are considering future commercially mature systems, contingencies will be lower. We assign the power island and air separation unit equipment contingencies of 5%. The gasifier and gas cleanup areas involve inherently larger uncertainties associated with construction, so we assign a contingency of 10% for these areas. Thus, the total percentages of TDC used to calculate indirect costs were 32% for gasifier and gas cleanup islands and 27% for the ASU and power island areas. Table 5 summarizes the assumptions we used to estimate indirect costs.

Table 5. Our assumptions regarding indirect costs.

	Gasifier and gas cleanup islands	Air separation unit and power island
Engineering & head office	15%	15%
Contingency	10%	5%
Startup	5%	5%
Royalties, fees, etc.	1%	1%
Spare parts	1%	1%
Total	32%	27%

Finally, we define the sum of TDC and IC as the total overnight capital cost (TOC) for the plant.

Interest During Construction (IDC). We assume that construction of a plant will require four years, that a loan with interest rate, r, is taken to pay the TOC in equal annual end-of-the-year installments over the construction period, and that the plant starts generating revenue (at full capacity) immediately after the last payment. Then the total interest during construction (IDC) is calculated from the TOC by Equation 10:

$$IDC = (TOC/4)\cdot\left(1+(1+r)+(1+r)^2+(1+r)^3\right)-1 \qquad (10)$$

If r = 7.8%/yr,[27] then IDC is 12.3% of TOC. The total capital investment (TCI) is:

$$TCI = TOC + IDC = (TOC/4)\cdot\left(5+(1+r)+(1+r)^2+(1+r)^3\right)-1 \qquad (11)$$

Production cost. To calculate production costs, we use a capital charge rate (*ccr*) of 15% per year, which corresponds to financial parameter values shown in Table 6. We also assume annual non-fuel O&M costs (m_a) are 4% of TOC, which is an accepted value for gasification-based coal

[27] The interest rate of 7.8% per year is the after tax real cost of capital based on the financial calculation methodology of the Electric Power Research Institute Technical Assessment Guide (TAG), which assumes a 30 year book life and 20 year tax life with MACRS depreciation schedule.

power plants (Williams, 2000) and thus is probably also appropriate for gasification-based biomass plants.

Table 6. Financial parameter assumptions.

Parameter values for capital charge rate, *ccr* = 15% per year	
Debt fraction	75%
Equity fraction	25%
Interest rate on debt, %/year	9%
Return on equity, %/year	15%
Federal + state taxes	40%
Property taxes and insurance	2%
Economic lifetime, years	25
Depreciation method	20-yr MACRS[a]
Other parameter values in financial analysis	
Construction Time, years	3
Operating Capacity Factor, *CF*	85%
Annual cost maintenance as % of TOC, m_a	4%
Alternative biomass prices, P_b ($/GJ)	2.1, 3.0, 3.4

(a) Modified Accelerated Cost Recovery System (MACRS) is a property depreciation system defined by the Internal Revenue Service that applies to assets placed in service after 1986. It results in more rapid depreciation than straight-line depreciation.

For stand-alone electricity production and for fuels production with co-produced electricity, the levelized production costs are, respectively:

$$\text{Stand-alone Electricity (\$/kWh)} = \frac{(ccr \times \text{TCI}) + (m_a \times \text{TOC}) + (P_b \times \text{B}_\text{T})}{\text{E} \times (24 \times 365 \times CF \text{ hrs/yr})} \quad (12)$$

and

$$\text{Fuel cost (\$/GJ)} = \frac{(ccr \times \text{TCI}) + (m_a \times \text{TOC}) + (P_b \times \text{B}_\text{T}) - (e \times P_e)}{\text{F} \times (24 \times 365 \times CF \text{ hrs/yr})} \quad (13)$$

where E is the rated plant electricity production capacity, F is the rated plant fuel production capacity, CF is the plant capacity factor, P_b is the cost of switchgrass, B_T is the total amount of biomass consumed each year, *e* is the amount of co-product electricity sold by a fuel producer, and P_e is the price at which this electricity is sold. Table 6 shows other financial parameter values assumed for these calculations. Of particular note is the capacity factor of 80%. This relatively low value (for baseload operation) is used because we assume no spare gasifier capacity. (Assuming a higher capacity factor could be justified if a spare gasifier were included in the capital cost estimate.)

5.2 Capital and Production Cost Estimates

5.2.1 Stand-Alone Electricity Production

5.2.1.1 Capital Costs

Table 7 gives values of S_o, S_{max}, C_o, and f used to develop the capital cost estimate for the BIGCC-VENT case.[28] Sources of the estimates are detailed in the table notes. Table 8 shows the resulting estimated total capital investment is \$481 million, or \$1090 per kW_e of installed capacity.

Table 7. Reference capacities, capital costs, and scaling factors for major plant areas and sub-units used in cost analysis of the B-IGCC-VENT case.

		Capacities (in indicated units)			Cost (in million 2003 $)	
		Base	Max. unit	Unit of Capacity	Base	Scaling exponent
Plant Area	**Sub-Unit**	S_o	S_{max}		C_o[a]	f
Gasifier Island	Feed preparation[b]	64.6	n.a.	wet tonne/hr biomass	9.84	0.77
	Gasifier[c]	41.7	120	dry tonne/hr biomass	6.41	0.7
	Ash Cyclone[d]	68.7	180	actual m^3/s gas feed	0.91	0.7
	Lockhopper N_2 boost comp[h]	10	n.a.	MW_e consumed	4.14	0.67
Gas Cleanup	Syngas cooler[e]	77	n.a.	MW_{th} heat duty	25.4	0.60
	Ceramic filter[f]	14.4	n.a.	actual m^3/s gas feed	18.6	0.65
Air Separation Unit	ASU[g]	76.6	n.a.	tonne/hr pure O_2	22.7	0.5
	O_2 compressor[h]	10	n.a.	MW_e consumed	5.54	0.67
	N_2 compressor[h]	10	n.a.	MW_e consumed	4.14	0.67
Power Island	Gas turbine[i]	266	334	GT MW_e	56.0	0.75
	HRSG + heat exchangers[j]	355	n.a.	MW_{th} heat duty[k]	41.2	1.0
	Steam cycle[l]	136	n.a.	ST gross MW_e	45.5	0.67

Notes to Table 7

(a) The GDP implicit price deflator (Council of Economic Advisors, February 2004) has been used to convert to constant 2003 dollars from other year dollars when necessary.

(b) Weyerhaeuser (2000) gives the following installed "N^{th} plant" equipment costs (in 1999$) for feed preparation to feed 64.6 wet tonnes/hr wood chips to a near-atmospheric pressure gasifier: conveyor, \$851,000; dried wood chip storage, \$561,000; feed bin, \$233,000; rotary air lock, \$329,000; and water cooled feed screw, \$54,000. We have multiplied these by 1.45 (Guthrie, 1969) to calculate the cost of a feed preparation system rated for 30 bar, and by a factor of 3.1 to account for the lower bulk density of chopped switchgrass compared to wood chips. [The ratio of the average bulk density for softwood chips to chopped straw is given by Jenkins (1989) to be 3.1. We assume equipment cost scales linearly with bulk density.] We derived the value of f by calculating an overall scaling factor for a feed preparation system with a base capacity of 33.5 wet tonnes/hour from Hamelinck and Faaij (2001) consisting of conveyors (C_o = $\$_{2001}$ 0.35M, f = 0.8), storage (\$1.0M, 0.65), and a feeding system such as a lock hopper and feed screw (\$0.41M, 1). Scaling the resulting total feed preparation cost for values of S/S_o between 1 and 3.5 gives an overall scaling factor of 0.77. The cost estimates from Hamelinck and Faaij (2001) were not used directly here for C_o because they represent first-of-a-kind plant cost estimates, whereas Weyerhaeuser (2000) gives estimates for an N^{th} plant.

(c) From Hughes (2003), the cost of an oxygen-blown GTI gasifier operating at 7.93 bar processing 400 dry tpd of bagasse (20% moisture content) is \$5 million in 2002 dollars. This price includes installation labor and is given for an N^{th} plant design. From Guthrie (1969), the cost of a pressure vessel rated for 30 bar (the gasifier used in the simulation) is 1.26 times that of a pressure vessel rated for 7.93 bar. Therefore the reference cost of \$5 million is multiplied by 1.26 to obtain a base cost, C_o, of \$6.3 million. Following Lau, *et al.* (2003), the maximum capacity of an oxygen-blown GTI gasifier operating at atmospheric pressure is roughly 625 dry tpd, at 25 bar is roughly 2500 tpd, and at 30 bar is roughly 15% greater than that at 25 bar (i.e. 2875 tpd). All three of these units would have the same physical dimensions; the increased capacity comes from

[28] The basis for estimating capital costs for stand-alone power generation systems developed previously by the authors (Larson *et al.*, 2004) is updated here.

the smaller volume of gas per tonne of biomass produced in the higher pressure gasifiers. From this information, the maximum capacity of a GTI gasifier in tpd can be calculated at any pressure by 77.8x + 549, where x is the pressure in bar. The maximum capacity at 7.93 bar is 1165 tpd, roughly 40% of the capacity at 30 bar. This means that a 400 tpd gasifier (7.93 bar) could process 2.5 x 400 tpd, or 1000 tpd, if it were pressurized up to 30 bar. For this reason, 1000 tpd (41.7 tonnes/hr) is used as the value of S_o corresponding to a 30 bar gasifier with the same dimensions as the 7.93 bar gasifier from Hughes (2003). S_{max} is taken from the above discussion of Lau, et al. (2003) where the maximum capacity of a 30 bar GTI gasifier is roughly 2875 tpd or 119.8 tonnes/hr. f for a GTI gasifier is assumed to have a value of 0.7 based on Katofsky (1993), Williams *et al*. (1995), Tijmensen (2000), Hamelinck and Faaij (2001), Tijmensen *et al*. (2002), and Hughes (2003).

(d) From Weyerhaeuser (2000), a cost of $584k (1999 dollars), was extracted for a cyclone separator. The ash cyclone is similar to a combustor primary cyclone, and the cost scales with the volumetric flowrate of gas through the unit. Installation labor is included in this cost. This cost is multiplied by 1.45 (Guthrie, 1969) to calculate the cost of a cyclone separator rated for 30 bar. The combustor primary cyclone in Weyerhaeuser (2000) is only rated for near-atmospheric pressure operation. Cost is given for an N^{th} plant design. S_o is volumetric gas feed to the combustor primary cyclone in Weyerhaeuser (2000), calculated from the gas mass flow using the temperature, pressure, average molecular weight, and the ideal gas law (for simplicity). S_{max} and f are taken from Hamelinck *et al*. (2003) for a cyclone separator.

(e) Based on Simbeck (2004), who gives $\$310/kW_{th}$ of saturated steam produced in a firetube syngas cooler producing 77 MW of such steam from 1000°C input syngas, or $24 million (year 2000$). This cost excludes BOP and indirects. The latter are included (using methodology discussed in text) when total plant costs are estimated later in this paper. Scaling exponent for high-temperature heat exchangers is taken from Hamelinck *et al*. (2003).

(f) From Newby *et al*. (1998), a cost of $14.6 M (1997 dollars) was extracted for a ceramic candle filter ($36.0/kW for a 406 MW coal IGCC plant). This cost does not include installation labor, so 15% is added (Craig and Mann, 1996). It is given for a N^{th} plant. S_o is the gas feed rate to the ceramic filter evaluated in Newby *et al*. (1998). f is taken to have the same value as for a fabric filter in Hamelinck *et al*. (2003).

(g) From Kreutz *et al*. (2005), we extracted a cost estimate of $40.4 million (in 2002$) for a standalone air separation unit with an air compressor. This cost includes installation, BOP, engineering and contingency, and is given for an N^{th} plant design. In order to achieve a consistent basis in accounting for indirect costs, engineering and contingency costs were removed from the costs reported in Kreutz *et al*. (2005) to obtain C_o. In Kreutz *et al*. (2005), the total direct cost (TDC) is the sum of the installed equipment cost and BOP. For the ASU, engineering is 10% of TDC, and contingency is 5% of TDC + engineering. Therefore, to subtract engineering and contingency from Kreutz's cost we divide by (1.1x1.05), yielding $35.0 million (or $35.6 million when converted to 2003$). Thus BOP is included in C_o for the ASU, while indirect costs are not. Values of S_o and f are also taken from Kreutz *et al*. (2005). The ASU used in this study is integrated with the gas turbine, and so no separate air compressor is needed. It has been estimated (using our own Aspen Plus model of a standalone ASU) that a 76.6 tonne/hr O_2 ASU plant requires a 25.7 MW air compressor which costs $7.7M (see note h below for derivation of air compressor costs). Thus, the cost of the integrated ASU (w/o air compressor) is estimated as $35.0M less $7.7M, or $27.3M. The ASU used in this study also operates at a higher pressure than a standalone ASU due to the integration with the gas turbine and thereby higher input air pressure. This means that the dimensions of the ASU "cold box" (which includes the high pressure and low pressure distillation columns and the low temperature heat exchangers - essentially everything except the air compressor) are smaller than those needed for a standalone plant producing the same rate of pure oxygen. According to Moore (2003), doubling the pressure in the cold box would reduce the physical size of the required distillation columns and other cold box equipment by about half while producing the same rate of pure oxygen. For the ASU, the cost scales with physical size according to a scaling exponent of 0.5 (Kreutz *et al*. 2005, Moore 2003), so halving the size leads to a cost of (1/2)^0.5 = 0.707 times the larger size. In our case, the pressure of cold box units are on average 1.5 times those in a standalone ASU, so the roughly 1.5x reduction in size leads to a cost that is (1/1.5)^0.5 = 0.81 times the cost of the lower pressure unit, or a final value of $22.3M (2002 dollars) for C_o ($22.7M in 2003 dollars).

(h) From Kreutz *et al*. (2005), the following original costs, in millions of 2002 dollars, were extracted for compressors: for oxygen compressors, $6.3M; nitrogen compressors, $4.7M; and PSA purge gas compressors, $6.28M. Here, air compressors are assumed to cost the same as nitrogen compressors, and syngas compressors are assumed to cost the same as purge gas compressors. The former assumption rests on the fact that air is mostly nitrogen. The latter assumption rests on the fact that both the biomass gasification-based syngas in this study and the PSA purge gas in Kreutz *et al*. (2005) are low heating value gases consisting mainly of CO, CO_2, H_2O, and H_2. These costs include installation, BOP, engineering and contingency, and are given for an N^{th} plant design. In order to achieve a consistent basis in accounting for indirect costs, engineering and contingency costs were removed from the costs reported in Kreutz *et al*. (2005) to obtain C_o. In Kreutz *et al*. (2005), the total direct cost (TDC) is the sum of the installed equipment cost and BOP. For oxygen and nitrogen compressors, engineering is 10% of TDC, and contingency is 5% of TDC + engineering. For purge gas compressors, engineering is 15% of TDC, and contingency is 15% of TDC + engineering. Therefore, to obtain C_o for oxygen and nitrogen compressors, the cost from Kreutz *et al*. (2005) is divided by (1.1x1.05), and to obtain C_o for purge gas compressors, the cost is divided by (1.15x1.15). Thus BOP is included in C_o for compressors, while indirect costs are not. Values of S_o and f are also taken from Kreutz *et al*. (2005).

(i) Kreutz *et al*. (2005) indicates an installed cost of $72.8 million (2002$) for a Siemens V94.3A gas turbine (266 MW_e outpute), the turbine design on which our simulation is based. This cost includes BOP, installation, engineering (15% of installed gas turbine +BOP), and contingencies (15% of installed gas turbine +BOP +engineering). The value in this table for base cost excludes the engineering and contingencies and has been converted to 2003$. Engineering and contingencies are included (using methodology discussed in text) when total plant cost is estimated later in this paper. The assumed scaling exponent was obtained by taking a power-series regression of equipment-only costs vs. power output for all simple cycle gas

turbine generators in Gas Turbine World's 2003 Handbook (Anonymous, 2003). The value for S_{max} is the power rating of the largest simple-cycle gas turbine generator in Gas Turbine World's 2003 Handbook. For some of the plant designs discussed later, the included gas turbine capacity is considerably smaller than the capacity of a Siemens V94.3A turbine. Our process simulation assumes the unit performance will be the same in all cases, but our cost estimation methodology accounts for higher costs for smaller units.

(j) Based on Simbeck (2004), who indicates a cost of $\$110/kW_{thermal}$ of superheated steam for an "HRSG Boiler" (year 2000$), or $39 million for a unit producing 355 MW superheated steam. Simbeck excludes BOP and indirects. We include the latter (using methodology discussed in text) when total plant costs are estimated later in this paper. We apply this cost to the heat transfer duty (based on our pinch analysis) that takes place in all heat exchangers throughout the plant (except for the syngas cooler and any water gas shift reactors, since we account for the cost for the syngas cooler and WGS heat exchangers separately). Most of the heat transfer in the process is associated with raising superheated steam. (For example, in the B-IGCC-VENT case, approximately 80% of total system heat transfer is accounted for as superheated steam.) Residual heat transfer includes raising warm water for saturators in some cases and heat rejection to cooling water. Our calculation method here implicitly costs heat exchangers needed for these low-temperature heat transfer functions at the same cost per kW transferred as for raising superheated steam. This may overestimate the costs of these lower-temperature heat exchangers. We assume a scale factor of unity, since this cost element for a full plant will typically include several heat exchangers.

(k) Total heat transfer rate considering all heat exchange in the process, except for heat transfer in the syngas cooler and (when present in a system) water gas shift reactors. See previous note for additional discussion.

(l) Kreutz *et al*. (2005) indicates an installed cost of $59.2 million (2002$) for a steam cycle (steam turbine and condenser) with a gross output of 136 MW_e. This cost includes installation BOP, engineering (15% of installed gas turbine +BOP), and contingencies (15% of installed gas turbine +BOP +engineering). The value in this table for base cost is expressed in 2003$, excluding the engineering and contingencies. The latter are included (using methodology discussed in text) when total plant cost is estimated later in this paper. Scale factor is from Kreutz *et al.* (2005)

The overnight capital cost ($\$970/kW_e$) is somewhat lower than most previously published cost estimates for BIGCC plants. This apparent discrepancy is largely resolved when one accounts for the scale of the BIGCC plants examined in the different cost studies. Figure 17 shows the total overnight capital cost as a function of plant scale for the BIGCC system examined here. (Discontinuities in the BIGCC curve reflect changes in the number of gasifier trains or gas turbine trains.) Overnight capital costs estimated by others for N^{th} plant BIGCC systems (with various equipment configurations) are shown as points on this graph. The largest plant for which we found a cost estimate in the literature is 215 MW_e. Below this scale, our costs fall within the range of costs reported in the literature.[29] This provides some basis for confidence in our cost estimates at the larger scales.

One further calibration of our cost estimate can be made by a comparison against estimated N^{th} plant costs for coal-IGCC (C-IGCC). Kreutz, *et al.* (2005) have developed such estimates for several C-IGCC plant configurations with net electricity generation of about 400 MW_e. (A number of the major component costs in our BIGCC estimates are derived from the work of Kreutz, *et al.*) For specificity, we consider their plant design that uses a Texaco-type quench gasifier and generates 390 MW_e of electricity. Kreutz *et al.*'s estimated overnight capital cost for this plant is shown in Table 9 alongside our results for a 390 MW_e scale BIGCC. The C-IGCC overnight installed capital cost is $470 million. Our BIGCC cost estimate is $391 million. The difference between these costs can be explained as follows:

- Feed preparation for biomass is more costly than for coal due primarily to the lower bulk density of biomass.

[29] Our cost curves were developed assuming electricity generating efficiency is the same at all scales. Since efficiency would actually decrease somewhat with decreasing scale, our cost estimates in Figure 17 may underestimate actual costs at the lower end of the scale range.

Table 8. Capital cost estimate for the B-IGCC-VENT case.

		Capacities (in indicated units)				Costs (in million 2003 $)		
		Required capacity	Number of units	Capacity per unit	Unit of Capacity	Cost per unit	Train cost	Overnight Cost
Plant Area	Sub-Unit	S_r	n[a]	S[b]		C[c]	C_m[d]	OC[e]
Gasifier Island	Feed preparation	236	2	118	wet tonne/hr biomass	15.7	29.2	46.6
	Gasifier	189	2	94.5	dry tonne/hr biomass	11.4	21.2	33.9
	Ash Cyclone	16.3	2	8.1	actual m^3/s gas feed	0.21	0.38	0.61
	Lockhopper N_2 boost comp	0.33	1	0.33	MW_e consumed	0.42	0.42	0.54
Gas Cleanup	Syngas cooler	124	2	62	MW_{th} heat duty	21.9	40.9	65.4
	Ceramic filter	8.1	2	4.0	actual m^3/s gas feed	8.1	15.2	24.2
Air Separation Unit	ASU	61.3	1	61.3	tonne/hr pure O_2	20.3	20.3	25.7
	O_2 compressor	5.3	1	5.3	MW_e consumed	3.6	3.6	4.6
	N_2 compressor	10.8	1	10.8	MW_e consumed	4.4	4.4	5.5
Power Island	Gas turbine	268	1	268	GT MW_e	56.2	56.2	71.4
	HRSG + heat exchangers	433	1	433	MW_{th} heat duty[f]	50.3	50.3	77.2
	Steam cycle	190	1	458	ST gross MW_e	57.0	57.0	72.4
Total Overnight Capital Cost (million $)						428		
Interest during construction (million $)[g]						53		
Total Capital Investment (million $)						481		
Total Capital Investment per unit capacity ($/$kW_e$)						1090		

(a) Number of units determined by rounding $n = S_r / S_{max}$ up to the nearest integer. This gives $n = 1$ whenever $S_r \leq S_{max}$ and leads to multiple units whenever $S_r > S_{max}$. We assume each gasifier is coupled to its own feed preparation area and gas clean up island. Thus, the number of feed preparation/clean up trains equals the number of gasifiers as determined by the equation above. The values of S_r are determined from the process simulation results for a 4536 tonnes/day plant.

(b) Capacity of each unit given by $S = S_r / n$. If $n = 1$, $S = S_r$.

(c) Cost per unit given by $C = C_o \cdot (S/S_o)^f$. See Table 7for values of C_o, S_o, and f for individual process units. For some units, C will include BOP (see notes g, h, and i in Table 7), but indirect costs are not included in any values of C (see note e below for discussion of indirect costs).

(d) C_m is the cost after accounting for scale economies involved with multiple trains. The cost for all n multiples of a unit is given by $C_m = C \cdot n^m$, where $m = 0.9$.

(e) Overnight capital cost (OC) for each capital unit is the installed cost, plus the balance of plant, plus the indirect costs, or OC = C_m + BOP + IC. Some installed costs (C_m) in Table 7already include BOP (see note c). For the power island, BOP is estimated as a separate component based on Kreutz *et al.* (2005). For all other components, we estimate BOP to be 20.9% of installed cost. This percentage was determined as follows. Hamelinck and Faaij (2001) note that the total cost of a plant as a whole grows more quickly with capacity than the BOP cost, so BOP as a % of total cost will be smaller the larger the plant size. We have estimated the % BOP as a function of energy input (biomass HHV MW_{th}) to a B-IGCC plant from a best fit of several literature sources' estimates (Katofsky 1993, DeLong 1995, Stone and Webster *et al*. 1995, Weyerhaeuser 2000, Hamelinck and Faaij 2001, Kreutz *et al*. 2005) for similar plants at varying scales. BOP (%) = 0.8867 / {(biomass MW_{th})$^{0.2096}$}. For the 4536 tonne/day scale investigated in this project, the thermal input (HHV) is 983.2 MW, so that BOP is 20.9 % of the installed cost. Indirect costs were estimated from review of several literature sources (Katofsky 1993, DeLong 1995, Stone and Webster *et al*. 1995, Mann and Spath 1997, Washington Group and Southern Company 2000, Weyerhaeuser 2000, Hamelinck *et al*. 2003, Kreutz *et al*. 2005). For gasifier island and gas cleanup units, IC = 32% of TDC, and for power island and air separation unit units, IC = 27% of TDC. Thus for a typical gasifier island or gas cleanup unit, OC = C_m x (1.209) x (1.32) = 1.60 C_m. For an air separation unit or power island unit, since BOP is already included in C_o or accounted for as a separate item, OC = C_m x (1.27).

(f) Total heat transfer rate considering all heat exchange in the process, except for heat transfer in the syngas cooler. See note (j) in Table 7 for additional discussion.

(g) This is 12.3% of the overnight cost, which is based on a four-year construction period, cost of capital of 7.8%/year, and equal payouts at the end of each construction year.

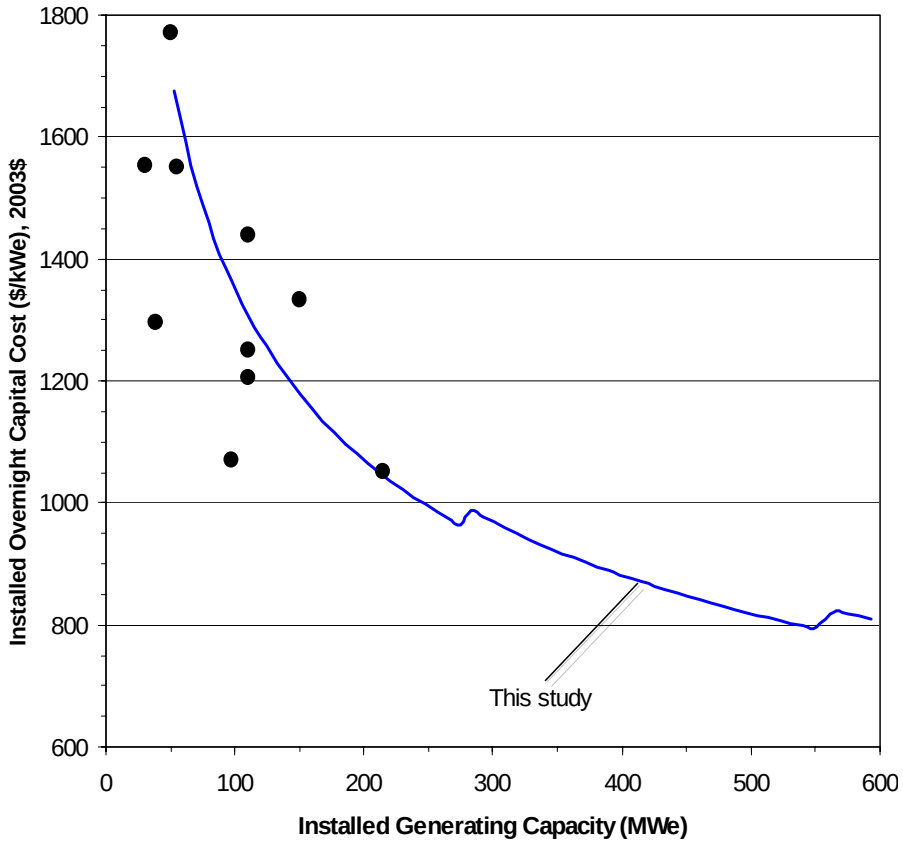

Figure 17. Estimates of installed overnight capital cost ($/kW) for electricity generating plants with BIGCC-VENT design (solid line), with comparisons to literature cost estimates (points) for commercially-mature (N^{th} plant) gasification-based power plant designs. The literature estimates are from USDOE and EPRI (1997), Faaij, *et al.* (1998), and Bain, *et al.* (2003).

- The biomass gasifier operates at a lower pressure (30 bar) than the coal gasifier (70 bar), and without ash slagging, but the resulting cost savings[30] are largely offset by the high cost for both a syngas cooler and hot-gas particle filter in the BIGCC case. (Neither of these are present in the C-IGCC design.)
- The low sulfur content of switchgrass obviates the need for any sulfur capture and recovery in the BIGCC case, since NSPS sulfur emission standards can be met without sulfur removal. In contrast, the C-IGCC cost includes $70 million in sulfur-related capital costs.
- Differences in the scale and design of the ASU account for the difference in ASU costs between the two systems. Unlike coal, biomass contains some oxygen and therefore requires less added oxygen for gasification. Also biomass is gasified at lower temperatures than coal, further reducing the required capacity of the ASU. For the systems in Table 9, the coal gasifier consumes 101 t/hr of O_2 and the biomass gasifier uses 61 t/hr O_2. Since the cost for a stand-alone ASU scales with the square root of capacity (Table 7), the BIGCC ASU could be expected to cost 77% of the C-IGCC ASU, if the ASU designs were otherwise the same. The ASU in the C-IGCC case is a stand-alone unit. In the BIGCC case it is integrated with the gas turbine, which eliminates the large air compressor needed with a stand-alone ASU. Based on Smith, *et al.* (1997) the air compressor accounts for about 20% of the total ASU

[30] Based on Guthrie (1969), a gasifier operating at 70 bar would cost about 70% more than a gasifier operating at 30 bar, if all other design features are the same.

cost at the ASU scale considered here. Moreover, with an integrated ASU, the pressure of air delivered to the ASU (from the gas turbine) will be higher than that from a standalone ASU's air compressor. The elevated pressure would result in cost savings due to smaller equipment in the ASU cold box. As detailed in Note g of Table 7, a higher-pressure cold box is estimated to cost 81% of a lower-pressure cold box. The smaller oxygen requirement, the elimination of the air compressor, and the smaller cold box for the BIGCC case explain the $23 million difference in ASU costs shown in Table 9.[31] Also, because of the integrated ASU design, lower pressure-ratio (less costly) oxygen and nitrogen compressors can be used in the BIGCC case compared with the C-IGCC case.

- The power island components in the BIGCC design are less costly than their counterparts in the C-IGCC design in absolute terms, but individual costs for the gas turbine and the steam turbine are consistent between the two designs. For the C-IGCC, the gross ouput of the gas turbine is 294 MW, which gives a unit cost of $252/kW. For the BIGCC design, the gross gas turbine output is 236 MW, for a unit cost of $275/kW. Similarly, for the steam turbine and condenser, the gross output in the C-IGCC case is 179 MW, for a unit cost of $403/kW. For the BIGCC case, the gross steam turbine output is 168 MW, for a unit cost of $396/kW.

Thus, our BIGCC cost estimate appears consistent with N^{th} plant cost estimates for C-IGCC technology at the scale of about 400 MW_e.

Table 9. Comparison of overnight installed capital costs for a 390 MW_e coal-IGCC plant as estimated by Kreutz et al. (2005) (case EVQ[a]) and a 390-MW_e B-IGCC (developed using methodology and inputs discussed in this report).

	Million 2003 $	
Plant area	**Coal-IGCC**	**Biomass-IGCC**
Feed preparation, handling	36.0	42.5
Gasifier	76.3	31.7
Syngas cooler, gas cleanup		83.3
Air separation unit	47.0	24.2
Oxygen compressor	9.0	4.2
Nitrogen compressor	10.7	5.1
Sulfur capture	41.5	0.0
Sulfur recovery	28.2	0.0
Gas turbine	74.0	64.9
HRSG and heat exchangers	72.4	68.4
Syngas expander	3.0	--
Steam cycle (turbine + condenser)	72.2	66.5
Total	**470**	**391**

(a) Texaco-type gasifier, with quench gas cooling, Selexol H_2S removal, Claus/SCOT sulfur recovery, stand-alone ASU, Siemens 94.3A gas turbine combined cycle. Costs originally in 2002$ converted to 2003$ using GDP deflator.

Compared to the BIGCC-VENT case, stand-alone power production with carbon capture (BIGCC-CCS) requires substantial additional capital expenditure for water gas shift reactors and a CO_2 removal system. Table 10 shows the reference costs used to developed the capital cost

[31] The coal-IGCC ASU cost is $47.2 million. Accounting for the smaller required O_2 capacity reduces this to (0.77*47.2 =) $36.3 million. Eliminating the air compressor reduces this to (0.80*36.3 =) $29.1 million. Finally, reflecting the cost reduction with a higher-pressure cold box reduces this to (0.81*29.1 =) $23.6 million.

estimate for the BIGCC-CCS system. The estimated overnight installed cost for a system consuming 5000 dry tonnes per day of switchgrass is estimated to be $502 million (Table 11), or a seemingly modest 17% more than the cost for a BIGCC-VENT system processing the same amount of biomass. However, because the system with CCS produces about 20% less electricity than the VENT design, the overnight cost per kW of installed net generating capacity is about 45% higher with CCS. Figure 18 compares the overnight installed costs for the VENT and CCS designs as a function of the net installed generating capacity.

Table 10. Reference capacities, capital costs, and scaling factors for major plant areas and sub-units used in cost analysis of the B-IGCC-CCS case.[a]

		Capacities (in indicated units)			Cost (in million 2003 $)	
		Base	Max. unit	Unit of Capacity	Base	Scaling exponent
Plant Area	Sub-Unit	S_o	S_{max}		C_o	f
Gasifier Island	Feed preparation	64.6	n.a.	wet tonne/hr biomass	9.84	0.77
	Gasifier	41.7	120	dry tonne/hr biomass	6.41	0.7
	Ash Cyclone	68.7	180	actual m^3/s gas feed	0.91	0.7
Gas Cleanup	External tar cracker[b]	47.1	52	actual m^3/s gas feed	0.732	0.7
	Syngas cooler	77	n.a.	MW_{th} heat duty	25.4	0.60
	Ceramic filter	14.4	n.a.	actual m^3/s gas feed	18.6	0.65
Carbon Capture Island	Saturator[c]	20.9	n.a.	actual m^3/s gas feed	0.30	0.70
	WGS reactors[d]	1377	n.a.	MW_{LHV} biomass input	30.6	0.67
	Rectisol AGR[e]	0.20	n.a.	million Nm^3/hr gas feed	20	0.65
	AGR compressor[f]	10	n.a.	MW compressor power	4.83	0.67
	CO_2 compressor[g]	10	n.a.	MW compressor power	4.75	0.67
	Supercritical CO_2 comp.[h]	13	n.a.	MW compressor power	7.28	0.67
Air Separation Unit	ASU	76.6	n.a.	tonne/hr pure O_2	22.7	0.5
	O_2 compressor	10	n.a.	MW compressor power	5.54	0.67
	N_2 compressor	10	n.a.	MW compressor power	4.14	0.67
Power Island	Gas turbine	266	334	GT MW_e	56.0	0.75
	HRSG + heat exchangers	355	n.a.	MW_{th} heat duty	41.2	1
	Steam cycle (turbine + cond.)	136	n.a.	ST gross MW_e	45.5	0.67

(a) Unless otherwise noted, numbers are taken from Table 7.

(b) Cost is based on Weyerhaeuser (2000), who gives a cost of $0.678 million (in 1999$) for a tar cracker passing 50.2 metric tonnes per hour of gas (or 47.1 m^3/s of gas at the actual temperature and pressure in the Weyerhaeuser study, assuming ideal gas). The estimated maximum capacity and scaling factor are taken from Hamelinck, *et al.* (2003).

(c) The cost for a saturator has been modeled from that for a gas cleanup scrubber (Weyerhaeuser, 2000), since the technologies are similar. Weyerhaeuser (2000) gives a cost of $0.206 million (in 1999$) for a scrubber processing 50.2 tonnes of synthesis gas at close to atmospheric pressure (or 47.1 m^3/s of gas at the actual temperature and pressure in the Weyerhaeuser study, assuming ideal gas). The cost in the table above is a result of converting to 2003$ and multiplying by a pressure factor (derived from Guthrie, 1969) of 1.35 to account for operating at 27.6 bar instead of atmospheric pressure. The scaling factor is based on Hamelinck, *et al.* (2003).

(d) Based on Kreutz *et al.* (2005), who give a cost of $39.8 million (in 2002$) for a 2-stage water gas shift system (including heat recovery) processing all syngas from a Texaco-type coal gasifier with input of 1377 MW coal (LHV). The cost includes BOP, indirects (15%), and contingencies (15%). The number in this table excludes the indirects and contingencies and is expressed in 2003$. (Indirects and contingencies are included in the total plant costs calculated later in this report, e.g., see Table 11 for B-IGCC-CCS case.)

(e) This installed cost estimate is from a personal communication (in 2003) with U. Koss of Lurgi, which licenses Rectisol technology. We assume this estimate excludes BOP and indirect costs. The latter are included (using methodology discussed in text) in estimating total installed capital cost for the B-IGCC-CCS and other cases utilizing a Rectisol unit.

(f) The Rectisol system captures small amounts of CO, H_2, and CH_4 in addition to CO_2 and H_2S (as discussed in text). The CO, H_2, and CH_4 are separated from the CO_2 and H_2S and fed back to the syngas stream downstream of the Rectisol plant. This compressor raises the pressure of the CO, H_2, and CH_4 to the main syngas stream pressure. The cost for this compressor is modeled after that for a syngas compressor, as indicated by Kreutz *et al.* (2005). See note (h) of Table 7 for discussion.

(g) This compressor is used to pressurize the CO_2 stream captured by the Rectisol plant up to a pressure of 31.4 bar (as required for use in the feed lockhopper). Cost is based on Kreutz et al. (2005), who give a cost of $6.28 million (in 2002$) for a 3-stage intercooled purge-gas compressor at a scale of 10 MW_e compressor capacity. The $6.28 million includes BOP, indirects (15%), and contingencies (15%). The cost in this table includes BOP, but indirects and contingencies have been factored out (to enable a consistent percentage indirects and contingencies to be included in the cost estimates for specific plants). See note (h) of Table 7 for additional discussion of compressor costing.

(h) This compressor pressurizes captured CO_2 from 31.4 bar (see previous note) up to 150 bar (supercritical). Kreutz et al. (2005) give a cost of $14.8 million (in 2002$) for a CO_2 dehydration and compression system (to 150 bar) at a scale of 13 MW_e. Of this total, 36% is due to the dehydration equipment, which is not needed in our designs because the CO_2 emerges dry from the Rectisol area. Kreutz's cost includes BOP, indirects (15%), and contingencies (15%). The cost in this table includes BOP, but indirects and contingencies have been factored out (to enable a consistent percentage indirects and contingencies to be included in the cost estimates for specific plants).

Table 11. Capital cost estimate for the B-IGCC-CCS case.[a]

		Capacities (in indicated units)				Costs (in million 2003 $)		
		Required capacity	Number of units	Capacity per unit	Unit of Capacity	Cost per unit	Train cost	Overnight Cost
Plant Area	**Sub-Unit**	S_r	n	S		C	C_m	OC
Gasifier Island	Feed preparation	236	2	118	wet tonne/hr biomass	15.7	29.2	46.64
	Gasifier	189	2	94.5	dry tonne/hr biomass	11.4	21.2	33.9
	Ash Cyclone	15.7	2	7.9	actual m^3/s gas feed	0.20	0.37	0.60
Gas Cooling and Cleanup	External tar cracker	15.7	2	7.9	actual m^3/s gas feed	0.21	0.39	0.62
	Syngas cooler	81.1	2	41	MW_{th} heat duty	17.3	32.2	51.4
	Ceramic filter	9.1	2	4.6	actual m^3/s gas feed	8.82	16.5	26.3
Carbon Capture Island	Pre-WGS saturator	8.5	1	8.5	actual m^3/sec	0.16	0.16	0.25
	WGS reactors[b]	849	1	849	MW_{LHV} biomass input	22.1	22.1	29.2
	Rectisol AGR	363314	1	363314	Nm^3/hour gas feed	29.5	29.5	47.1
	AGR compressor	0.05	1	0.05	Compressor MW_e	0.14	0.14	0.19
	CO_2 compression	22.78	1	22.78	Compressor MW_e	8.38	8.38	11.1
	Supercritical CO_2 comp.	9.01	1	9.01	Compressor MW_e	5.69	5.69	7.51
Air Separation Unit	ASU	61.9	1	61.9	tonne/hr pure O_2	20.4	20.4	25.9
	O_2 compressor	5.4	1	5.4	MW_e consumed	3.65	3.65	4.64
	N_2 compressor	10.9	1	10.9	MW_e consumed	4.39	4.39	5.57
Power Island	Gas turbine	241.5	1	241.5	GT MW_e	51.0	51.0	66.1
	HRSG + heat exchangers	451.9	1	451.9	MW_{th} heat duty[c]	52.1	52.1	80.6
	Steam cycle	164	1	164	ST gross MW_e	52.5	52.5	65.5

Total Overnight Capital Cost (million $)	503
Interest during construction (million $)[d]	62
Total Capital Investment (million $)	565
Total Capital Investment per unit capacity ($/$kW_e$)	1605

(a) See the relevant notes to Table 8 for descriptions of the column-heading parameters in this table.

(b) Kreutz et al. (2005) gives a cost for WGS that is scaled with the lower heating value of coal input to the plant. In some plant configurations we have analyzed, the WGS reactor does not process all of the syngas from the gasifier. Therefore, we assume that the WGS area in our plant configuration for maximum hydrogen production (H-MAX-VENT) is the WGS area most closely resembling the WGS area modeled by Kreutz (in his coal-H_2 production designs). The molar flow of syngas to the WGS in that case is 6.24 kmol/s. The molar flow of syngas to the WGS reactors in the B-IGCC-CCS case is 6.90 kmol/s (due to added water vapor absorbed by the syngas in the saturator immediately preceding the WGS). We adjust the WGS reactor cost by molar gas flow (relative to H-MAX-VENT case), and this adjustment is reflected in the input biomass LHV rate shown here.

(c) Total heat transfer rate considering all heat exchange in the process, except for heat transfer in the syngas cooler and associated with water gas shift reactors. See note (j) in Table 7 for additional discussion.

(d) See note g of Table 8.

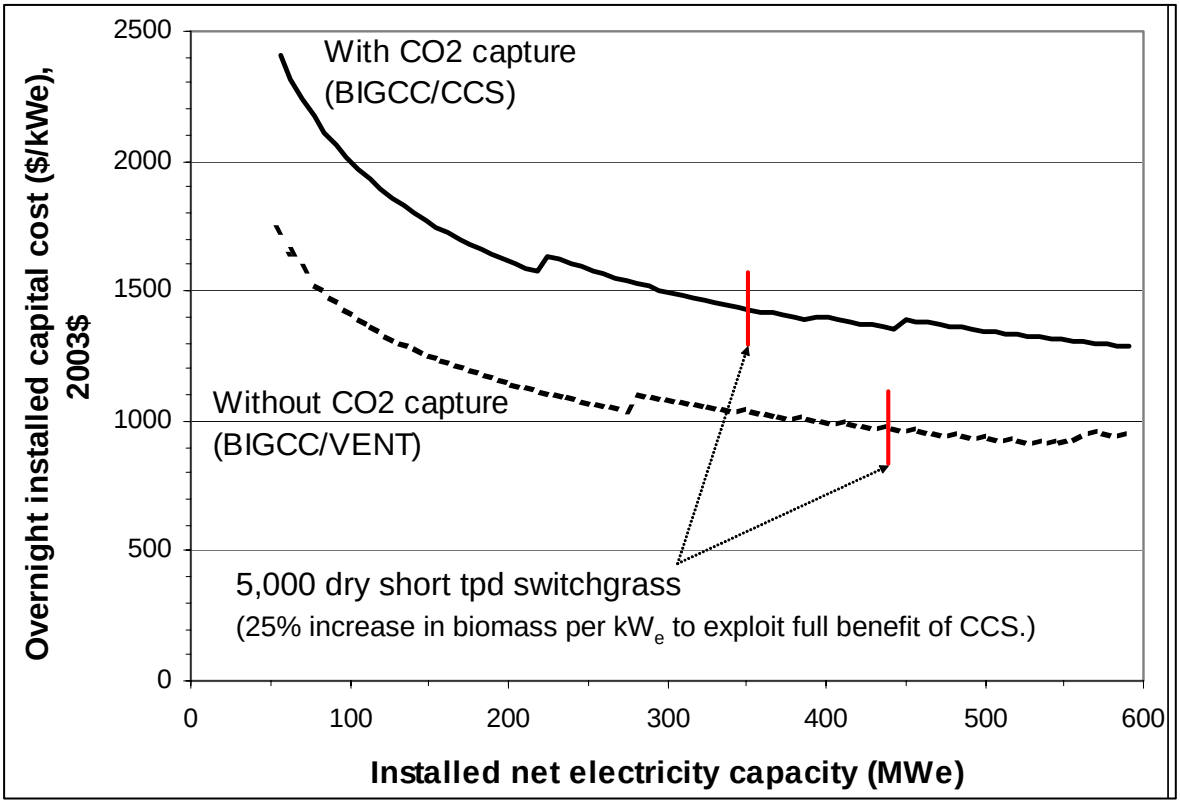

Figure 18. Comparison of installed overnight capital cost per kW for BIGCC without and with carbon capture and storage.

5.2.1.2 Levelized Electricity Costs

Based on the capital costs described above, and using the financial parameter assumptions discussed earlier, the levelized cost of electricity generation for the BIGCC-VENT case at the reference plant scale (4,536 metric tons/day switchgrass input, dry basis) is shown in Table 12. For the range of biomass prices considered, the BIGCC system generates electricity for 4.5 to 6.1 ¢/kWh. For comparison, the estimated costs of power from a comparable-scale steam Rankine power plant are also shown. These range from 5.1 to 7.4 ¢/kWh. For the three biomass prices, Figure 19 shows the total generating cost as a function of plant size for the BIGCC-VENT case. At the reference plant scale, most of the benefits of scale economies have been achieved.

In the absence of any value for captured carbon, the cost of electricity from the BIGCC-CCS design will far exceed the cost of electricity from the BIGCC-VENT system. Figure 20 compares the levelized cost of electricity for the two systems for a range of carbon prices, assuming a switchgrass feedstock price of $3/GJ$_{HHV}$. The generating cost in the VENT case is independent of the carbon price, since the system is essentially carbon-neutral with respect to the atmosphere.[32] On the other hand, the electricity cost for the CCS case falls as the value of captured carbon increases. The CCS electricity cost still exceeds the VENT case cost, with the given assumptions, until the carbon price approaches $110/tC ($30/tCO_2) (Figure 20).

[32] For simplicity, we ignore any net emissions of CO_2 that might be associated with the VENT case, e.g., emissions that might occur during production and harvesting of the switchgrass. Such emissions will be small or non-existent.

Table 12. Levelized cost of electricity generation at the reference plant scale (4,536 metric tons/day switchgrass input, dry basis) for B-IGCC and steam Rankine systems.

	B-IGCC-VENT			Steam Rankine[a]		
Total Installed Capital cost, $/kW	1087			975		
O & M cost, $/kW·yr	38.7			34.2		
Efficiency, HHV %	45.0%			30.0%		
Heat Rate, MJ_{th}/kWh_e	8.00			12.01		
Switchgrass price, $/GJ	2.0	3.0	4.0	2.0	3.0	4.0
Electricity Generating Cost, $/kWh						
Capital charges	0.023			0.021		
O & M charges	0.0055			0.0049		
Biomass charges	0.016	0.024	0.032	0.024	0.036	0.048
Total Cost, $/kWh	**0.045**	**0.053**	**0.061**	**0.051**	**0.061**	**0.074**

(a) The steam-Rankine system is based on a stoker boiler with high-pressure steam conditions of 160 bar, 550°C. The turbine includes 3 stages, with one reheat. Net power output is 295 MW_e.

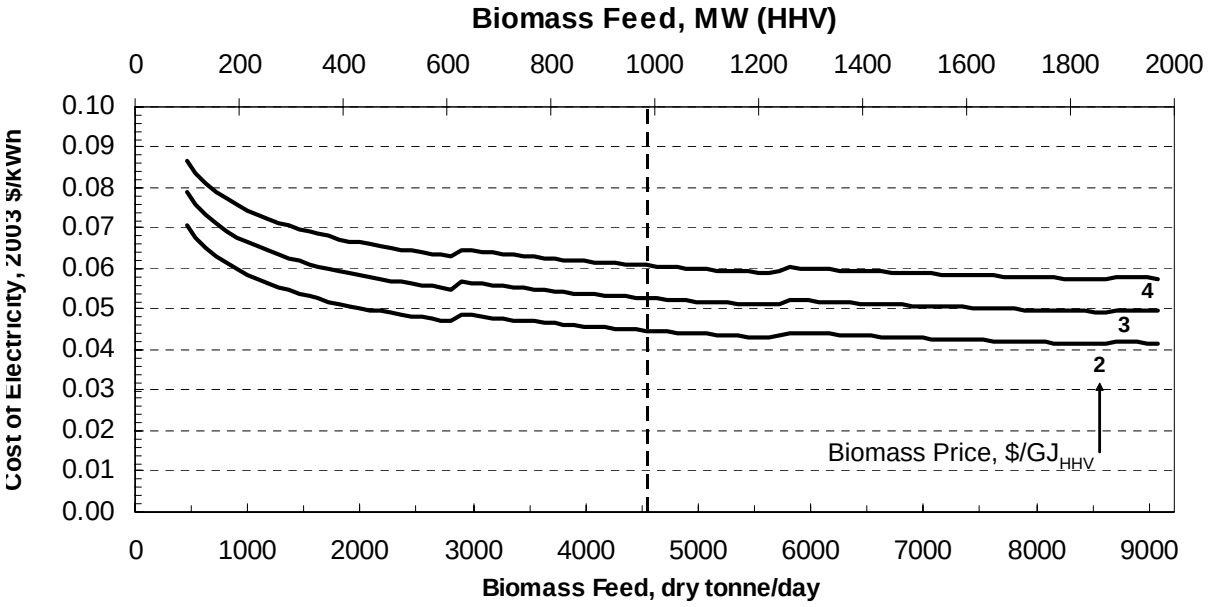

Figure 19. Total levelized cost of electricity production as a function of plant size for BIGCC-VENT process design with three different switchgrass prices.

In many parts of the United States, biomass-generated electricity will likely need to compete with new baseload coal electricity in the future. Assuming that coal-IGCC might well be the coal generating technology of choice in the future, we compare the cost of electricity from coal-IGCC and biomass-IGCC systems (Figure 21).[33] For the conditions indicated in the figure, a coal-IGCC system would provide the least costly power when there is no carbon price, but the biomass option would be favored when the carbon price is above about $25/tC. Figure 21 also

[33] The coal-IGCC electricity generating costs are based on Kreutz *et al.*, 2005.

shows a carbon price of about $90/tC would be needed before there would be sufficient incentive for coal generators to adopt CCS.

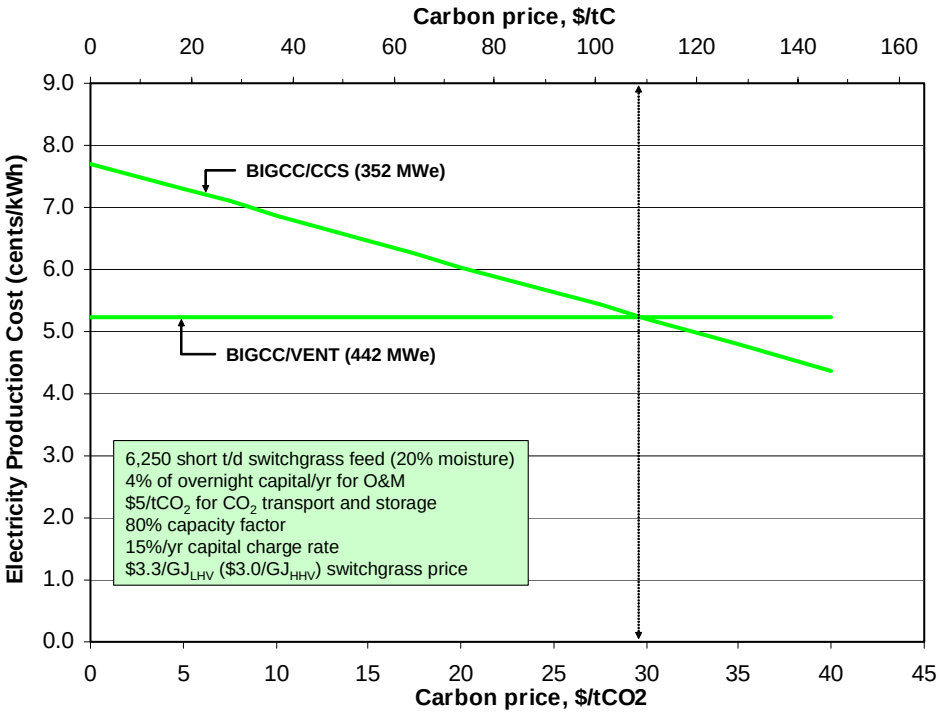

Figure 20. Total levelized cost of electricity production from BIGCC systems as a function of carbon price.

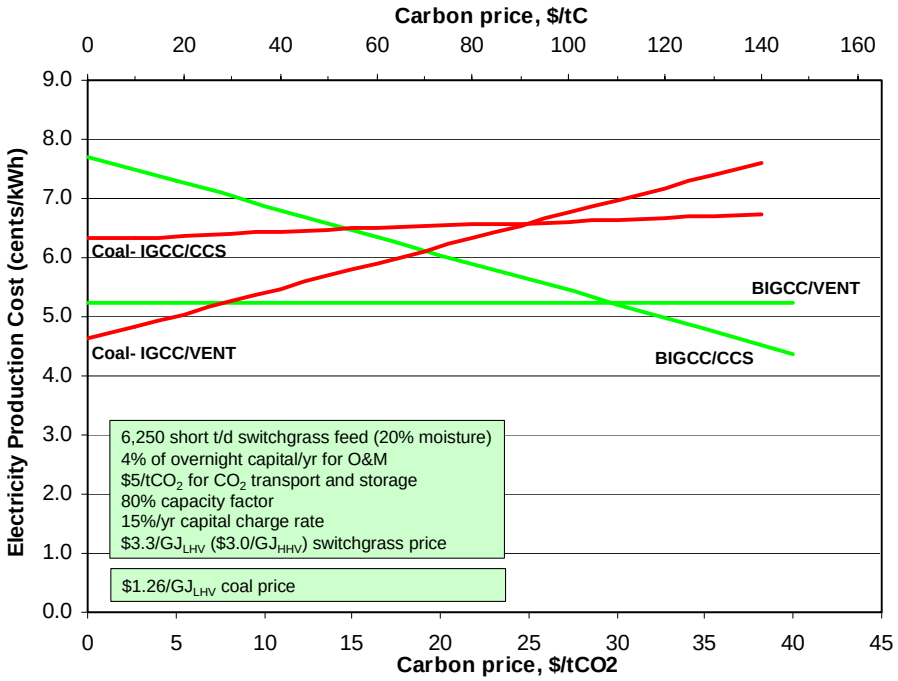

Figure 21. Comparison of total levelized cost of electricity production with coal and biomass IGCC systems as a function of the carbon price.

5.2.2 Fuels Production

5.2.2.1 Capital Costs

Following a similar approach to estimating capital costs as with the BIGCC systems, we have developed a set of reference costs by major plant area for the plant configurations producing DME, FT fuels, and hydrogen described in Section 4 (Table 13). The costs for upstream components (gasifier, ASU, etc.) and for the power island are consistent with the estimates used for these components in the BIGCC systems. Costs for the fuel synthesis and hydrogen purification areas are derived from Celik *et al.* (2004), Larson and Ren (2003), discussions with industry experts, and other sources, as detailed in the notes to Table 13.

Using the reference costs shown in Table 13, we have estimated the installed capital costs for all fuels production systems described in Section 4. Details of the capital costs are given in Table 14 through Table 18 for the five fuels production systems in which CO_2 is vented to the atmosphere. A summary of the capital costs for all systems, including those incorporating CCS, is given in Table 19. (BIGCC costs are also summarized in this table.) The common characteristic of all systems in Table 19 is the capacity of switchgrass input: 5000 short dry tons per day. Because all of the fuel production systems also produce some level of saleable electricity as a co-product, the cost of producing the fuel depends to some extent on the price received for the electricity, as discussed further below.

Table 13. Reference capacities, capital costs, and scaling factors for for fuels production plants.

Plant Area	Sub-Unit	Capacities (in indicated units)			Cost (in million 2003 $)	
		Base	Max. unit	Unit of Capacity	Base	Scaling exp.
		S_o	S_{max}		C_o[a]	f
Gasifier Island	Feed preparation[a]	64.6	n.a.	wet tonne/hr biomass	3.17	0.77
	GTI Gasifier[a]	41.7	120	dry tonne/hr biomass	6.41	0.7
	Ash Cyclone[a]	68.7	180	actual m^3/s gas feed	0.91	0.7
Gas Cleanup and carbon capture	External tar cracker[b]	47.1	52	Actual m^3/s gas feed	0.732	0.7
	Syngas cooler[a]	77	n.a.	MW_{th} heat duty	25.4	0.6
	Ceramic filter[a]	14.4	n.a.	actual m^3/s gas feed	18.60	0.65
	Rectisol AGR[b,c]	200000	n.a.	Nm^3/hr gas feed	20.00	0.65
	AGR compressor[b]	10	n.a.	MW_e consumed	4.83	0.67
	CO_2 compression[b]	10	n.a.	MW_e consumed	4.75	0.67
	CO_2 drying/compression[b]	13	n.a.	MW compressor power	7.28	0.67
FT Synthesis, Fuel Upgrading and Refinery	Slurry phase F-T reactor[d]	2.52	n.a.	million scf/hr feed gas	10.5	0.72
	Hydrocarbon recovery unit[e]	14.44	200	thousand lbs/hr feed	0.56	0.7
	H_2 recovery unit[f]	0.033	0.1	million scf/hr H_2 prod	0.65	0.7
	Wax hydrocracker[g]	8.984	575	thousand lbs/hr feed	7.21	0.7
	Distillate hydrotreater[h]	2.871	650	thousand lbs/hr feed	1.93	0.7
	Naphtha hydrotreater[i]	2.05	650	thousand lbs/hr feed	0.58	0.7
	Naphtha reformer[j]	3.43	750	thousand lbs/hr feed	4.02	0.7
	C_5/C_6 isomerization[k]	1.158	250	thousand lbs/hr feed	0.74	0.7
	CO shift reactor[l]	0.040	0.080	million scf/hr feed gas	0.79	0.7
	Fuel gas compressor[m]	10	n.a.	MW compressor power	4.83	0.67
DME Synthesis and Separation	Once-through LP synthesis[n]	2.91	n.a.	kmol/sec feed gas	15.8	0.65
	Recycle LP synthesis[o]	8.68	n.a.	kmol/sec total feed gas	88.8	0.65
	DME distillation plant[p]	6.75	n.a.	kg/s DME product	21.3	0.65
	MeOH dehydration[q]	2.91	n.a.	kmol/s MeOH feed	15.8	0.65
	Syngas expander[r]	10	n.a.	MW_e generated	2.41	0.67
	Syngas compressor[m]	10	n.a.	MW compressor power	4.83	0.67
Hydrogen production	Water Gas Shift[s]	1377	n.a.	MW_{LHV} biomass input	30.6	0.67
	PSA[t]	0.294	n.a.	kmol/s purge gas flow	5.46	0.74
	PSA purge gas compressor[u]	10	n.a.	MW_e compressor power	4.83	0.67
	H_2-rich gas compressor[v]	10	n.a.	MW_e compressor power	4.83	0.67
Air Separation Area	ASU, if stand-alone[w]	76.6	n.a.	tonne/hr pure O_2	35.6	0.50
	ASU, if integrated[a]	76.6	n.a.	tonne/hr pure O_2	22.7	0.50
	O_2 compressor[a]	10	n.a.	MW_e consumed	5.54	0.67
	N_2 compressor[a]	10	n.a.	MW_e consumed	4.14	0.67
	N_2 expander[r]	10	n.a.	MW_e generated	2.41	0.67
Power Island	Saturator[b]	20.9	n.a.	actual m^3/s gas feed	0.30	0.70
	Gas turbine[a]	266	334	GT MW_e	56.0	0.75
	HRSG + heat exchangers[a]	355	n.a.	MW_{th} heat duty[a]	41.2	1
	Steam cycle (turbine + cond.)[a]	136	n.a.	ST gross MW_e	45.5	0.67

Notes to Table 13

(a) See corresponding note in Table 7.

(b) See corresponding note in Table 10.

(c) In the case where there is both upstream and downstream decarbonization (D-OT-DCAP), the total cost for the upstream and downstream Rectisol units is calculated as the cost of a single unit with capacity equal to the upstream capacity plus one-half of the downstream capacity (U. Koss, Lurgi, personal communication, 2003). Among other factors, this calculation accounts for the upstream and downstream absorber columns sharing a single solvent regenerating stripper column.

(d) Based on an "inside battery limits" cost estimate (assumed here to exclude BOP and indirect costs) from Bechtel (1998) for a slurry-phase F-T reactor operating at an average temperature and pressure of 253ºC and 21.4 bar, with a feed gas H_2/CO ratio of 0.52, and having a feed gas capacity of 2.52 million standard cubic feet per hour (mmSCF/hr). Bechtel's cost estimate is $9.5 million (in 1997$). They indicate a maximum single-reactor capacity of 8.1 mmSCF/hr, which is approximately the capacity needed in the systems described in this report. The cost scaling factor is from Hamelinck *et al.* (2003).

(e) Based on an "inside battery limits" cost estimate (assumed here to exclude BOP and indirect costs) from Bechtel (1998) for a hydrocarbon recovery plant with a feed of 14.44 thousand lbs/hour of $0.507 million (in 1997$). The maximum capacity for such a plant is indicated by Bechtel to be 200 thousand lbs/hr feed rate. We have assumed the indicated scale factor.

(f) Based on an "inside battery limits" cost estimate (assumed here to exclude BOP and indirect costs) from Bechtel (1998) for a hydrogen recovery plant utilizing pressure-swing adsorption. Bechtel indicates a cost for a unit producing 0.033 million SCF/hr of H_2 of $0.583 million (in 1997$) and a maximum capacity for such a system of 0.1 million SCF/hr. We have assumed the indicated scale factor.

(g) Based on an "inside battery limits" cost estimate (assumed here to exclude BOP and indirect costs) from Bechtel (1998) for a wax hydrocracker with a feed rate of 8.984 thousand lbs/hr of $6.509 million (in 1997$). Bechtel indicates a maximum unit capacity for such a hydrocracker to be 575 thousand lbs/hr. We have assumed the indicated scale factor.

(h) Based on an "inside battery limits" cost estimate (assumed here to exclude BOP and indirect costs) from Bechtel (1998) for a distillate hydrotreating unit with a feed rate of 2.871 thousand lbs/hr of $6.509 million (in 1997$). Bechtel indicates a maximum unit capacity for such a hydrotreater to be 650 thousand lbs/hr. We have assumed the indicated scale factor.

(i) Based on an "inside battery limits" cost estimate (assumed here to exclude BOP and indirect costs) from Bechtel (1998) for a naphtha hydrotreating unit with a feed rate of 2.05 thousand lbs/hr of $0.528 million (in 1997$). Bechtel indicates a maximum unit capacity for such a hydrotreater to be 650 thousand lbs/hr. We have assumed the indicated scale factor.

(j) Based on an "inside battery limits" cost estimate (assumed here to exclude BOP and indirect costs) from Bechtel (1998) for a naphtha reformer with a feed rate of 3.43 thousand lbs/hr of $3.628 million (in 1997$). Bechtel indicates a maximum unit capacity for such a reformer to be 750 thousand lbs/hr. We have assumed the indicated scale factor.

(k) Based on an "inside battery limits" cost estimate (assumed here to exclude BOP and indirect costs) from Bechtel (1998) for a C_5/C_6 isomerization plant with a feed rate of 1.158 thousand lbs/hr of $0.669 million (in 1997$). Bechtel indicates a maximum unit capacity for this type of unit to be 250 thousand lbs/hr. We have assumed the indicated scale factor.

(l) Based on an "inside battery limits" cost estimate (assumed here to exclude BOP and indirect costs) from Bechtel (1998) for a CO shift reactor with a feed rate of 0.04 million scf/hr of $0.715 million (in 1997$). Bechtel indicates a maximum unit capacity for this type of unit to be 0.080 million scf/hr. We have assumed the indicated scale factor.

(m) For plant designs involving F-T synthesis, this compressor is used to deliver unconverted syngas plus purge gases from the F-T product upgrading area to the gas turbine. For DME synthesis designs, this compressor raises the pressure of the syngas after the Rectisol unit to the required synthesis reactor pressure. In both cases, the cost of this compressor is modeled on that of a purge gas compressor, as discussed in note (h) of Table 7.

(n) This cost is based on a projected scaled-up cost for Nth-plant version of the liquid-phase synthesis reactor demonstrated at the Eastman Chemical facility in Kingsport, Tennessee, as provided by Moore (2003). See also Larson and Ren (2003). The original estimate provided by Moore was $15.76 million (2002$) for a reactor with a gas feed rate of 2.91 kmol/sec. The scale factor was recommended by Moore (2003). We assume BOP (15%, according to Moore) and indirect costs (assumed to be 32%) are not included in the cost shown in this table. These latter costs are added in later when the total installed capital costs for the DME cases are developed.

(o) Larson and Ren (2003) indicate a cost for recycle-based synthesis (including recycle compressor) of $87.37 million (in 2002$) for a total feed gas flow (fresh feed plus recycled unconverted gas) of 8.69 kmol/s.

(p) A cost estimate of $21.26 million (2002$) for a DME distillation plant delivering 6.75 kg/sec of DME was provided by Moore (2003). See also Larson and Ren (2003). The scale factor was recommended by Moore (2003). We assume BOP (15%, according to Moore) and indirect costs (assumed to be 32%) are not included in the cost shown in this table. These latter costs are added in later when the total installed capital costs for the DME cases are developed.

(q) Since equipment for once-through liquid-phase DME synthesis has many similarities to MeOH dehydration equipment, we assume that the installed cost per kmol of feed to the MeOH dehydration area would be the same as that for once-through LPDME synthesis. BOP (15%) and indirect costs (32%) are not included in the cost shown in this table. These are added in later when the total installed capital costs for the DME cases are developed.

(r) The cost for a syngas expander is based on Kreutz *et al.* (2005), who give an estimate of $3.14 million (in 2002$) for the installed cost of a unit producing 10 MW_e. We assume the cost for a nitrogen expander is the same as for a syngas expander. We assume Kreutz, *et al.*'s cost includes BOP, engineering, and contingencies. The latter two items are assumed to be 15% each, giving a base cost (including BOP) of $2.37 million, or $2.41 million in 2003$. Engineering and contingency costs are included (using methodology discussed in text) when total plant costs are estimated later in the paper. Scale factor is from Kreutz, *et al.* (2005).

(s) The estimate here is for a two-stage water gas shift system (adiabatic first stage, isothermal second stage, with heat recovery), as discussed in note d of Table 10. For a single-stage (adiabatic) WGS, Moore (2003) indicates that the cost would be about 40% of the cost for the two-stage system.

(t) Kreutz *et al.* (2005) gives an estimated cost for a PSA unit recovering 85% of hydrogen in a shifted syngas stream of $7.1 million (in 2002$). The unit has a purge gas flow rate of 0.294 kmol/sec. Factoring out 15% indirect cost and 15% engineering costs, gives $5.37 million, or $5.46 million when converted to 2003$.

(u) The cost for a PSA purge gas compressor is modeled as described in note h of Table 7.

(v) The cost for a hydrogen compressor, based on Kreutz *et al.* (2005), is taken to be the same as the cost for a syngas compressor, as described in note (h) of Table 7.

(w) See note g of Table 7.

Table 14. Capital cost estimate for DME and electricity co-production with D-OT-VENT design.[a]

Plant Area	Sub-Unit	Capacities (in indicated units): Required capacity S_r	Number of units n	Capacity per unit S	Unit of Capacity	Costs (in million 2003 $): Cost per unit C	Train cost C_m	Overnight Cost OC
Gasifier Island	Feed preparation	236	2	118	wet tonne/hr biomass	15.7	29.2	46.6
	Gasifier	189	2	94.5	dry tonne/hr biomass	11.4	21.2	33.9
	Ash Cyclone	15.6	2	7.9	actual m^3/s gas feed	0.20	0.37	0.59
Gas Cleanup	Tar cracker	15.6	2	7.8	actual m^3/s gas feed	0.21	0.39	0.62
	Syngas cooler	81.7	2	40.8	MW_{th} heat duty	17.3	32.3	51.6
	Ceramic filter	9.1	2	4.5	actual m^3/s gas feed	8.79	16.4	26.2
	Rectisol AGR	363314	1	363314	Nm^3/hour gas feed	27.4	27.4	43.7
	AGR Compressor	0.094	1	0.094	MW_e consumed	0.21	0.21	0.28
	Syngas compressor	11.6	1	11.6	MW_e consumed	5.35	5.35	7.06
	CO_2 compressor	11.6	1	11.6	MW_e consumed	5.34	5.34	7.04
	CO_2 boost compressor	0.07	1	0.1	MW_e consumed	0.17	0.17	0.23
DME Synthesis	LPDME synthesis	2.61	1	2.61	kmol/s feed gas	14.67	14.67	22.3
	DME distillation	7.53	1	7.53	kg/s DME output	22.83	22.83	34.7
	MeOH dehydration	0.082	1	0.082	kmol/s MeOH feed	1.55	1.55	2.36
	Syngas Expander	1.68	1	1.7	MW_e consumed	0.73	0.73	0.97
	Syngas Compressor	0.024	1	0.024	MW_e consumed	0.08	0.08	0.11
Air Separation	ASU	61.3	1	61.3	tonne/hr pure O_2	20.28	20.28	25.8
	O_2 compressor	5.44	1	5.44	MW_e consumed	3.69	3.69	4.68
	N_2 expander	2.57	1	2.57	MW_e produced	0.97	0.97	1.23
Power Island	Saturator	2.65	1	2.65	actual m^3/s gas feed	0.07	0.07	0.11
	Gas Turbine	151	1	151	GT MW_e	36.55	36.55	46.4
	HRSG + heat exchangers	477	1	477	MW_{th} heat duty[b]	55.42	55.42	85.1
	Steam cycle (turb. + cond.)	144	1	144	ST gross MW_e	47.32	47.32	60.1
Total Overnight Capital Cost (million $)				502				
Interest during construction (million $)[c]				62				
Total Capital Investment (million $)				563				

(a) See the relevant notes to Table 8 for descriptions of the column-heading parameters in this table.

(b) Total heat transfer rate considering all heat exchange in the process, except for heat transfer in the syngas cooler. See note (j) in Table 7 for additional discussion.

(c) See note g of Table 8.

Table 15. Capital cost estimate for DME and electricity co-production with D-R-VENT design.[a]

Plant Area	Sub-Unit	Capacities (in indicated units): Required capacity S_r	Number of units n	Capacity per unit S	Unit of Capacity	Costs (in million 2003 $): Cost per unit C	Train cost C_m	Overnight Cost OC
Gasifier Island	Feed preparation	236	2	118	wet tonne/hr biomass	15.7	29.2	46.6
	Gasifier	189	2	94.5	dry tonne/hr biomass	11.4	21.2	33.9
	Ash Cyclone	15.6	2	7.9	actual m^3/s gas feed	0.20	0.37	0.59
Gas Cleanup	Tar cracker	15.6	2	7.8	actual m^3/s gas feed	0.21	0.39	0.62
	Syngas cooler	81.7	2	40.8	MW_{th} heat duty	17.3	32.3	51.6
	Ceramic filter	9.1	2	4.5	actual m^3/s gas feed	8.79	16.4	26.2
	Rectisol AGR	294202	1	294202	Nm^3/hour gas feed	25.7	25.7	41.0
	AGR Compressor	0.094	1	0.094	MW_e consumed	0.21	0.21	0.28
	Syngas compressor	11.34	1	11.34	MW_e consumed	5.25	5.25	6.93
	CO_2 compressor	12.46	1	12.46	MW_e consumed	5.59	5.59	7.38
	CO_2 boost compressor	0.068	1	0.068	MW_e consumed	0.17	0.17	0.23
DME Synthesis	LPDME synthesis, DME distillation, recycle comp.	14.38	1	14.38	kmol/s total feed gas (fresh + recycled)	123.3	123.3	187.2
	MeOH dehydration	0.32	1	0.32	kmol/s MeOH feed	3.76	3.76	5.71
	Syngas Expander	12.1	1	12.1	MW_e consumed	2.74	2.74	3.62
	Syngas Compressor	0.043	1	0.043	MW_e consumed	0.12	0.12	0.16
Air Separation	ASU	61.3	1	61.3	tonne/hr pure $_{O2}$	20.28	20.28	25.8
	O_2 compressor	5.44	1	5.44	MW_e consumed	3.69	3.69	4.68
	N_2 compressor	6.69	1	6.69	MW_e consumed	3.16	3.16	4.01
	N_2 expander	1.29	1	1.29	MW_e produced	0.61	0.61	0.78
Power Island	Saturator	0.81	1	0.81	actual m^3/s gas feed	0.03	0.03	0.05
	Gas Turbine	53.3	1	53.3	GT MW_e	16.75	16.75	21.3
	HRSG + heat exchangers	466	1	466	MW_{th} heat duty[b]	54.13	54.13	83.1
	Steam cycle (turb. + cond.)	90.5	1	90.5	ST gross MW_e	34.63	34.63	44.0
Total Overnight Capital Cost (million $)					596			
Interest during construction (million $)[c]					73			
Total Capital Investment (million $)					669			

(a) See the relevant notes to Table 8 for descriptions of the column-heading parameters in this table.
(b) Total heat transfer rate considering all heat exchange in the process, except for heat transfer in the syngas cooler. See note (j) in Table 7 for additional discussion.
(c) See note g of Table 8.

Table 16. Capital cost estimate for F-T and electricity co-production with FT-OT-VENT design.[a]

Plant Area	Sub-Unit	Capacities (in indicated units): Required capacity S_r	Number of units n	Capacity per unit S	Unit of Capacity	Costs (in million 2003 $): Cost per unit C	Train cost C_m	Overnight Cost OC
Gasifier Island	Feed preparation	236	2	118	wet tonne/hr biomass	15.7	29.2	46.6
	Gasifier	189	2	94.5	dry tonne/hr biomass	11.4	21.2	33.9
	Ash Cyclone	15.6	2	7.9	actual m^3/s gas feed	0.20	0.37	0.59
Gas Cleanup	Tar cracker	15.6	2	7.8	actual m^3/s gas feed	0.21	0.39	0.62
	Syngas cooler	81.7	2	40.8	MW_{th} heat duty	17.3	32.3	51.6
	Ceramic filter	9.1	2	4.5	actual m^3/s gas feed	8.79	16.4	26.2
	Rectisol AGR	323748	1	323748	Nm^3/hour gas feed	27.35	27.35	43.7
	AGR Compressor	0.094	1	0.094	MW_e consumed	0.21	0.21	0.28
	CO_2 compressor	12.44	1	12.44	MW_e consumed	5.59	5.59	7.37
	CO_2 boost compressor	0.068	1	0.068	MW_e consumed	0.17	0.17	0.23
FT Synthesis and Upgrading	Slurry phase F-T reactor	8.04	1	8.04	million scf/hr feed gas	24.29	24.29	38.8
	Hydrocarbon recovery unit	242.7	2	242.7	thousand lbs/hr feed	2.49	4.65	7.42
	H_2 recovery unit	0.15	2	0.15	million scf/hr H_2 prod	1.17	2.19	3.49
	Wax hydrocracker	43.4	1	43.4	thousand lbs/hr feed	21.71	21.71	34.7
	Distillate hydrotreater	6.81	1	6.81	thousand lbs/hr feed	3.53	3.53	5.63
	Naphtha hydrotreater	12.86	1	12.86	thousand lbs/hr feed	2.11	2.11	3.37
	Naphtha reformer	18.79	1	18.79	thousand lbs/hr feed	13.21	13.21	21.1
	C_5/C_6 isomerization	5.80	1	5.8	thousand lbs/hr feed	2.29	2.29	3.65
	CO shift reactor	0.070	1	0.070	million scf/hr feed gas	1.17	1.17	1.86
	Fuel gas compressor	5.70	1	5.70	MW_e consumed	2.93	2.93	3.87
Air Separation	ASU	61.3	1	61.3	tonne/hr pure O_2	20.28	20.28	25.8
	O_2 compressor	5.44	1	5.44	MW_e consumed	3.69	3.69	4.68
	N_2 expander	2.57	1	2.57	MW_e produced	0.97	0.97	1.23
Power Island	Gas Turbine	86.7	1	86.7	GT MW_e	24.13	24.13	30.7
	HRSG + heat exchangers	476	1	476	MW_{th} heat duty[b]	55.2	55.2	84.8
	Steam cycle (turb. + cond.)	141	1	141	ST gross MW_e	46.59	46.59	59.2
Total Overnight Capital Cost (million $)					541			
Interest during construction (million $)[c]					67			
Total Capital Investment (million $)					608			

(a) See the relevant notes to Table 8 for descriptions of the column-heading parameters in this table.
(b) Total heat transfer rate considering all heat exchange in the process, except for heat transfer in the syngas cooler. See note (j) in Table 7 for additional discussion.
(c) See note g of Table 8.

Table 17. Capital cost estimate for hydrogen and electricity co-production with H-MAX-VENT design.[a]

Plant Area	Sub-Unit	Capacities (in indicated units): Required capacity S_r	Number of units n	Capacity per unit S	Unit of Capacity	Costs (in million 2003 $): Cost per unit C	Train cost C_m	Overnight Cost OC
Gasifier Island	Feed preparation	236	2	118	wet tonne/hr biomass	15.7	29.2	46.6
	Gasifier	189	2	94.5	dry tonne/hr biomass	11.4	21.2	33.9
	Ash cyclone	15.6	2	7.9	actual m^3/s gas feed	0.20	0.37	0.59
Gas Cleanup	Tar cracker	15.6	2	7.8	actual m^3/s gas feed	0.21	0.39	0.62
	Syngas cooler	81.7	2	40.8	MW_{th} heat duty	17.3	32.3	51.6
	Ceramic filter	9.10	2	4.5	actual m^3/s gas feed	8.79	16.4	26.2
Water Gas Shift	Saturator	9.10	1	9.10	actual m^3/s gas feed	0.17	0.17	0.27
	2-stage WGS	887	1	887	MW_{LHV} biomass input	22.78	22.78	30.1
CO_2 Removal	Rectisol AGR	359305	1	359305	Nm^3/hour gas feed	29.27	29.27	46.7
	AGR compressor	0.052	1	0.052	MW_e consumed	0.14	0.14	0.19
	CO_2 compressor	1.38	1	1.38	MW_e consumed	1.28	1.28	1.69
PSA area	PSA	1.0	1	1.0	kmol/s purge gas flow	13.79	13.79	18.20
	PSA purge gas compressor	7.27	1	7.27	MW_e consumed	3.90	3.90	5.15
	H_2-rich gas compressor	9.74	1	9.74	MW_e consumed	4.74	4.74	6.26
Air Separation	ASU	61.3	1	61.3	tonne/hr pure O_2	31.82	31.82	40.4
	O_2 compressor	7.26	1	7.26	MW_e consumed	4.47	4.47	5.68
Power Island	HRSG + heat exchangers	201	1	201	MW_{th} heat duty[b]	23.36	23.36	35.9
	Steam cycle (turb. + cond.)	98.6	1	98.6	ST gross MW_e	36.67	36.67	46.57
Total Overnight Capital Cost (million $)					396.6			
Interest during construction (million $)[c]					48.8			
Total Capital Investment (million $)					445.4			

(a) See the relevant notes to Table 8 for descriptions of the column-heading parameters in this table.
(b) Total heat transfer rate considering all heat exchange in the process, except for heat transfer in the syngas cooler and that associated with the WGS reactors. See note (j) in Table 7 for additional discussion.
(c) See note g of Table 8.

Table 18. Capital cost estimate for hydrogen and electricity co-production with H-5050-VENT design.[a]

Plant Area	Sub-Unit	Capacities (in indicated units): Required capacity S_r	Number of units n	Capacity per unit S	Unit of Capacity	Costs (in million 2003 $): Cost per unit C	Train cost C_m	Overnight Cost OC
Gasifier Island	Feed preparation	236	2	118	wet tonne/hr biomass	15.7	29.2	46.6
	Gasifier	189	2	94.5	dry tonne/hr biomass	11.4	21.2	33.9
	Ash cyclone	15.6	2	7.9	actual m^3/s gas feed	0.20	0.37	0.59
Gas Cleanup	Tar cracker	15.6	2	7.8	actual m^3/s gas feed	0.21	0.39	0.62
	Syngas cooler	81.7	2	40.8	MW_{th} heat duty	17.3	32.3	51.6
	Ceramic filter	9.10	2	4.5	actual m^3/s gas feed	8.79	16.4	26.2
Water Gas Shift	Saturator	9.10	1	4.89	actual m^3/s gas feed	0.11	0.11	0.17
	Single-stage WGS	443	1	443	MW_{LHV} biomass input	5.73	5.73	7.56
CO_2 Removal	Rectisol AGR	176789	1	176789	Nm^3/hour gas feed	18.46	18.46	29.5
	AGR compressor	0.026	1	0.026	MW_e consumed	0.090	0.090	0.12
	CO_2 compressor	6.44	1	6.44	MW_e consumed	3.59	3.59	4.74
	CO_2 boost compressor	0.068	1	0.068	MW_e consumed	0.17	0.17	0.23
PSA area	PSA	0.33	1	0.33	kmol/s purge gas flow	5.94	5.94	7.85
	PSA purge gas compressor	3.39	1	3.39	MW_e consumed	2.34	2.34	3.09
	H_2-rich gas compressor	4.43	1	4.43	MW_e consumed	2.8	2.8	3.69
Air Separation	ASU	61.3	1	61.3	tonne/hr pure O_2	20.28	20.28	25.8
	O_2 compressor	5.44	1	5.44	MW_e consumed	3.69	3.69	4.68
	N_2 expander	2.57	1	2.57	MW_e produced	0.97	0.97	1.23
Power Island	Saturator	5.5	1	5.5	actual m^3/s gas feed	0.12	0.12	0.18
	Gas Turbine	166.6	1	166.6	GT MW_e	39.39	39.39	50.03
	HRSG + heat exchangers	317	1	317	MW_{th} heat duty[b]	36.73	36.73	56.4
	Steam cycle (turb. + cond.)	131.1	1	131.1	ST gross MW_e	44.4	44.4	56.39
Total Overnight Capital Cost (million $)					411.1			
Interest during construction (million $)[c]					50.6			
Total Capital Investment (million $)					461.7			

(a) See the relevant notes to Table 8 for descriptions of the column-heading parameters in this table.
(b) Total heat transfer rate considering all heat exchange in the process, except for heat transfer in the syngas cooler and that associated with the WGS reactor. See note (j) in Table 7 for additional discussion.
(c) See note g of Table 8.

Table 19. Installed capital costs for all thermochemical conversion systems included in this analysis.

2003 US $	DME & Electricity Coproduction					FT + Elec		Electricity Only		Hydrogen			
	OT-VENT	OT-UCAP	OT-DCAP	RC-VENT	RC-UCAP	OT-VENT	OT-UCAP	B-IGCC	B-IGCC CCS	H-5050 VENT	H-MAX VENT	H-5050 CCS	H-MAX CCS
Energy capacities													
Switchgrass input, MW HHV	983	983	983	983	983	983	983	983	983	983	983	983	983
Switchgrass input, MW LHV	893	893	893	893	893	893	893	893	893	893	893	893	893
DME production, MW LHV	217	218	218	468	469								
Hydrogen production, MW LHV										240	526	249	528
FT gasoline, MW LHV						117	117						
FT diesel, MW LHV						188	189						
Electricity output, MW	270	257	229	79	67	207	191	442	352	281	41	218	10
Physical capacities													
Switchgrass input, dry metric tons/day	4545	4545	4545	4545	4545	4545	4545	4545	4545	4545	4545	4545	4545
Liquids output, barrels/day diesel equiv.	3357	3368	3368	7226	7253	4630	4641	--	--	--	--	--	--
CO2 captured, million tCO2/yr	0	1.31	2.10	0	1.42	0	1.42	0	2.57	0	0	2.56	2.57
Annual Quantities (80% capacity factor)													
Switchgrass, PJ/yr (HHV)	24.81	24.81	24.81	24.81	24.81	24.81	24.81	24.81	24.81	24.81	24.81	24.81	24.81
CO2 for storage, million tCO2/yr	0.00	1.05	1.68	0.00	1.14	0.00	1.14	0.00	2.06	0.00	0.00	0.00	0.00
DME, PJ/yr (HHV)	6.02	6.04	6.04	12.97	13.02			0.00	0.00				
Hydrogen, PJ/yr (HHV)										7.15	15.69	7.42	15.74
FT gasoline, PJ/yr (HHV)						3.24	3.25						
FT diesel, PJ/yr (HHV)						5.07	5.08						
Electricity, TWh/yr	1.89	1.80	1.61	0.55	0.47	1.45	1.34	3.10	2.46	1.97	0.29	1.53	0.07
Overnight Installed Capital Costs (million 2003 $)													
Biomass preparation & handling	46.6	46.6	46.6	46.6	46.6	46.6	46.6	46.6	46.6	46.6	46.6	46.6	46.6
Gasifier and ash cyclone	34.5	34.5	34.5	34.5	34.5	34.5	34.5	34.5	34.5	34.5	34.5	34.5	34.5
Syngas cooler	51.6	51.63	51.6	51.6	51.6	51.6	51.6	65.4	51.4	51.6	51.6	51.6	51.6
Gas cleaning (tar cracker + ceramic filter)	26.8	26.8	26.8	26.8	26.8	26.8	26.8	24.2	26.9	26.8	26.8	26.8	26.8
Upstream water gas shift	--	--	--	--	--	--	--	--	29.5	7.73	30.3	30.3	30.3
Rectisol (upstream +downstream)	43.7	43.8	51.4	41.0	41.1	43.7	41.1	--	47.1	29.5	46.7	46.8	46.7
Rectisol recovery compressor	0.28	0.28	0.28	0.28	0.28	0.28	0.28	--	0.19	0.12	0.19	0.18	0.19
Syngas compressor	7.06	7.07	7.07	6.93	6.94	--	--	--	--	--	--	--	--
CO2 compression	7.27	7.33	9.77	7.61	7.68	7.60	7.68	--	11.06	4.97	1.69	11.03	11.04
Supercritical CO2 compressor	--	4.79	6.57	--	5.05	--	5.04	--	7.51	--	--	7.50	7.50
DME synthesis	22.27	22.30	22.30	187.20	186.90	--	--	--	--	--	--	--	--
DME distillation	34.66	34.73	34.74			--	--	--	--	--	--	--	--
Byproduct MeOH dehydration to DME	2.36	2.36	2.35	5.71	5.72	--	--	--	--	--	--	--	--
Syngas Expander	0.97	0.97	0.97	3.62	3.61	--	--	--	--	--	--	--	--
Syngas compressor in DME distillation	0.11	0.11	0.00	0.16	0.16	--	--	--	--	--	--	--	--
PSA	--	--	--	--	--	--	--	--	--	7.85	18.20	6.14	18.15
PSA purge gas compressor	--	--	--	--	--	--	--	--	--	3.09	5.15	2.82	5.13
Hydrogen compressor	--	--	--	--	--	--	--	--	--	3.69	6.26	3.78	6.27
FT synthesis	--	--	--	--	--	38.77	43.99	--	--	--	--	--	--
HC recovery plant	--	--	--	--	--	7.42	7.43	--	--	--	--	--	--
H2 Recovery	--	--	--	--	--	3.49	3.49	--	--	--	--	--	--
Wax Hydrocracking	--	--	--	--	--	34.65	34.65	--	--	--	--	--	--
Distillate H.T.	--	--	--	--	--	5.63	5.63	--	--	--	--	--	--
Naphtha H.T.	--	--	--	--	--	3.37	3.37	--	--	--	--	--	--
Naphtha Reforming	--	--	--	--	--	21.09	21.09	--	--	--	--	--	--
C5/C6 Isomerization	--	--	--	--	--	3.65	3.65	--	--	--	--	--	--
CO shift reactor plant	--	--	--	--	--	1.86	1.87	--	--	--	--	--	--
Fuel gas compressor	--	--	--	--	--	3.87	3.88	--	--	--	--	--	--
Saturator for WGS (scrubber)	--	--	0.14	--	--	--	--	--	--	--	--	--	--
WGS reactors, heat exchangers	--	--	17.41	--	--	--	--	--	--	--	--	--	--
Recovery compressor for Rectisol 2	--	--	0.15	--	--	--	--	--	--	--	--	--	--
Pressure Booster	--	--	1.67	--	--	--	--	--	--	--	--	--	--
ASU	25.75	25.75	25.75	25.75	25.75	25.75	25.75	25.74	25.89	25.75	40.41	25.75	40.41
O2 compressor	4.68	4.68	4.68	4.68	4.68	4.68	4.68	4.61	4.64	4.68	5.68	4.68	5.68
N2 expander	--	--	--	0.78	--	1.23	--	--	--	1.23	--	1.23	--
N2 compressor	1.23	5.68	5.67	4.01	6.39	--	6.34	6.07	5.57	--	--	--	--
Saturator	0.11	0.11	0.09	0.05	0.05	--	--	--	--	0.18	--	0.12	--
Gas Turbine	46.41	49.44	47.76	21.27	22.20	30.65	33.96	71.35	66.11	50.03	--	43.64	--
HRSG + heat exchangers	85.10	86.70	88.55	83.13	85.73	84.77	86.02	77.18	80.55	56.41	35.87	60.61	43.60
Steam cycle (ST + condenser)	60.10	58.71	56.48	43.98	43.98	59.17	57.62	72.37	65.50	56.39	46.57	54.10	46.31
Total overnight capital cost	501	514	543	596	606	541	557	428	503	411	397	458	421
Interest during construction (4yr,7.8%/yr)	62	63	67	73	75	67	69	53	62	51	49	56	52
Total installed capital cost, MM$	563	578	610	669	680	608	626	481	565	462	445	515	473

5.2.2.2 Fuels Production Costs without CCS

Figure 22 shows the average total cost (capital, O&M, fuel, and coproduct electricity credit) of producing a mix of FT gasoline and diesel blend stocks over a range of electricity prices and for three different switchgrass prices (FT-OT-VENT case). The upper graph shows the plant-gate cost of FT production in $ per GJ_{LHV}. The lower figure shows the corresponding breakeven crude oil price, i.e. the world oil price at which the FT fuel would be competitive with petroleum

diesel, assuming that a GJ of diesel can be substituted by a GJ of the FT fuel.[34] For the higher range of electricity prices (6 to 7 c/kWh), the cost of FT would be competitive with petroleum diesel when the crude oil price is $45 - $55/barrel (for the mid-range biomass price of $3/GJ$_{HHV}$).

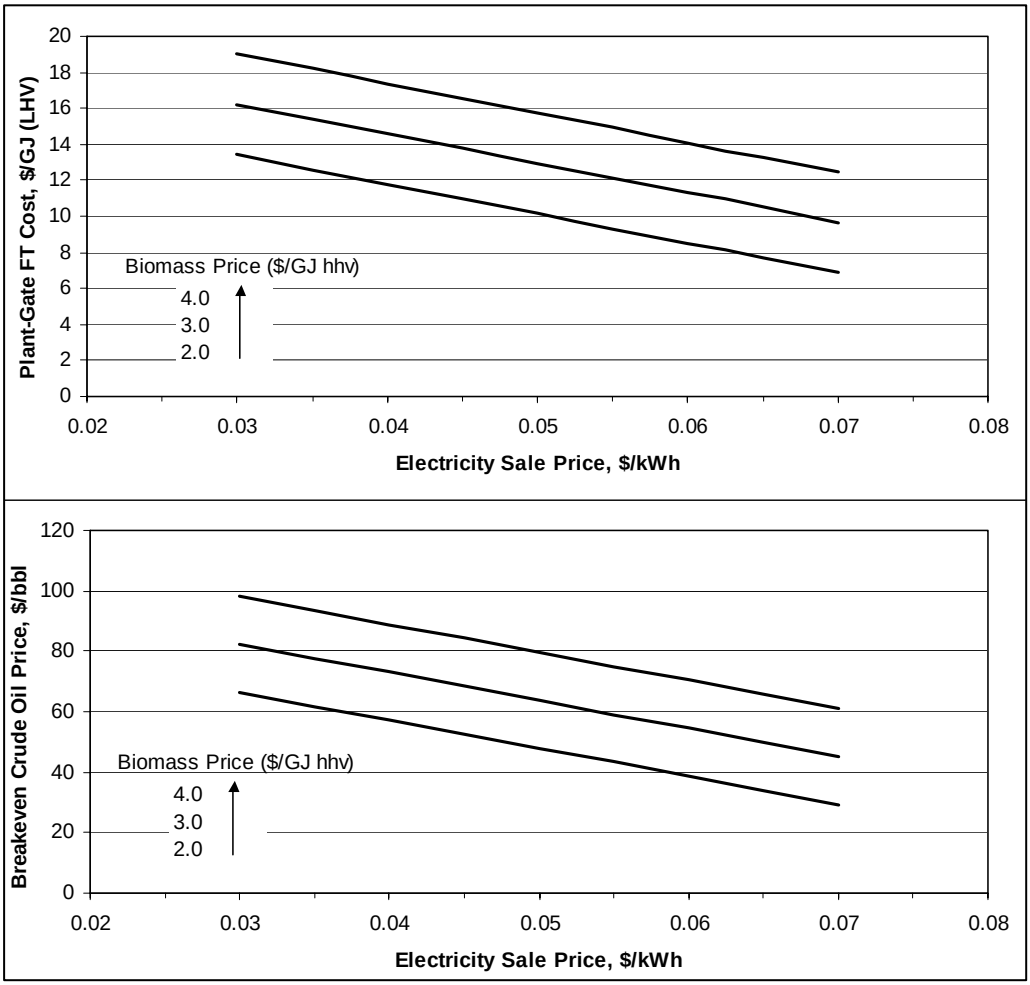

Figure 22. Estimated average factory-gate cost of a mix of F-T diesel and gasoline blendstocks (based on FT-OT-VENT process) as a function of electricity co-product price and for three switchgrass prices. Upper diagram shows cost in terms of $/GJ. Lower diagram shows the crude oil price at which the F-T liquids would be cost-competitive with the average U.S. refiner petroleum diesel price to resellers, if the cost of the diesel fraction of the F-T product were the same as the average cost of the mix of F-T diesel and gasoline.

For a fixed electricity sale price of $0.04/kWh, Figure 23 shows the production cost of FT fuel (without CCS) as a function of plant capacity. By comparing to the analogous curves for a BIGCC system (Figure 19), one can see a somewhat greater sensitivity of cost to scale for fuels production.

[34] We have estimated the breakeven crude oil price (BCOP) as follows (Williams and Larson, 2003):
BCOP ($/liter crude) = [Synfuel cost ($/MJ LHV) * 35.68 MJ/lit (diesel LHV)] – Refinery Margin.
For US refiners, the Refinery Margin averaged $0.0465/liter diesel (2002$) during 1992-2001. Adding a projected cost for 2007 sulfur standards compliance, the refinery margin would be $0.0597/lit. Converting to 2003$ gives a refinery magin of 1.0164*0.0597 = $0.0607/lit.

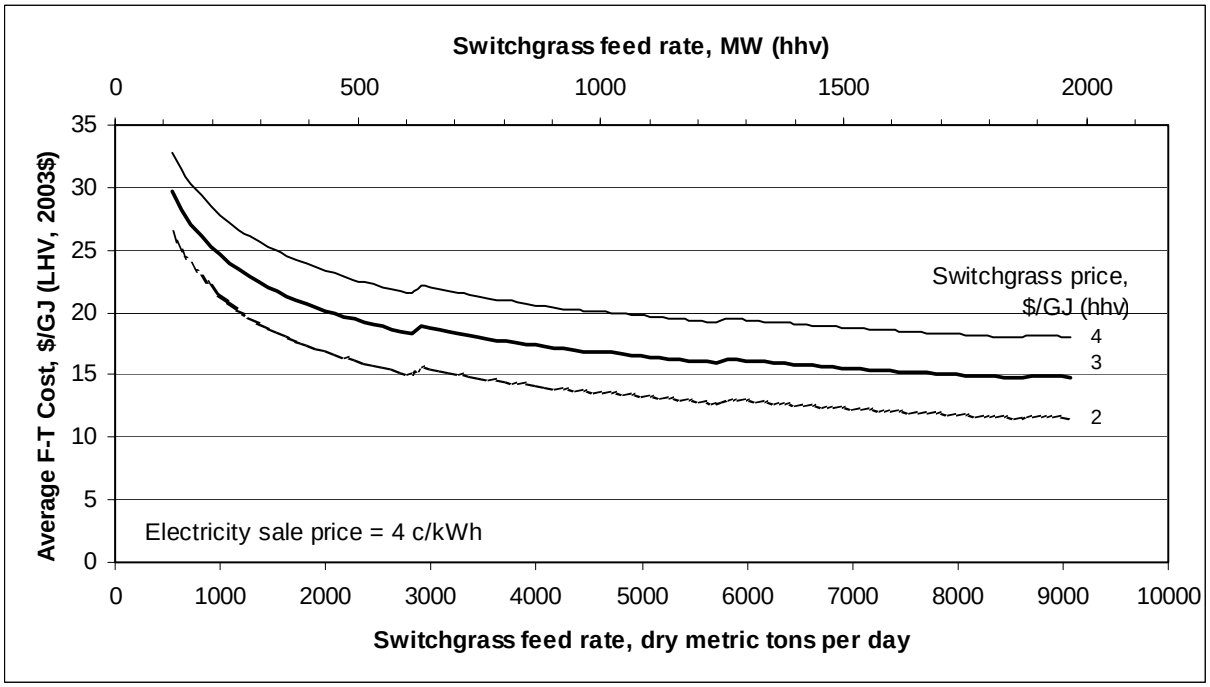

Figure 23. Total levelized cost of F-T fuels production (mix of diesel and gasoline) with FT-OT-VENT design as a function of plant size for fixed electricity sale price and three different switchgrass prices.

Figure 24 shows the cost of DME production over a range of electricity prices and for three different switchgrass prices (without carbon capture and storage in all cases). As for Figure 22, the upper graph has units of \$ per GJ_{LHV} and the lower figure shows the corresponding breakeven crude oil price.[35] As evident from Figure 24, the cost of DME with the recycle configuration (RC-VENT) is less sensitive to electricity price than for the once-through configuration (OT-VENT) due to much lower electricity production per unit of fuel produced.

In comparing the OT-VENT case for DME (Figure 24) versus that for FT (Figure 22), one observes a greater sensitivity to electricity price for DME. This is due to the relatively high one-pass conversion of syngas to fuel in an FT synthesis reactor compared to a DME synthesis reactor, resulting in a greater amount of unconverted syngas being used for power generation in the DME case.

Figure 25 shows the production cost of DME (without CCS) as a function of plant capacity for both the RC and OT configurations. The scale sensitivity is similar to that observed for FT production (Figure 23).

[35] Comparing the plant-gate cost of DME with a refiner's resale price for petroleum diesel (implicit in estimates of the breakeven crude oil price) ignores the difference in costs for delivering DME to a refueling station and vehicle compared to delivering diesel. However, a preliminary analysis suggests that the added costs for delivering DME (due to requirement for slight pressurization to remain as a liquid at normal temperatures) would roughly offset the pollution control costs that would be avoided on the vehicle due to the much cleaner burning nature of DME (Williams, 2005).

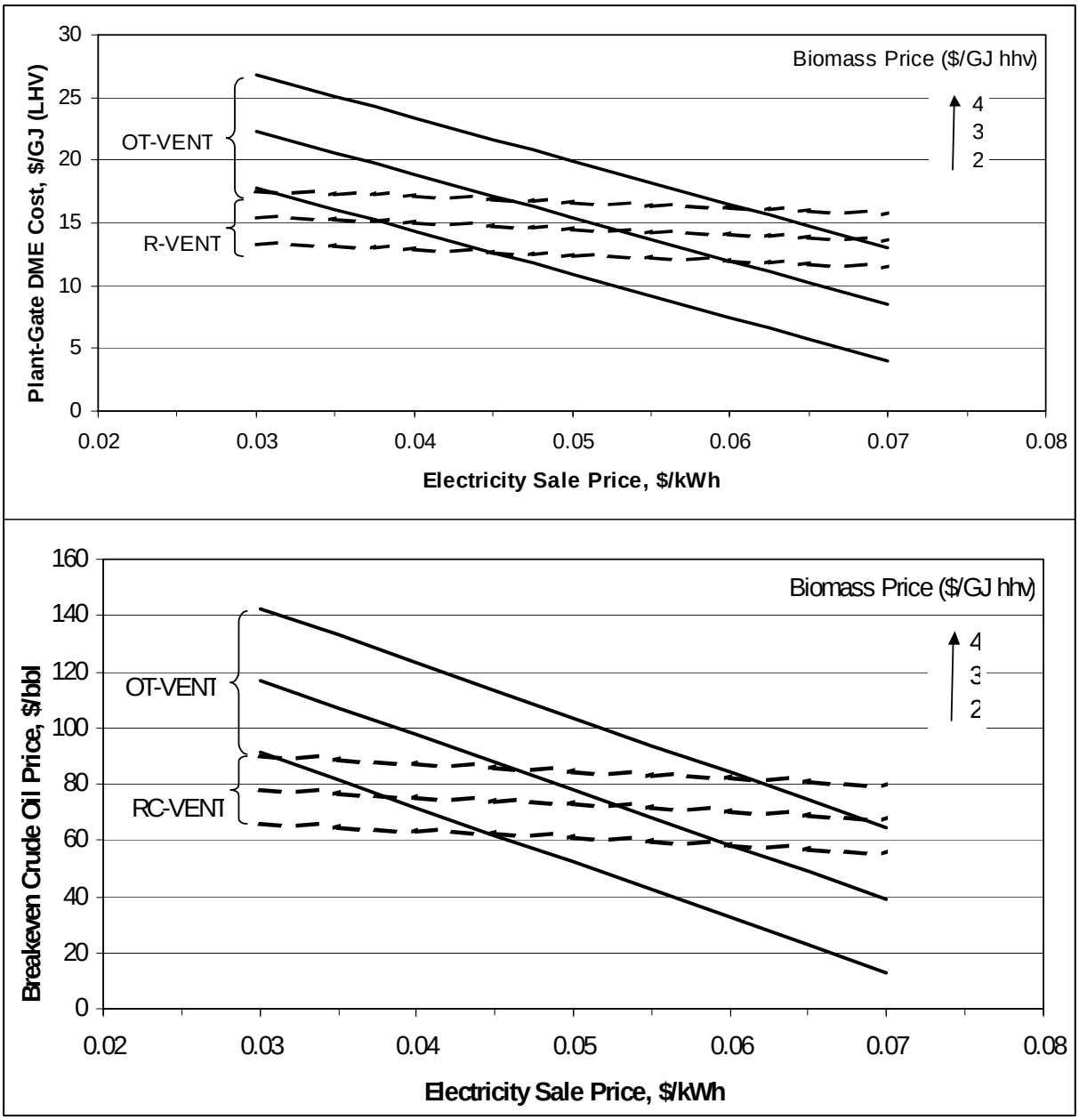

Figure 24. Estimated factory-gate cost of DME as a function of electricity co-product price and for three different switchgrass prices. Results are shown for both the D-OT-VENT and D-RC-VENT configurations. The upper diagram shows DME cost in terms of $/GJ. The lower diagram shows the crude oil price at which DME would be cost-competitive with the average U.S. refiner petroleum diesel price to resellers.

Figure 26 shows the production costs for hydrogen (without CCS) as a function of electricity sale price. Hydrogen costs are considerably lower than costs for liquid fuels due to intrinsically simpler and more-efficient processing. Figure 27 shows the sensitivity of H_2 cost to conversion plant scale. The plant configuration with greater electricity output (H-5050-VENT) shows a stronger dependence on scale than the case with maximum H_2 production.

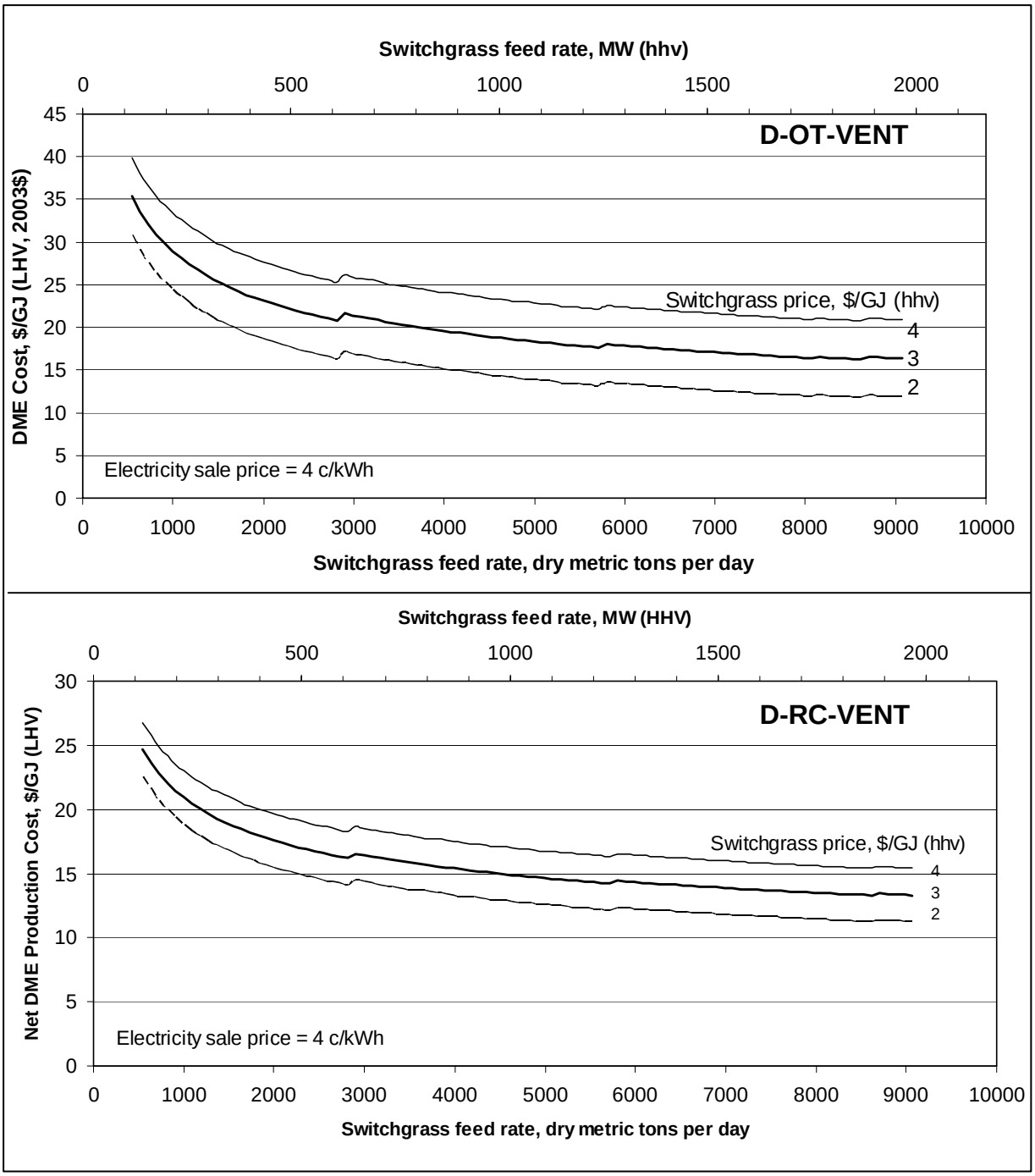

Figure 25. Total levelized cost of DME production with once-through synthesis (D-OT-VENT) and recycle synthesis (D-RC-VENT) process configurations as a function of plant size for fixed electricity sale price and three different switchgrass prices.

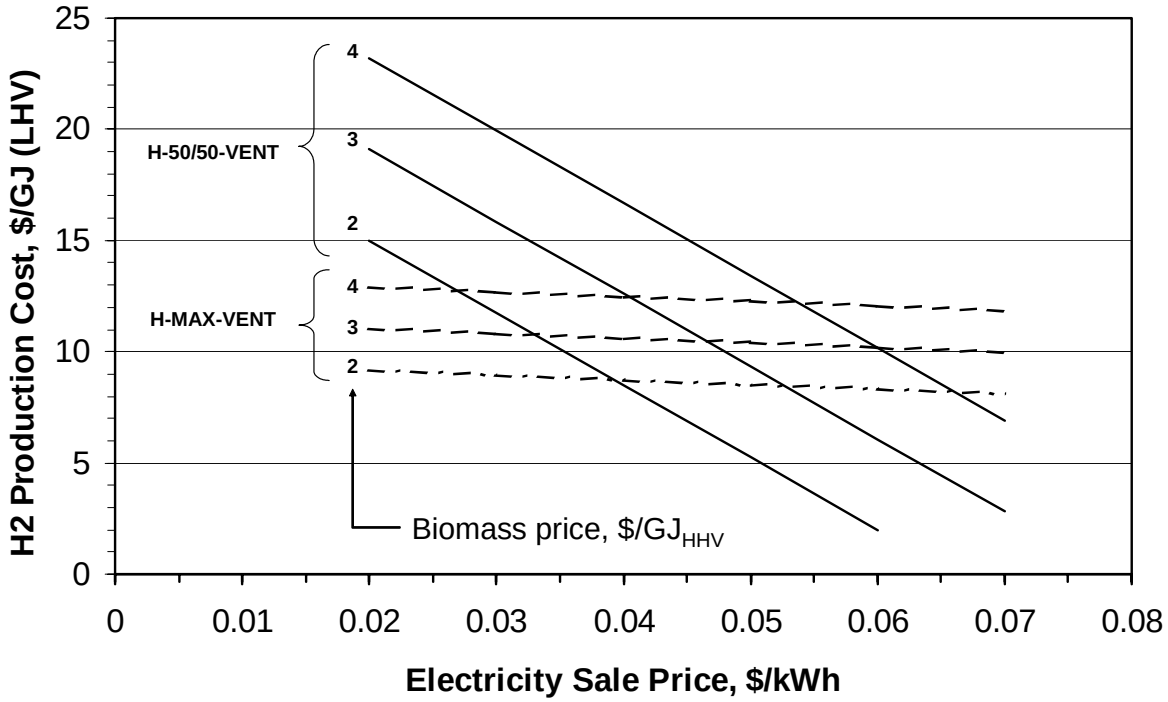

Figure 26. Total levelized hydrogen production costs (without CCS) for H-MAX-VENT and H-50/50-VENT process configurations as a function of electricity sale price for three switchgrass prices.

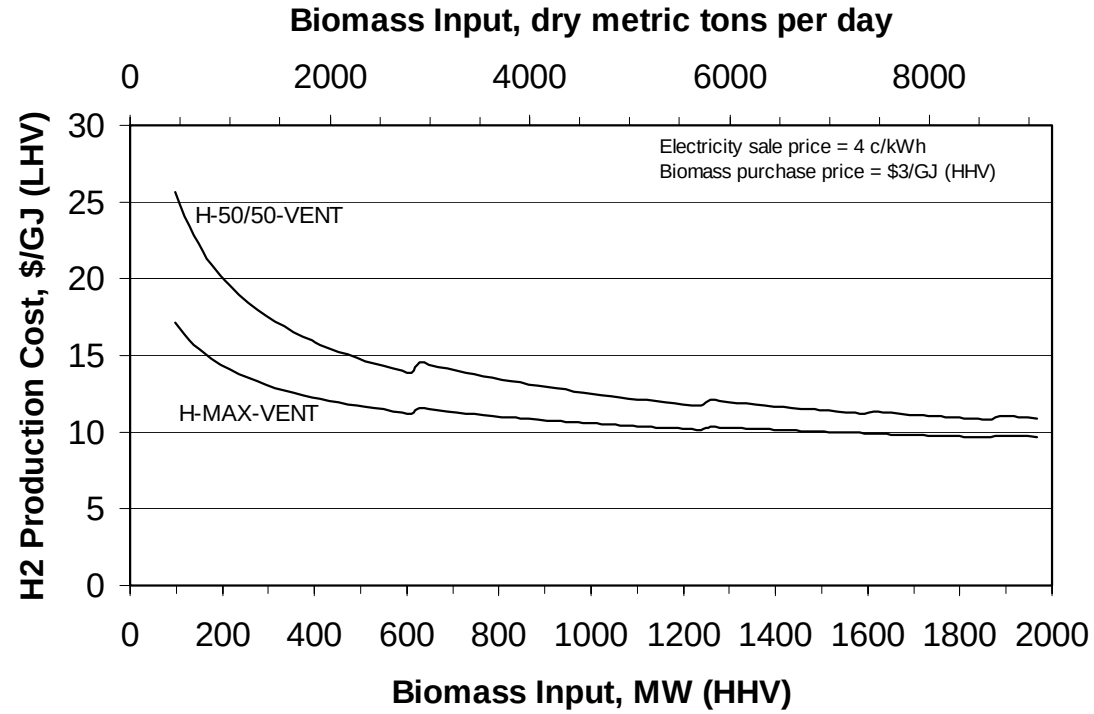

Figure 27. Total levelized costs of hydrogen production as a function of plant size for a fixed electricity price and switchgrass price.

5.2.2.3 Fuels Production Costs with CCS

Figure 28 illustrates the impact on production cost of liquid synfuels when carbon capture and storage are included. The total levelized cost of production is shown (with a switchgrass plant gate price of $3/GJ$_{HHV}$), including the net impact of revenues for electricity sales and for carbon emissions avoided. The assumed electricity sale price is the estimated generating cost for the least-expensive coal-IGCC electricity. When the carbon price is zero (left set of bars in Figure 28), the least costly coal-IGCC electricity is with venting of CO_2, and the electricity sale price is 4.6 c/kWh (see Figure 21, Coal-IGCC/VENT). For a carbon price of $100/tC (right bars in Figure 28), the electricity sale price is 6.6 c/kWh (in Figure 21, see Coal-IGCC/CCS).

Shown for comparison in Figure 28 is the cost of petroleum diesel (average U.S. refiner's resale price) corresponding to world crude oil prices of $30/bbl and $60/bbl. Our results suggest that even with oil at $60/bbl, liquid fuels are not cost-competitive with diesel in the absence of a carbon price. With a carbon price of $100/tC, several of the options are cost-competitive with diesel when the oil price is $30/bbl, and all five options are more than competitive when the oil price is $60/bbl.

Figure 29 shows the cost components that go into the net production cost shown in Figure 28. The importance of the electricity revenues (especially with the $100/tC carbon price) can be seen clearly there.

Finally, Figure 30 shows results for hydrogen that parallel those shown in the Figure 28 and Figure 29 for the liquid fuels. The electricity prices assumed to generate costs shown in Figure 30 are as described above.

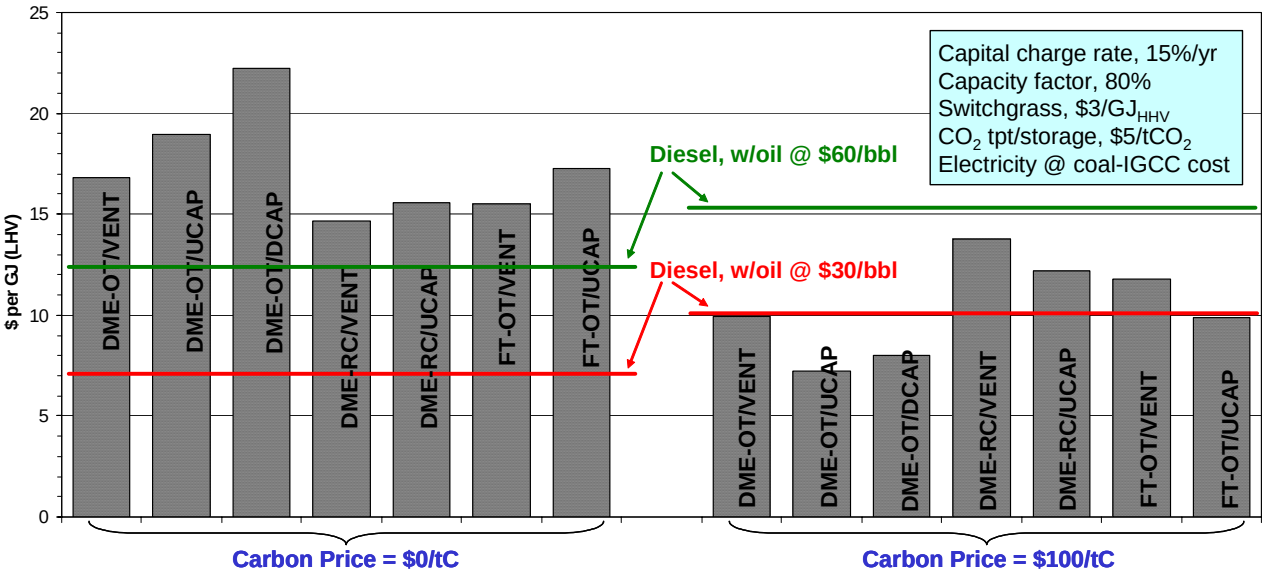

Figure 28. Net plant-gate cost of liquid fuels production from switchgrass, including sale of co-product electricity, for all liquid-fuel producing process configurations examined in this study.

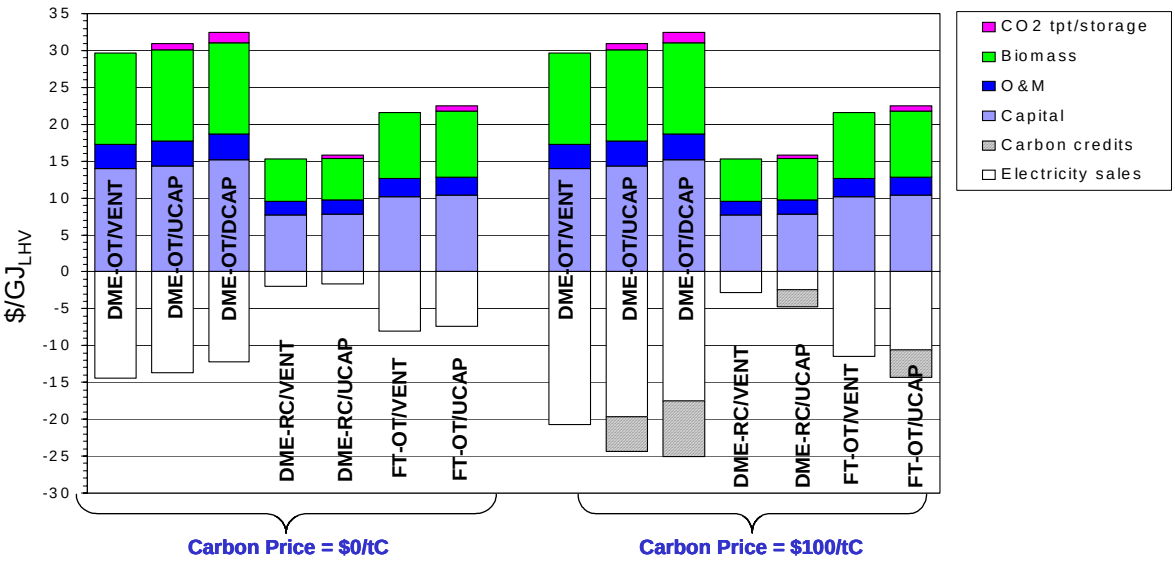

Figure 29. Components of the net plant-gate cost of liquid fuels production from switchgrass (Figure 28) for all liquid-fuel producing process configurations examined in this study.

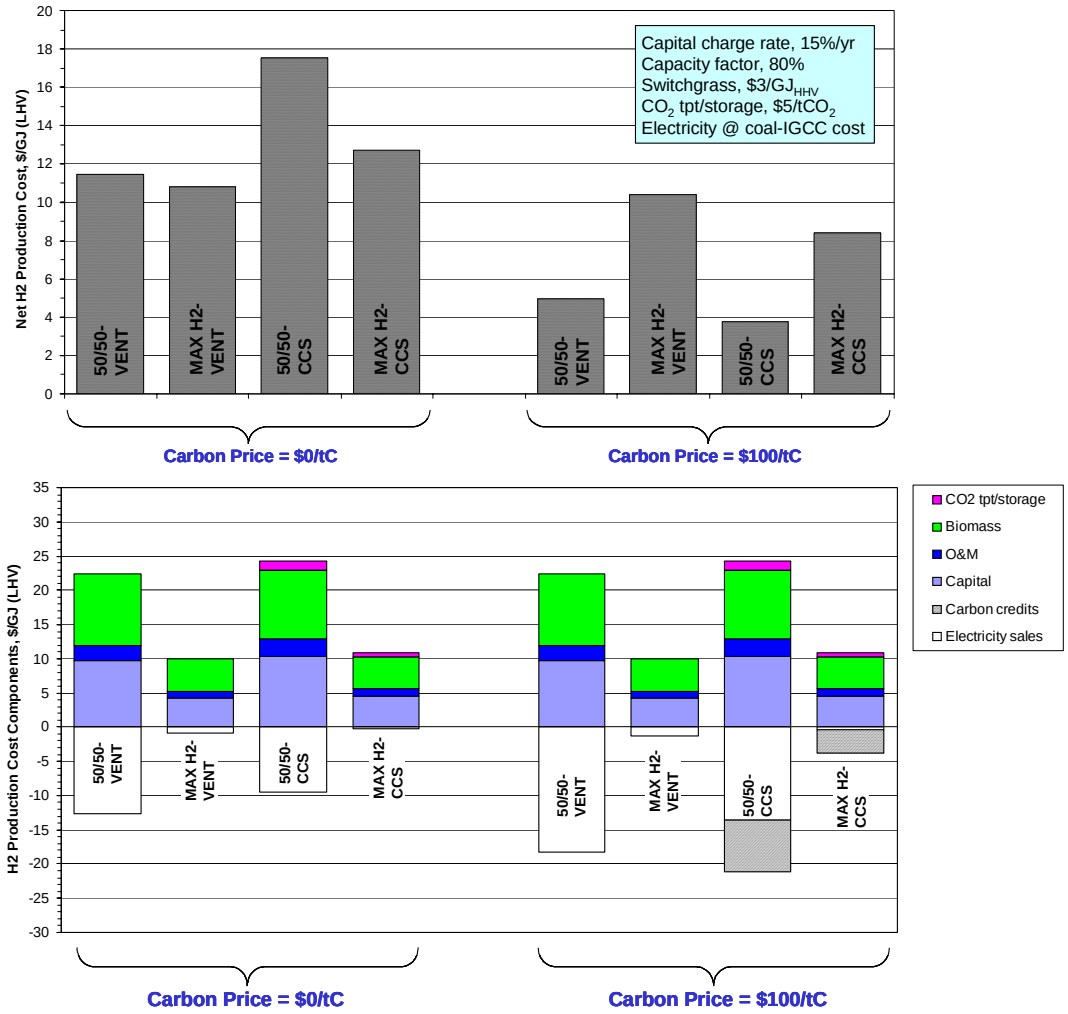

Figure 30. Net levelized plant-gate cost of hydrogen production from switchgrass for all process configurations examined in this study (upper), and components of the net cost (lower).

6 Acknowledgements

The authors thank Robert Williams for many valuable discussions in the course of preparing this report. For financial support, the authors thank Dartmouth College, the National Renewable Energy Laboratory, Princeton University's Carbon Mitigation Initiative (funded by BP and Ford), the William and Flora Hewlett Foundation, and the Blue Moon Fund.

7 References

Adachi, Y., Komoto, M., Watanabe, I., Ohno, Y. and Fujimoto, K. 2000. "Effective Utilization of Remote Coal Through Dimethyl Ether Synthesis," *Fuel*, **79**: 229-234.

Air Products and Chemicals, Inc. 1993. "Synthesis of Dimethyl Ether and Alternative Fuels in the Liquid Phase from Coal-Derived Synthesis Gas," report DOE/PC/89865-T8, U.S. Dept. of Energy, Pittsburgh Energy Tech. Center, Pittsburgh, PA, Feb.

Air Products and Chemicals, Inc. 2001. "Liquid Phase Dimethyl Ether Demonstration in the LaPorte Alternative Fuels Development Unit," prepared for US Dept. of Energy by APCI, Allentown, Pennsylvania, January.

Air Products and Chemicals, Inc. 2002. "Market Outlook for Dimethyl Ether (DME)," prepared for US Dept. of Energy by APCI, Allentown, Pennsylvania, April.

Anderson, R.B. 1984. *The Fishcer-Tropsch Synthesis*, Academic Press, Inc., Orlando, Florida.

Anonymous. 2003. *Gas Turbine World Handbook*, Vol. 23, Pequot Publishing Inc., Fairfield, CT.

Bachu, S. and Gunter, W.D. 2005. "Overview of Acid-Gas Injection Operations in Western Canada**,"** in *Proceedings of 7th International Conference on Greenhouse Gas Control Technologies. Volume 1: Peer-Reviewed Papers and Plenary Presentations* (E.S. Rubin, D.W. Keith and C.F. Gilboy, eds.), IEA Greenhouse Gas Programme, Cheltenham, UK (in press).

Bain, R.L., Amos, W.P., Downing, M., and Perlack, R.L. 2003. "Highlights of Biopower Technical Assessment," NREL/TP-510-33132, ORNL and NREL, January 2003.

Bechtel. 1998. "Aspen process flowsheet simulation model of a Battelle biomass-based gasification, Fischer-Tropsch liquefaction and combined-cycle power plant," DE-AC22-93PC91029-16, May, US Dept. of Energy, Pittsburgh, Pennsylvania.

Bechtel Group, Inc. 1990. *Slurry Reactor Design Studies. Slurry vs. Fixed-Bed Reactors for Fischer-Tropsch and Methanol: Final Report*, US Dept. of Energy Project No. DE-AC22-89PC89867, Pittsburgh Energy Technology Center, Pittsburgh.

Bechtel Corporation, Global Energy Inc., and Nexant Inc. 2003a: *Gasification Plant Cost and Performance Optimization, Final Report*, prepared for the National Energy Technology Laboratory, US Department of Energy under Contract No. DE-AC26-99FT40342, September.

Bechtel Corporation, Global Energy Inc., and Nexant Inc. 2003b: *Gasification Plant Cost and Performance Optimization, Task 2 Topical Report: Coke/Coal Gasification with Liquids Coproduction*, prepared for the National Energy Technology Laboratory, US Department of Energy under Contract No. DE-AC26-99FT40342, September.

Boerrigter, H. and van der Drift, A. 2003. "Liquid Fuels from Biomass: The ECN Concept(s) for Integrated FT-Diesel Production Systems," presented at the Biomass Gasification Conference, Leipzig, Germany, 1-2 October.

Boerrigter, H. and van der Drift, A. 2004. "Biosyngas: Description of R&D trajectory necessary to reach large-scale implementation of renewable syngas from biomass," ECN-C-04-112, Energy Research Centre of the Netherlands, Petten, December, 29 pages.

Brooks, F.J. 2000. *GE gas turbine performance characteristics*, GE Power Systems, GER-3567H, Oct.

Brown, R.L. and Galloway, A.E. 1929. "Methanol from Hydrogen and Carbon Monoxide, II: Dimethyl Ether," *Industrial and Engineering Chemistry*, **21**(4): 310-313.

Brown, D.M., Bhatt, B.L., Hsiung, T.H., Lewnard, J.J. and Waller, F.J. 1991. "Novel Technology for the Synthesis of Dimethyl Ether from Syngas," *Catalysis Today*, **8**:279-304.

Bukur, D.B., Ma, W.P., Carreto-Vazquez, V., Nowicki, L., and Adeyiga, A.A. 2004). "Attrition resistance and catalytic performance of spray-dried iron Fischer-Tropsch catalysts in a stirred-tank slurry reactor," *Ind. Eng. Chem. Res.*, 43: 1359-1365.

Celik, F., Larson, E.D., and Williams, R.H. 2004. "Transportation Fuel From Coal With Low CO_2 Emissions," *Proceedings of 7th Int'l. Conf. on Greenhouse Gas Control Technologies*, Vancouver, BC, Canada (5-9 September).

Cerovski, T. (GE Power Systems). 2003. Personal communications.

Chiesa, P., Consonni, S., Kreutz, T. and Williams, R. 2005. "Co-Production of Hydrogen, Electricity and CO_2 from Coal with Commercially Ready Technology. Part A: Performance and Emissions," *International Journal of Hydrogen Energy*, 30: 747-767.

Cicero, D., Gupta, R., Turk, B., and Simbeck, D. 2003. "A Review of Desulfurization in Gasification Systems," *Proceedings of the 20th Annual International Pittsburgh Coal Conference*, National Energy Technology Center, Pittsburgh.

Council of Economic Advisors, 2004. *Economic Indicators*, US Government Printing Office, Wash., DC, February.

Craig, K.R. and Mann, M.K., 1996. "Cost and Performance Analysis of Biomass-Based Integrated Gasification Combined-Cycle (BIGCC) Power Systems," NREL/TP-430-21657, National Renewable Energy Laboratory, Golden, CO, 57 pp.

Dayton, D.C. 2001. *Fuel Cell Integration – A Study of the Impacts of Gas Quality and Impurities*, NREL/MP-510-30298, National Renewable Energy Laboratory, Golden, CO, June.

DeLong, M.M. 1995. "Economic Development Through Biomass System Integration: Summary Report," NREL/TP-430-20517, National Renewable Energy Laboratory, Golden, CO, December, 63 pp.

Devi, L., Ptasinski, K.J., Janssen, F.J.J.G. 2003. "A Review of the Primary Measures for Tar Elimination in Biomass Gasification Processes", *Biomass and Bioenergy*, 24: 125-140.

Dry, M.E. 2002. "The Fischer-Tropsch Process: 1950-2000," *Catalysis Today*, **71**: 227-241.

Eastman Chemical and Air Products and Chemicals, 2003. "Project Data on Eastman Chemical Company's Chemicals-from-Coal Complex in Kingsport, TN," prepared for US Department of Energy (under cooperative agreement DE-FC22-92PC90543).

Eilers, J., Posthuma, S.A., and Sie, S.T. 1990. "The Shell Middle Distillate Synthesis Process (SMDS)," *Catalysis Letters*, 7:253-270.

Engstrom, S., Lindman, N., Rensfelt, E., and Waldheim, L. 1981. "A New Synthesis Gas Process for Biomass and Peat," *Energy from Biomass and Wastes V*, Institute of Gas Technology, Chicago.

Evans, R.J., Knight, R.A., Onischak, M., and Babu, S.P. 1987. "Process Performance and Environmental Assessment of the Renugas Process," *Energy from Biomass and Wastes X*, D.L. Klass (ed.), Elsevier Applied Science (London) and Institute of Gas Technology (Chicago), pp. 677-694.

Faaij, A., Meuleman, B., and van Ree, R. 1998. *Long-Term Perspectives of Biomass Integrated Gasification/Combined Cycle (BIG/CC) Technology, Costs and Electrical Efficiency: a Comparison with Combustion*, for NOVEM (Dutch Organization for Energy and Environment), Department of Science, Technology and Society, Utrecht University, the Netherlands.

Fox III, J. M. and Tam, S.S. 1995. "Correlations of Slurry Reaction Fischer-Tropsch Yield Data", *Topics in Catalysis*, 2: 285-300.

Fujimoto, K., Shikada, T. and Yamaoka, Y. 1995. "Method of producing dimethyl ether," US pat. 5466720, Nov. 14.

Graaf, G.H. and Beenackers, A.A.C.M. 1996. "Comparison of Two-Phase and Three-Phase Methanol Synthesis Processes, *Chemical Engineering and Processing*, **35**: 413-427.

Graaf,, G.H., Stamhuis, E.J. and Beenackers, A.A.C.M. 1988a. "Kinetics of Low-Pressure Methanol Synthesis, *Chemical Engineering Science*, **43**(12): 3185-3195.

Graaf, G.H., Winkelman, J.G.M. and Stamhuis, E.J. 1988b. "Kinetics of Three-Phase Methanol Synthesis, *Chemical Engineering Science*, **43**(8): 2161-2168.

Graham, R.G. and Bain, R. 1993. *Biomass Gasification: Hot Gas Clean-Up*, report for IEA Biomass Gasification Working Group from Ensyn Technologies and National Renewable Energy Laboratory, Golden, Colorado, 44 pp.

Guthrie, K.M. 1969. "Capital Cost Estimating." *Chemical Engineering*. March 24, pp. 114-142.

Hamelinck, C.N. and Faaij, A.P.C. 2001. "Future Prospects for Production of Methanol and Hydrogen from Biomass," report NWS-E-2001-49, Copernicus Inst., Dept. of Science, Technology and Society, Utrecht University, Utrecht, The Netherlands, September, 81 pp.

Hamelinck, C.N. and Faaij, A.P.C. 2002. "Future prospects for production of methanol and hydrogen from biomass," Journal of Power Sources, 111:1-22.

Hamelinck, C.N., Faaij, A.P.C., den Uil, H., and Boerrigter, H. 2003. "Production of FT Transportation Fuels from Biomass; Technical Options, Process Analysis and Optimisation, and Development Potential," report NWS-E-2003-08, Copernicus Inst., Dept. of Science, Technology and Society, Utrecht University, Utrecht, The Netherlands, March, 69 pp.

Hamelinck C.N., Faaij, A.P.C., den Uil, H., and Boerrigter, H. 2004, "Production of FT Transportation Fuels from Biomass; Technical Options, Process Analysis and Optimisation, and Development Potential," *Energy*, 29:1743-1771.

Hansen, J.B., Voss, B., Joensen, F., and Sigurdardottir, I.D. 1995. "Large-Scale Manufacture of Dimethyl Ether -- a New Alternative Diesel Fuel from Natural Gas" SAE Paper 950063.

Hughes, E. (Electric Power Research Institute). 2003. Personal communications, Palo Alto, CA.

Jager, B. 1997. "SASOL's Advanced Commercial Fischer-Tropsch Processes," presented at the Spring Meeting of the American Institute of Chemical Engineers, Houston, Texas, 10-13 March.

Jenkins, B. 1989. "Physical Properties of Biomass," *Biomass Handbook*, O. Kitani and C.W. Hall (eds.), Gordon and Breach Science Publishers, New York, pp. 860-891.

Katofsky, R. 1993. "Production of fluid fuels from biomass," MSE thesis, Mechanical and Aerospace Engineering Dept., Princeton University, Princeton, NJ.

Kosowski, G.M., Onischak, M., and Babu, S.P. 1984. "Development of Biomass Gasification to Produce Substitute Fuels," *Proceedings of the 16th Biomass Thermochemical Conversion Contractors' Meeting*, Pacific Northwest Laboratory, Richland, WA, pp. 39-59.

Kreutz, T., Williams, R., Consonni, S. and Chiesa, P. 2005. "Co-Production of Hydrogen, Electricity, and CO_2 from Coal with Commercially Ready Technology. Part B: Economic Analysis," *International Journal of Hydrogen Energy*, 30: 769-784.

Larson, E.D. and Jin, H. 1999a. "Biomass Conversion to Fischer-Tropsch Liquids: Preliminary Energy Balances," *Proceedings of the 4th Biomass Conference of the Americas*, Elsevier Science, Oxford, UK, pp. 843-853.

Larson, E.D. and Jin, H. 1999b. "A Preliminary Assessment of Biomass Conversion to Fischer-Tropsch Cooking Fuels for Rural China," *Proceedings of the 4th Biomass Conference of the Americas*, Elsevier Science, Oxford, UK, pp. 855-863.

Larson, E.D. 2003, "Literature Review for Thermochemical Biomass Conversion," draft prepared for RBAEF project, 18 December, available from E. Larson, Princeton University.

Larson, E.D. and Ren, T. 2003, "Synthetic fuels production by indirect coal liquefaction," *Energy for Sustainable Development*, **VII**(4): 79-102.

Larson, E.D., Consonni, S., and Katofsky, R., 2003. *A Cost-Benefit Assessment of Biomass Gasification Power Generation in the Pulp and Paper Industry,*" Final Report, Princeton Environmental Institute, Princeton University, Princeton, NJ, 8 October. (available at www.princeton.edu/~energy/publications/).

Larson, E.D., Celik, F.E., and Jin, H. 2004, "Performance and Cost Analysis of Future, Commercially-Mature Gasification-Based Electric Power Generation from Switchgrass," final task report for RBAEF project, 19 November (available from E. Larson, Princeton University).

Lau, F.S., Bowen, D.A., Dihu, R., Doong, S., Hughes, E.E., Remick, R., Slimane, R., Turn, S.Q., and Zabransky, R. 2003. "Techno-economic analysis of hydrogen production by gasification of biomass," final technical report for the

period 15 Sept 2001 – 14 Sept 2002, contract DE-FC36-01GO11089 for US Dept. of Energy, Gas Technology Inst., Des Plaines, IL, June (rev.), 145 pp.

Lewnard, J.J., Hsiung, T.H., White, J.F. and Brown, D.M. 1990, "Single-Step Synthesis of Dimethyl Ether in a Slurry Reactor," *Chemical Engineering Science*, **45**(8): 2735-2741.

Lewnard, J.J., Hsiung, T.H., White, J.F. and Bhatt, B.L. 1993. "Liquid phase process for dimethyl ether synthesis," US pat. 5,218,003, June 8.

Li, Y.Y, Xiang, H.W., Yang, J.L, Xu, Y.Y, Li, Y.W, and Zhong, B. 2001, "Effect of reaction conditions on the product distribution during Fischer-Trpsch synthesis over an industrial Fe-Mn catalyst," *Applied Catalysis A: General*, 214: 77-86.

Linnhoff, B. 1993. "Pinch Analysis – A State-of-the-Art Overview," *Trans IchemE*, 71(Part A): 503-522, September.

Lucas, S.H. 2002. "Ningxi Petrochemical DME Project," prepared for the U.S. Trade and Development Agency, Washington, DC, September.

Maniatis, K. 2001. "Progress in Biomass Gasification: An Overview," downloaded 12/10/2003 from http://europa.eu.int/comm/energy/res/sectors/bioenergy_publications_en.htm.

Mann, M.K. and Spath, P.L. 1997. *Life Cycle Assessment of a Biomass Gasification Combined-Cycle System*, NREL/TP-430-23076, National Renewable Energy Laboratory, Golden, CO, September, 150 pp.

McLaughlin, S., Bouton, J., Bransby, D., Conger, B., Ocumpaugh, W., Parrish, D., Taliaferro, C., Vogel, K., and Wullschleger, S. 1999. "Developing Switchgrass as a Bioenergy Crop," Perspectives on New Crops and New Uses. J. Janick (ed.), ASHS Press, Alexandria, VA.

McGlaughlin, S.B., de la Torre Ugarte, D.G., Garten, C.T., Lynd, L.R., Sanderson, M.A., Tolbert, V.R., and Wolf, D.D. 2002. "High Value Renewable Energy from Prairie Grasses," *Environmental Sci. & Tech.*, 36(10): 2122-2129.

Milne, T.A., Evans, R.J., and Abatzoglou, N. 1998. *Biomass Gasifier 'Tars': Their Nature, Formation, and Conversion*, National Renewable Energy Laboratory, Golden, CO, 204 pp Ng, K.L., Chadwick, D. and Toseland, B.A., 1999. "Kinetics and Modeling of Dimethyl Ether Synthesis from Synthesis Gas," *Chemical Engineering Science*, **54**: 3587-3592.

Moore, R. (retired from Air Product and Chemicals, Inc.). 2003. Personal communications, Allentown, PA.

Newby, R.A., Bruck, G.J., Alvin, M.A., and Lippert, T.E. 1998. "Optimization of Advanced Filter Systems, Base Contract Topical Report." Report to DOE/OFE/FETC under Contract No. DE-AC26-97FT33007—03, April.

Ng, K.L., Chadwick, D., and Toseland, B.A. 1999. "Kinetics and modeling of dimethyl ether synthesis from synthesis gas," *Chemical Engineering Science*, 54: 3587-3592.

Niu Y. 2000. "Dimethyl Ether – Clean Fuel in the 21st Century," Inst. of Coal Chemistry, Chinese Academy of Sciences, presented at the Workshop on Polygeneration, Working Group on Energy Strategies and Technologies, China Council for International Cooperation on Environment and Development, Beijing, May.

NKK Corporation, 2003. (http://www.nkk.co.jp/nkknews/40-1/art02.html).

Ohman, M. and Nordin, A. 2000. " The role of Kaolin in prevention of bed agglomeration during fluidized bed combustion of biomass fuels," *Energy Fuels*, **14**(3): 618-624.

OPPA (Office of Policy, Planning, and Analysis), 1990. *Assessment of costs and benefits flexible and alternative fuel use in the US transportation sector, technical report V: costs of methanol production from biomass,* DOE/PE-0097P. Washington D.C. US Department of Energy, December.

Oukaci, R. 2002. "Fischer-Tropsch Synthesis," presented at the 2nd Annual Global GTL Summit, London, 28-30 May.

Pagani, G. 1978. "Process for the production of dimethyl ether," US pat. 4098809, July 4.

Pan, Y.G., Roca, X., Velo, E., and Puigjaner, L. 1999. "Removal of Tar by Secondary Air in Fluidised Bed Gasification of Residual Biomass and Coal," *Fuel*, 78: 1703-1709.

Peng, X.D., Toseland, B.A. and Tijm, P.J.A. 1999a. "Kinetic Understanding of the Chemical Synergy Under LPDME Conditions—Once-Through Applications,"*Chemical Engineering Science*, **54**: 2787-2792.

Peng, X.D., Wang, A.W., Toseland, B.A. and Tijm, P.J.A. 1999b. "Single-Step Syngas-to-Dimethyl Ether Processes for Optimal Productivity, Minimal Emissions, and Natural Gas-Derived Syngas," *IEC Research*, Nov.

Pitcher, K., Hilton, B., and Lundberg, H. 1998. "The Arbre Project: Progress Achieved," Biomass *and Bioenergy*, 15(3): 213-218.

Qadar, S.A., Qadar, Q.A., and Muzio, L.J. 1996. "Decomposition of Ammonia in IGCC Fuel Gas Streams," DOE/ER/81964-97/C0732, *Proceedings of the Advanced Coal-Fired Power Systems '96 Review Meeting*, USDOE, Morgantown, WV.

Rahmim, I.I. 2003. "Gas-to-Liquid Technologies: Recent Advances, Economics, Prospects," presented at the 26th IAEE Annual International Conference, Prague, June.

Raje, A., Inga, J.R., and Davis, B.H. 1997. "Fischer-Tropsch Synthesis: process Considerations Based on Performance of Iron Based Catalysts," *Fuel*, 76(3): 273-280.

Scholz, M. 2002. *GE "F-Class" gas turbines technology evaluation*, GE Power Systems, Aug.

Shell Deutschland Oil GmbH, 2005. "Shell Partners with CHOREN in the World's First Commercial SunFuel Development," press release, August 17.

Simbeck, D. 2004. "Existing Coal Power Plants - CO2 Mitigation Costs (Replacement Coal Gasification Combined Cycle)," draft worksheet for WestCarb by SFA Pacific, Inc., Oct. 26.

Smith, A.R., Klosek, J. and Woodward, D.W. 1997. "Next-generation integration concepts for air separation units and gas turbines," *ASME Journal of Engineering for Gas Turbines and Power*, **119**: 298-304.

Spath, P.L. and Dayton, D.C. 2003. *Syngas Analysis – Preliminary Screening, Technical Briefs, and Technical Barrier Assessment for Syngas to Fuels and Chemicals*, C-Milestone Completion Report, National Renewable Energy Laboratory, Golden, CO, 146 pp.

Steenari, B.M. and Lindqvist, O. 1998. "High-temperature reactions of straw ash and the anti-sintering additives kaolin and dolomite," *Biomass and Bioenergy*, **14**(1): 67-76.

Stevens, D.J., 2001. *Hot Gas Conditioning: Recent Progress with Larger-Scale Biomass Gasification Systems*, NREL/SR-510-29952, National Renewable Energy Laboratory, Golden, CO, 88 pp.

Stone and Webster, Weyerhaeuser, Amoco, and Carolina Power & Light, 1995. "New Bern Biomass to Energy Project Phase 1 Feasibility Study," for EPRI and NREL, Golden, CO, June, 242 pp.

Strom, E., Liinanki, L., Sjostrom, K., Rensfelt, E., Waldheim, L., and Blackadder, W. 1984. "Gasification of Biomass in the MINO-Process," *Bioenergy 84*, Vol. III (Biomass Conversion), H. Egneus and A. Ellegard (eds), Elsevier Applied Science Publishers, London, pp. 57-64.

Sydkraft, Elforsk, and Nutek, 2001. *Varnamo Demonstration Plant: The Demonstration Program, 1996-2000*, Berlings Skogs, Trelleborg, Sweden, 133 pp.

Tijmensen, M.J.A. 2000. "The Production of Fischer Tropsch Liquids and Power through Biomass Gasification," Ph.D. thesis, Dept. of Science, Technology and Society, Utrecht University, Utrecht, The Netherlands, November, 66 pp.

Tijmensen, M.J.A., Faaij, A.P.C., Hamelinck, C.N. nad van Hardeveld, M.R.M. 2002. "Exploration of the Possibilities for Production of Fischer Tropsch Liquids and Power via Biomass Gasification," *Biomass and Bioenergy*, **23**: 129-152.

US Department of Energy (DOE) and the Electric Power Research Institute (EPRI), 1997. *Renewable Energy Technology Characterizations*, Topical Report 109496, U.S. Department of Energy, Washington, DC.

Voss, B., Joensen, F. and Hansen, J.B., 1999. "Preparation of fuel grade dimethyl ether," US pat. 5908963, June 1.

Washington Group and Southern Company, 2000. *Black Liquor Gasification Study*, internal report, Southern Co. Services, Birmingham, AL.

Weist, E.L. 2005. personal communication, Air Products and Chemicals, Inc., Allentown, Pennsylvania.

Weyerhaeuser, 2000. "Biomass Gasification Combined Cycle," final report under contract DE-FC36-96GO10173 to US Dept. of Energy, Federal Way, WA, 160 pp.

Wilen, C. and Rautalin, A., 1993. “Handling and Feeding of Biomass to Pressurized Reactors: Safety Engineering”, *Bioresource Technology*, 46: 77-85.

Williams, R.H. 2000. “Advanced Energy Supply Technologies,” Ch. 8 in *World Energy Assessment: Energy the Challenge of Sustainability*, Bureau for Development Policy, United Nations Development Program, New York, pp. 274-329.

Williams, R.H. 2005. personal communication, Princeton University, Princeton, New Jersey.

Williams, R.H., Larson, E.D., Katofsky, R.E., and Chen, J. 1995. "Methanol and Hydrogen from Biomass for Transportation," *Energy for Sustainable Development*, **I**(5): 18-34.

Williams, R.H. and Larson, E.D. 2003. “A Comparison of Direct and Indirect Liquefaction Technologies for Making Fluid Fuels from Coal,” *Energy for Sustainable Development*, **VII**(4): 103-129.

Xu H., Ge Q., Li W., Hou S., Yu C. and Jia M. 2001. “The synthesis of dimethyl ether from syngas obtained by catalytic partial oxidation of methane and air,” presented at the 6th Natural Gas Conversion Conference, Girdwood, Alaska, 17-22 June.

Yang, J., Liu, Y., Chang, J., Wang, Y.N., Bai, L., Xu, Y.Y., Xiang, H.W., Li, Y.W., and Zhong, B. 2003, “Detailed kinetics of Fischer-Tropsch synthesis on an industrial Fe-Mn catalyst,” *Ind. Eng. Chem. Res.*, 42: 5066-5090.

Zahner, J.C. 1977. “Conversion of modified synthesis gas to oxygenated organic chemicals,” US pat. 4011275, March 8.